THEORETICAL AND TECHNICAL ASPECTS OF USING THE DOPPLER UMBILICAL FLOW WAVEFORM TO ASSESS COMPROMISED FOETAL CIRCULATION.

John Guy Cowper

University of Cape Town

Medical School

July 1996

THEORETICAL AND TECHNICAL ASPECTS OF USING THE DOPPLER UMBILICAL FLOW WAVEFORM TO ASSESS COMPROMISED FOETAL CIRCULATION.

John Guy Cowper

Submitted to the Faculty of Medicine at the University of Cape Town in partial fulfilment of the requirements for the degree of Master of Science in Medicine in the field of Biomedical Engineering

University of Cape Town

July 1996

Things do not change - We change.

Henry David Thoreau

DECLARATION

I, ***JOHN GUY COWPER,*** hereby declare that the work on which this thesis is based is my original work except where acknowledgements indicate otherwise. Neither the whole work nor any part thereof, is being, or has been submitted for another degree in this or any other university.

The university may reproduce, for the purpose of research, any part of this document in any manner whatsoever.

Signed by candidate

16-11-96.

Date

ACKNOWLEDGEMENTS

I would like to express my sincere thanks and appreciation to the following people who enabled me to complete this thesis.

- Wayne Capper, Department of Biomedical Engineering, UCT, for his support and guidance as thesis supervisor and mentor.

- Dr Gerald Mantel, Department of Obstetrics and Gynaecology, Groote Schuur Hospital, for his valuable clinical support and insights.

- The staff and fellow students, Department of Biomedical Engineering, UCT, for their contribution and constructive critique.

- The administrators of the Duncan Baxter research scholarship for financial assistance.

- Wendy Hands, for her commitment, support and tireless proof reading efforts.

- My family, and friends for their encouragement and support.

PRESENTATIONS

PUBLICATIONS

1) Cowper JG, Capper WL

(Abstract) 1996

Modelling of foetal blood flow under hypoxic conditions.

Journal of Maternal-Foetal Investigation, (in press)

POSTERS

1) Cowper JG, Capper WL, Mantel G

April 1995

The effect of maternal hyperoxygenation on umbilical blood flow in growth retarded foetuses

Bessa Conference, Gallagher Estate, Midrand, Gauteng.

2) Cowper JG, Capper WL

August 1996

Modelling of foetal blood flow under hypoxic conditions

9th Congress of the IPDS and Workshop on foetal asphyxia, Long Island, New York.

TABLE OF CONTENTS

DECLARATION iii

ABSTRACT iv

ACKNOWLEDGEMENTS vi

PRESENTATIONS vii

TABLE OF CONTENTS viii

LIST OF FIGURES xii

LIST OF TABLES xiv

1. INTRODUCTION 1

2. NORMAL FOETAL CIRCULATION 5

2.1 INTRODUCTION 5

2.2 Foetal blood flow distribution 5

2.2.1 Ductus Arteriosus 7

2.2.2 Ductus Venosus 8

2.2.3 Foramen Ovale 8

2.3 FOETAL BLOOD 9

2.3.1 Foetal haemoglobin 9

2.3.2 Double Bohr effect 10

2.4 THE FOETAL HEART 10

2.5 NORMAL FOETAL BLOOD PRESSURE 11

2.6 UMBILICAL PLACENTAL UNIT 12

2.7 NORMAL GROWTH PATTERNS 14

2.8 BLOOD FLOW WAVEFORM CHARACTERISATION 16

2.9 FOETAL RESPONSE TO ADVERSE CONDITIONS 19

3. COMPROMISED FOETAL CIRCULATION 19

3.1 INTRODUCTION 19

3.2 ACUTE HYPOXIA 19

3.2.1 Sporadic uterine contractions 20

3.2.2 Umbilical cord compression 20

3.2.3 Foetal haemorrhage 20

3.3 CHRONIC HYPOXIA 21

3.3.1 Growth impairment 21

3.3.2 Oxygen delivery and consumption 22
3.4 CARDIAC RESPONSE TO HYPOXIA 24
3.5 SEVERE FOETAL HYPOXIA 24
3.6 AETIOLOGY OF GROWTH IMPAIRMENT 25
3.7 CLINICAL INTERVENTIONS 26
3.8 CLINICAL ASSESSMENT WITH DOPPLER ULTRASOUND 27
4. A MODEL OF THE FOETAL CIRCULATION 29
4.1 INTRODUCTION 29
4.2 FUNCTIONAL SIMPLIFICATIONS OF THE FOETAL CIRCULATION 29
4.3 AN ANALOGOUS ELECTRICAL MODEL 32
4.3.1 An electrical equivalent of a short segment of vessel 33
4.3.2 Non-parabolic blood flow considerations 36
4.3.3 The approximation for the foetal heart 37
4.3.4 Placental vascular approximation 38
4.4 TWO PORT ANALYSIS 40
4.5 TRANSFER FUNCTION ANALYSIS 42
4.6 NORMAL DATA RANGES AND VESSEL DIMENSIONS 45
4.7 FOETAL MODEL 46
5. SIMULATIONS OF FOETAL BLOOD FLOW UNDER HYPOXIC CONDITIONS 47
5.1 INTRODUCTION 47
5.2 METHODS 48
5.2.1 Model validation for a normal 28 week old foetus 48
5.2.2 The effect of non-parabolic flow on the umbilical PI. 48
5.2.3 the effect of heart pulsatility on the umbilical PI 48
5.2.4 the effect of placental blood distribution on the PI 49
5.2.5 Preferential blood flow shunting on the umbilical PI 50
5.3 RESULTS 52
5.3.1 Umbilical blood flow for a normal 28 week old foetus 52
5.3.2 The effect of non-parabolic flow on the umbilical PI. 52
5.3.3 The effect of heart pulsatility on the umbilical PI. 53
5.3.4 The effect of placental blood distribution on the umbilical PI. 56

5.3.5 Blood flow shunting 57
5.4 DISCUSSION 60
5.4.1 Validation 61
5.4.2 Placental impedance 62
5.4.3 Blood flow shunting 65
5.5 CONCLUSION 66
6. THEORETICAL AND PRACTICAL ASPECTS OF DOPPLER ULTRASOUND MEASUREMENTS. 68
6.1 INTRODUCTION 68
6.2 MATERIALS USED FOR THE FLOW PHANTOM 70
6.3 METHODS 70
6.3.1 Investigation of the effect of changing Doppler Gain 70
6.3.2 Reverse flow during diastole 71
6.3.3 Opposite flow in adjacent vessels 71
6.3.4 Maternal breathing 71
6.4 RESULTS 73
6.4.1 Doppler Gain 73
6.4.2 Reversal of flow within a vessel 73
6.4.3 Flow in opposite directions 75
6.4.4 Maternal breathing 77
6.5 DISCUSSION 78
6.5.1 Doppler gain 78
6.5.2 Signal strength 79
6.5.3 Opposite flow in adjacent vessels 81
6.5.4 Effect of the Doppler wall filter on the MFW 82
6.5.5 Maternal Breathing 84
6.6 CONCLUSION 84
7. THE EFFECT OF MATERNAL HYPEROXYGENATION ON THE UMBILICAL BLOOD FLOW WAVEFORM. 86
7.1 INTRODUCTION 86
7.2 METHODS 87
7.2.1 Clinical trial 87

7.2.2 Doppler waveform acquisition 88
7.2.3 Doppler waveform validation 90
7.2.4 Waveform Analysis 91
7.3 RESULTS 92
7.3.1 Patient summary and outcomes 92
7.3.2 Patient measurement register 92
7.3.3 Low frequency flow modulation 93
7.3.4 PI index versus gestational age 94
7.4 DISCUSSION 95
7.5 CONCLUSION 99
8. DISCUSSION 101
8.1 LITERATURE SURVEY 102
8.1.1 Normal foetal circulation. 102
8.1.2 Compromised foetal circulation 103
8.2 FOETAL CIRCULATORY MODEL 104
8.2.1 Simulations 105
8.3 DOPPLER LIMITATIONS 106
8.4 CLINICAL TRIAL 108
9. CONCLUSIONS AND RECOMMENDATIONS 111
9.1 THEORETICAL CONCLUSIONS 111
9.2 CLINICAL RECOMMENDATIONS 111

APPENDIX A SEGMENT LENGTH A-1
APPENDIX B UNIT VALIDATION B-1
APPENDIX C TWO PORT ANALYSIS C-1
APPENDIX D SPECTRAL ANALYSIS D-1
APPENDIX E WORMERSLEY CONDITIONS E-1
APPENDIX F SHUNT CONDUCTANCES F-1
APPENDIX G STATISTICAL ANALYSIS G-1
APPENDIX H DOPPLER FREQUENCY SPECTRUM H-1
REFERENCES R-1

LIST OF FIGURES

Figure		Page
2-1	Normal circulation of the human foetus close to term.	6
2-2	Circulation in the foetal heart and cardiac vessels.	8
2-3	Foetal and adult oxygen saturation curves.	10
2-4	A plan of the placental and umbilical arteries.	13
2-5	Placenta growth versus gestational age.	14
2-6	Normal foetal weights with respect to gestational age.	16
2-7	a Typical normal umbilical waveform with defined index parameters.	18
3-1	Redistribution of the combined ventricular output to the heart and brain.	22
3-2	Correlation between oxygen delivery and oxygen consumption.	23
3-3	Diagrammatic representation of the trophoblastic invasion of the placenta.	26
3-4	Absent end diastolic flow in the umbilical artery.	28
4-1	Arterial simplification of the foetal arterial system.	31
4-2	Electrical representation of the simplified foetal circulation.	31
4-3	Analogous electrical circuit for vessel segment of length δx.	33
4-4	Equivalent electrical circuit for vessel segment of length δx.	34
4-5	Resistance and inductance scaling factors for different alpha values.	37
4-6	Proximal aorta flow profile and corresponding frequency spectrum.	38
4-7	Schematic representation of the placental branching and equivalent circuit.	39
4-8	A lumped parameter equivalent circuit representing the placental vessels.	40
4-9	Two port analysis for the foetal arterial forward flow transfer function (A_{22}).	42
4-10	Flow diagram of the output flow waveform generation.	44
5-1	Measured and modelled umbilical flow waveforms.	52
5-2	Pulsatility index versus distributed impedance of terminating villi.	56
5-3	Extreme placenta impedance and obstruction of umbilical blood flow.	57
5-4	Simulated maximum flow waveforms under severely hypoxic conditions.	60
5-5	PI versus the number of terminating villi.	63
5-6	3 D plot of placental impedance versus umbilical flow magnitudes.	64
5-7	Cerebral oxygen consumption versus ascending oxygen content.	66
6-1	Relative movement of sample volume with respect to the insonated vessels.	72

6-2 Flow phantom investigation, factors affecting acquisition of the MFW 72
6-3 Increasing Doppler gain 73
6-4 The effect of flow reversal on the MFW 74
6-5 Dual flow for laminar and pulsatile flow conditions 75
6-6 Vessels conducting pulsatile and laminar flow 77
6-7 Pulsatile flow with vessel movement 78
7-1 Sampling protocol 89
7-2a Maximum umbilical flow waveform with periodic vessel movement 94
7-3 PI versus gestational age for growth-impaired foetuses 94
7-4 PI for SGA foetuses of 25 to 27 weeks gestation 95
7-5 HRSI versus PI 99
C-1 A matrix cascading parameters C-1
C-2 Two port equivalents of vessels shunting blood C-2
D-1 Input flow waveform and corresponding frequency spectrum D-1
E-1 Development of a steady parabolic velocity profile E-1
E-2 Alpha and different types of flow E-3
H-1 Frequency power spectrum H-1
H-2 Sonogram of the Doppler power spectral density H-2
H-3 Velocity flow profiles and corresponding velocity distribution histograms H-2

LIST OF TABLES

Table		Page
2-1	Percentage blood flows to anatomical regions in foetal sheep	7
2-2	Reference limits (5th, 50th, 95th centiles) for gestation of PI	17
4-1	Electrical definitions of flow parameters	34
4-2	Vessel dimensions for normal foetuses of 28-30 weeks gestation	45
4-3	Properties and dimensions of a normal placenta	46
4-4	Normal ranges for lobes and TSV of the placenta	46
5-1	Comparison of PI when including or neglecting non parabolic flow	53
5-2	Smoothing of the heart flow waveform	54
5-3	Input waveform profile and corresponding PI's	54
5-4	Systolic time intervals versus umbilical pulsatility index	55
5-5	Effect of clinical blood flow shunting on the umbilical PI	58
5-6	Experimental flow distributions (%CO - percentage cardiac output)	61
6-1	The sizes and concentrations of blood constituents	80
6-2	Approximate attenuation coefficients of common	81
7-1	Clinical trial summary	92
7-2	Patient measurement register	93
A-1	Phase velocity and wavelength calculations for various harmonics	A-3
A-2	Derivation of segment length for various arterial vessels	A-3
B-1	CGS units	B-1
F-1	Percentage conductance and absolute conductance per section	F-1
G-1	Comparison of coefficient of variation for inter and intra variability	G-1
G-2	Sample size versus required detectable difference of PI index	G-2

LIST OF ABBREVIATIONS

AEDF	- Absent end diastolic flow
AGA	- Average for gestational age
BP	- Blood pressure
BPD	- Bi-parietal diameter
bpm	- Beats per minute
BPP	- Bio-physical profile
CTG	- Cardio tachograph
D	- Diastolic minimum
dB	- Decibels
FFT	- Fast Fourier transform
FHR	- Foetal heart rate
GPH	- Gestational proteinuric hypertension
HRSI	- High resistive state index
Hz	- Hertz (frequency)
IFFT	- Inverse Fast Fourier transform
MFW	- Maximum flow waveform
mmHg	- Millimeters mercury (Pressure)
msec	- Milliseconds
PCO_2	- Partial pressure of carbon dioxide
PI	- Pulsatility index
PImp	- Peripheral impedance
PO_2	- Partial pressure of oxygen
r	- Inner lumen vessel radius
RI	- Resistive index
S	- Systolic maximum
SGA	- Small for gestational age
SV	- Stroke volume
TSV	- Terminal stem villi

1. INTRODUCTION

There are several anatomical and haemodynamic differences between the foetal and adult circulations. These differences result from special adaptations of the foetus to its developmental environment within the uterus. One such adaptation is the placenta. Diffusion of substances between mother and foetus is controlled by the placental membranes that separate the maternal and foetal circulations.

Conditions within the uterus are normally conducive to controlled growth and development of the foetus. All the foetal requirements in terms of gaseous exchange, supply of nutrients and removal of waste products are accomplished, via diffusion, across the placenta. The foetus is, therefore, entirely dependent on the mother and the integrity of the placenta for its well-being.

If any maternal, placental or foetal pathology were to compromise the optimised exchange of nutrients and oxygen across the placenta, the foetus would be affected directly. The foetus, however, has the ability to minimise or counteract the effect of changes in its surroundings by appropriately adjusting physiological variables such as heart rate, blood distribution and growth rate.

The change in foetal blood flow distribution results from the ability of the foetus to shunt blood preferentially to more vital regions, namely the brain and heart, when nutrients and oxygen are in short supply. The small fraction of nutrients that does reach the peripheral regions is therefore used for sustenance as opposed to growth. Preferential blood flow shunting results in foetal growth impairment and disproportionate development of the foetal organs and body.

Common signs of compromise and abnormal foetal development include:

- Abnormal foetal heart rate patterns, detected using cardiotocography (CTG).
- Small foetal size for gestational age, as assessed by using ultrasound imaging.
- Reduction in the liquor volume surrounding the foetus, considered when performing a bio-physical profile (BPP).
- Decreased end diastolic flow velocity in the umbilical arterial blood flow waveform, determined by using Doppler ultrasound.

Early detection of foetal compromise allows the clinician an opportunity to take corrective action to minimise the damage caused by the pathology. Alterations to blood flow resulting from a change in the foetal condition have been shown to precede any changes detected by CTG, BPP and ultrasound imaging.(Schulman et al 1989). This study, therefore, investigated the feasibility of using the maximum umbilical flow waveform, as detected by Doppler ultrasound, to characterise blood flow in growth impaired foetuses that have been exposed to chronic hypoxic conditions.

The maximum umbilical flow waveform shape was characterised by the pulsatility index which is defined from the mean, maximum systolic and minimum diastolic values of the maximum flow velocity waveform. The sensitivity of the umbilical PI to various factors such as the flow waveform generated by the foetal heart, the placental impedance and foetal blood flow distribution were investigated, using an analogous flow model. This model simplified the foetal circulation into a number of distributed units, based on the foetal anatomy. Each unit was modelled using electrically analogous flow parameters which were concatenated to derive a single expression, characterising the entire foetal circulatory system.

The model of the normal foetal circulation enabled the effect of progressive foetal compromise to be investigated. The foetal circulation was modelled by a single input and output system which considered the foetal vasculature as the transfer function relating foetal heart flow input and the umbilical arterial flow output.

A flow phantom was used to simulate flow conditions that are likely to occur when insonating the umbilicus of a growth-impaired foetus. Doppler measurements on the phantom highlighted potential errors which could limit the ability of Doppler ultrasound as an effective monitoring technique to investigate foetal growth impairment. Typical limitations of Doppler analysis occur as a result of :

- Reduced liquor volumes
- Vessel movement due to maternal breathing
- Low signal strength of the received Doppler signals
- The high pass wall filter under reduced blood flow conditions
- Simultaneous insonation of multiple vessels on the maximum flow waveform

Information obtained from the foetal circulatory modelling and the investigation of Doppler limitations using a flow phantom, was incorporated into the design of measurement and analysis protocols for a clinical trial. A small pilot study was performed to test these protocols and investigate potential technical and logistical problems that could arise when attempting a large, statistically significant clinical trial.

Clinical data was obtained from a small, controlled trial which investigated the effect of maternal hyper oxygenation in small for gestational age foetuses with absent end diastolic flow. Umbilical blood flow waveforms were captured from these high risk patients and two numerical indices, the pulsatility index and high resistance state index, were used to characterise the waveform shape. These numerical indices, measured at regular time intervals, were analysed to determine (i) the effect of maternal hyperoxygenation on growth-impaired foetuses, (ii) statistical variables regarding measurement variability and sample sizes, (iii) an appropriate analysis technique.

The aim of this thesis was to investigate the feasibility of using the shape of the umbilical flow waveform, obtained clinically with Doppler ultrasound, to monitor the condition growth impaired foetuses.

This aim was addressed via the following :

1. Survey the literature to obtain information regarding :
   a) the foetal blood flow distribution for normal foetuses.
   b) the effect of placental pathology and maternal hyperoxygenation in compromised foetuses.

2. Model the foetal circulation to investigate the effect, on the umbilical flow waveform, of physiological changes resulting from placental insufficiency.

3. Perform a theoretical and practical assessment of Doppler ultrasound by considering its suitability in monitoring foetal condition, through alterations in the umbilical blood flow waveform shape.

4. Clinically gather and analyse umbilical blood flow waveforms from foetuses currently on a trial to investigate appropriate protocols for the assessment of maternal hyperoxygenation.

2. NORMAL FOETAL CIRCULATION

2.1 INTRODUCTION

The foetal circulation is required to supply the foetus with sufficient oxygen and nutrients to enable normal foetal growth and development. Anatomical and haemodynamic adaptations optimise the transfer of oxygen and nutrients, via the placenta, from the maternal to the foetal circulation. During gestation and particularly during labour, when the blood supply to the maternal placenta is interrupted by uterine contractions, the foetal circulation must have the ability to tolerate acute periods of hypoxia. This chapter considers some of these adaptations, namely (i) the specialised distribution of foetal blood flow, (ii) the unique physiological characteristics of foetal blood, (iii) the anatomy of the foetal heart, (iv) the appropriate regulation and control of blood pressure and finally, the localised blood flow within the placenta.

2.2 FOETAL BLOOD FLOW DISTRIBUTION

There are a number of differences between the foetal and adult circulations since, whilst in utero, the placenta serves as the site for gaseous exchange rather than the lungs. Consequently, a unique feature of the foetal circulation is the relatively high proportion of combined ventricular output distributed, via the umbilical arteries, to the placenta (45%), as compared with the small percentage to the lungs (10%).

Oxygenated blood from the placenta passes through the umbilical vein. A large percentage of this blood is shunted through the liver via the ductus venosus and enters the right atrium (RA) of the foetal heart through the inferior vena cava (IVC). Venous blood from the upper body also drains into the right atrium via the superior vena cava (SVC). A high percentage of the right atrial blood (45%) is shunted between the atria, via the foramen ovale. The unshunted blood passes into the pulmonary artery where again, a high percentage (70%) is shunted into the foetal aorta via the ductus arteriosus (Dawes 1968).

The anatomical structure of vessels branching from the aorta is identical to that of an adult apart from the umbilical arteries, as seen in Figure 2-1. The two umbilical arteries each

branch from an internal iliac artery and, after passing through the foetal umbilicus, helix around the umbilical vein before anastomising with the placenta.

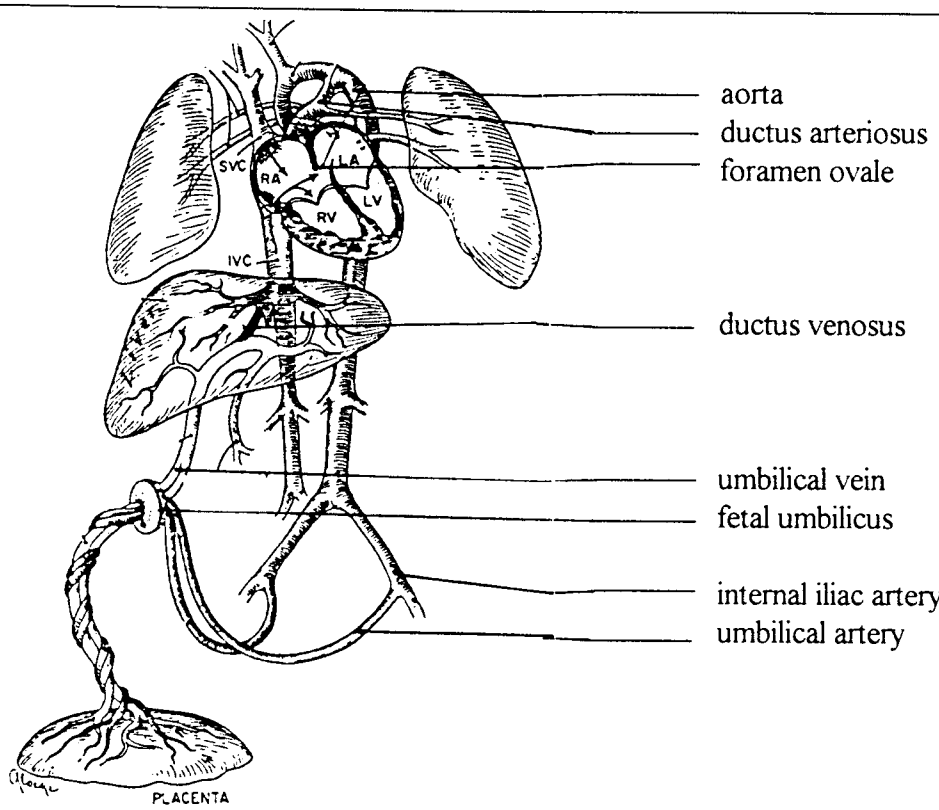

Figure 2-1 Normal circulation of the human foetus close to term.(Veth, 1976)

The total foetal circulation can be divided into several anatomical regions. The normal percentage of the total cardiac output distributed to each of these regions, is tabulated for ovine foetuses in Table 2-1. The major difference between ovine and human distributions, is the percentage blood flow to the respective brains, approximately 4% for sheep and 10% for humans.(Rudolph, 1984).

Percentage Cardiac Output					
Region	Rudolph et al. 1967	Rudolph et al. 1970	Toubas et al 1981	Itskovitz et al. 1987	Block et al. 1990
	%	%	%	%	%
Placenta	40	41	43	46	33
Heart	3	5	3	3	3
Brain	2	5	2	3	3
Thorax	6	4	7	8	7
Abdomen	7	9	9	8	8
Adrenal	0.1	0.1	0.2	0.5	0.08
Body	32	35	35	31	45

Table 2-1 Percentage blood flows to anatomical regions in foetal sheep, cited in Jensen & Berger, 1991 .

Anatomical circulatory adaptations facilitate the blood flow requirements of the foetus. These structural adaptations namely, the ductus arteriosus, foramen ovale and the ductus venosus are considered in detail.

2.2.1 DUCTUS ARTERIOSUS

The two ventricles of the foetal heart work in parallel. This can be seen in Figure 2-2 where the right atrium (RA) and right ventricle (RV) are in parallel with the left atrium (LA) and left ventricle (LV) respectively. The left and right ventricles eject the same volumes of blood and have nearly identical ejection pressures, (DeMuylder et al., 1984). A large percentage of total cardiac output ejected from the right ventricle, is shunted away from the pulmonary arteries (PA) into the aorta (Ao) via the ductus arteriosus (DA), (Dawes, 1968). The ductus arteriosus is sensitive to arterial PO_2 and constricts with an increase in the PO_2, (Heymann, 1975). At birth, when the PO_2 rises rapidly the ductus arteriosus constricts and the chambers of the neonate's heart begin to work serially rather than in parallel.

2.2.2 DUCTUS VENOSUS

The foetal hepatic vascular bed is different from that of the adult, since the ductus venosus connects the umbilical vein (UV) with the abdominal inferior vena cava (IVC) Figure 2-2. This configuration enables rich oxygenated blood to be shunted past the hepatic circulation directly to the right atrium of the foetal heart. Within the inferior vena cava, oxygenated blood returning from the placenta (P) via the ductus venosus (DV) is streamlined, and therefore it does not completely mix with blood returning from the lower body via the distal inferior vena cava, (Edelstone et al. 1979,1980 , Reuss et al. 1980,1981) cited in Polin & Fox, 1992 .The stream of oxygenated umbilical venous (UV) blood returning via the ductus venosus (DV) preferentially enters the left ventricle via the foramen ovale to be distributed to the upper body.

2.2.3 FORAMEN OVALE

Part of the blood returning via the inferior vena cava is shunted from the right atrium through to the left atrium via the foramen ovale (FO). The blood shunted through this opening is distributed almost exclusively to the upper body,(Rudolph, 1974). The foramen ovale therefore facilitates streamlining, which accentuates the difference in oxygen content between the blood distributed to the heart and brain, and that distributed to the lower body.

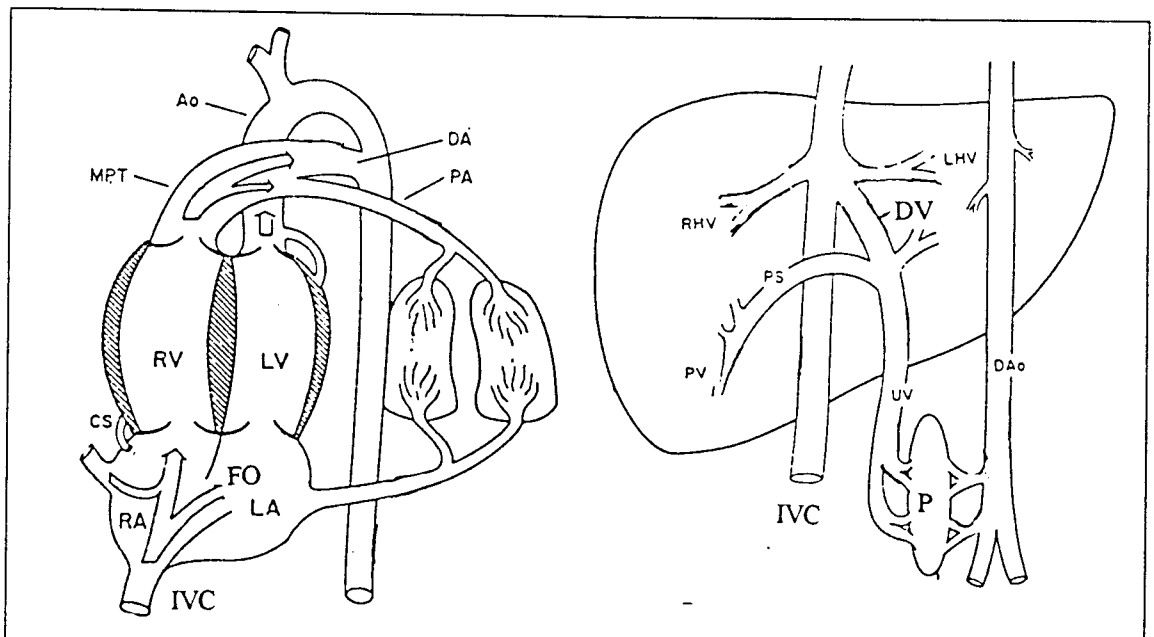

Figure 2-2 Circulation in the foetal heart and cardiac vessels(Polin & Fox, 1992)

2.3 FOETAL BLOOD

The PO_2 of blood contained within the placental sinuses is maintained at 50mmHg by the maternal circulation. The foetal vessels which are bathed in these pools have a much lower PO_2. This large difference in partial oxygen pressures creates a steep concentration gradient, optimising conditions for oxygen transfer from the mother to the foetus. The foetal blood returning from the placenta has a PO_2 of 30mmHg. Even with such a low PO_2, foetal blood is still able to transmit almost as much oxygen to foetal tissue as the maternal blood to the maternal tissue. This is due to three foetal haemodynamic adaptations which optimise oxygen transfer namely (i) the foetal haemoglobin has a higher affinity for oxygen than that of the adult; (ii) the foetal haemoglobin concentration within foetal blood is approximately 50% greater than that of the mother; (iii) the double Bohr effect which results from the high concentration of foetal haemoglobin and partial pressure of carbon dioxide within the foetal circulation (Guyton 1993).

2.3.1 FOETAL HAEMOGLOBIN

Foetal blood contains a high concentration of an entirely different type of haemoglobin to that of adult blood. Foetal haemoglobin combines with oxygen at a considerably lower PO_2 than adult haemoglobin which allows the foetal blood to carry up to 30% more oxygen in low PO_2 ranges (20-40mmHg), (Guyton ,1993). Itskovitz et al , 1984 cited in Itskovitz et al.(1987) showed a 60% decrease in the delivery of oxygen to the tissues of the foetus when foetal blood was replaced by maternal blood. The oxygen saturation curves for the foetus and the adult are shown in Figure 2-3. The foetal curve (F) illustrates the ability of foetal haemoglobin to maintain higher oxygen saturation levels for lower partial pressures compared to the adult/maternal curve (M).

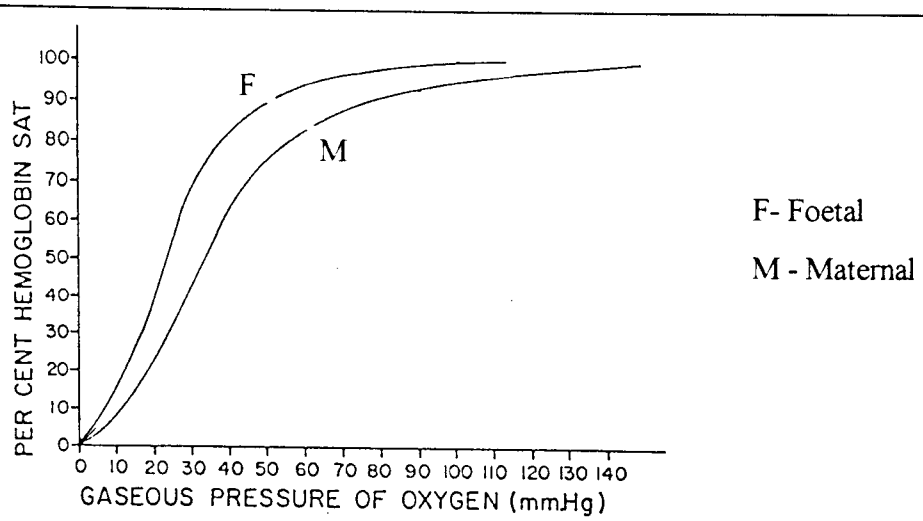

Figure 2-3 Foetal and adult oxygen saturation curves.(Guyton, 1993).

2.3.2 DOUBLE BOHR EFFECT

Haemoglobin can carry more oxygen at low PCO_2 than it can at high PCO_2. This phenomenon, known as the Bohr effect, facilitates optimal gaseous transfer across the pleural membranes. In the foetal circulation blood flowing into the placenta has a high PCO_2 which diffuses readily into the maternal blood. The loss of CO_2 from the foetal blood causes it to become more alkaline and the maternal blood more acidic. As a result of the Bohr effect, oxygen is actively forced from the maternal blood into the foetal circulation. The Bohr effect during placental exchange is twice as effective as it is during pleural exchange and is therefore referred to as the Double Bohr effect,(Guyton, 1993).

2.4 THE FOETAL HEART

The effective cardiac output is a function of the stroke volume and heart rate and is determined by the sum of blood flow from the left and right ventricles. The normal heart rate range is 120 to 160 bpm with an average of 140bpm,(Thompson & Trudinger, 1990). The values of cardiac output for foetal sheep reported in the literature vary between 200 and 500 ml/min/kg foetal weight,(Assali et al., 1968 , Dawes, 1968 , Makowski et al. 1968 and Rudolph & Heyman, 1970). Polin & Fox (1992) state that the approximate cardiac output in human foetuses is 450 ml/min/kg, which is similar to that of foetal sheep.

The stroke volume is constant for normal ranges of FHR in a developing foetus,(Goodlin et al., 1972). Thus the only way to change the cardiac output is by varying the FHR,(Polin & Fox, 1992). If the foetal heart rate exceeds a certain critical limit however, there is insufficient time for the atria to fill the ventricles effectively, and the stroke volume falls with a subsequent drop in cardiac output.

Another important parameter to be considered when modelling the foetal heart is the ejection time. It has been reported that the systolic time interval (ejection time) remains constant and the diastolic interval changes as the FHR is varied,(Veth, 1976),(Downing et al, 1991),(Thompson et al, 1987),(Maulik et al, 1992). The diastolic interval is thus inversely proportional to the heart rate. A mean ejection time of 180 msec is quoted in the literature and will be used in further calculations.

2.5 NORMAL FOETAL BLOOD PRESSURE

The average or mean blood pressure is determined from the stroke volume, the heart rate and the peripheral impedance according to Equation 2-1.

$$BP = SV \times FHR \times PImp \qquad \text{Equ 2-1}$$

BP = Blood Pressure SV = Stroke Volume

FHR = Foetal Heart Rate PImp = Peripheral Impedance

The mean arterial blood pressure in human foetuses is reported to be approximately 50 to 53 mmHg,(Hibbard, 1988 , Dawes, 1968). In foetal sheep, the mean arterial blood pressure ranges between 44 and 66 mmHg,(Polin & Fox, 1992 , Dawes, 1968 , Cohn et al, 1980 , Paulick et al, 1991). The mean pressure in the umbilical arteries is reported to be almost equal to the mean arterial pressure,(Veth, 1976).

The mean arterial blood pressure is controlled by reflexes which are initiated by the baro- and chemo-receptors which are found in the carotid sinus and the aortic arch. These reflexes have been shown to be developed in the foetus by the 3rd trimester. It is difficult to differentiate the specific control of either reflex because they are situated at the same site. The baroreflex and aortic chemoreflex respond to changes in FHR, the total peripheral impedance and the ventricular contractility,(Veth, 1976) These reflexes respond via

sympathetic and parasympathetic innervation to maintain the blood pressure. The aortic chemoreceptors sense partial pressure of oxygen, not oxygen saturation and are thought to play an active role in the response to hypoxemia in utero,(Giussani et al., 1993).

The mean arterial pressure of the foetus is affected by the foetal vascular impedance (Muijsers et al, 1991 , Adamson et al, 1989). The autonomic nervous system is actively involved in controlling the peripheral impedance and is thus also actively involved in controlling the blood pressure. (Veth, 1976) reports that the parasympathetic nervous system is capable of exerting significant control, and that this control increases as the foetus approaches full term. The alpha and beta adrenergic control of the resting heart rate and peripheral impedance is present in early foetal life and increases as the autonomic nervous system develops and matures.

Peripheral capillary beds are able to autoregulate peripheral blood flow. This regulation is independent of the autonomic nervous system and results from the metabolic activity and blood flow requirements of the tissue,(Liedtke et al, 1973 , Sagawa & Eisner, 1975).

2.6 UMBILICAL PLACENTAL UNIT

The placenta is required to supply the foetus with sufficient gasses and nutrients even during uterine contractions. During this time, blood supply to the maternal placenta is interrupted for extended periods. To facilitate the absence of maternal replenishment and supply, the foetal placental vessels are bathed within uterine blood pools. During intervals of absent maternal flow, the foetus can still obtain sustenance from the blood pools. Consequently, the foetus can accommodate numerous acute hypoxic insults lasting several minutes.

The umbilical cord consists of two umbilical arteries which spiral around the umbilical vein. The two arteries anastomose at the end of the cord before reaching the placenta. At the placenta the umbilical artery divides into several (4-8) smaller branches which run radially across the placental surface. These vessels branch quickly into secondary and tertiary stem villi before finally proliferating into the terminal villous vessels. The primary and secondary stem villi are collectively grouped into lobes and the tertiary stem villi into parallel

branching lobules, Figure 2-4. The dimensions of vessels contained within the umbilical placental unit are given in Table 4-2.

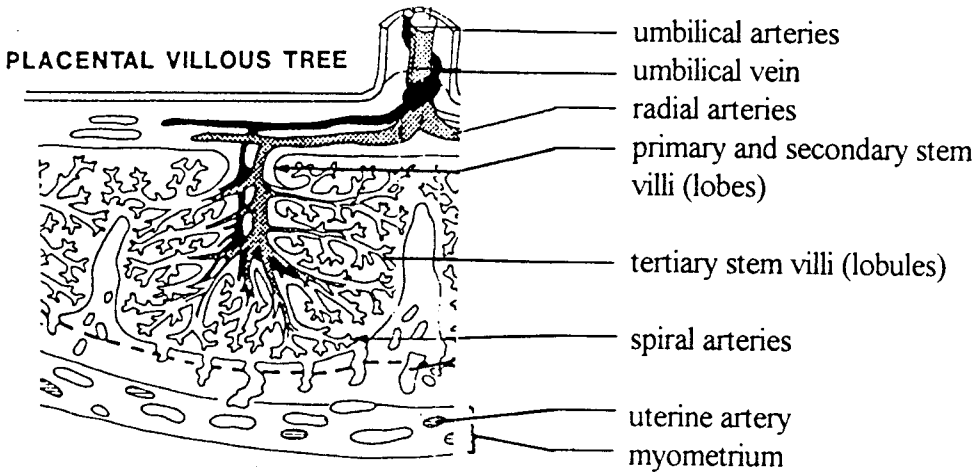

Figure 2-4 A plan of the placental and umbilical arteries,(Thompson & Trudinger, 1990).

The umbilical arteries and the placental bed are not innervated and are thus not controlled by the foetal autonomic nervous system,(Veth, 1976). The umbilical arteries and arteries of the placental bed have been shown to be under hormonal control as they are sensitive to catecholamines, (Adamson et al., 1989 , Dawes, 1968 , Howard et al., 1987). Umbilical placental impedance can thus be varied by hormonal action but not by neural control.

The development of the normal foeto-placental circulation and its impedance has been shown to depend on the proliferation and maintenance of small vessels in the secondary and tertiary villi. As their numbers increase, so the peripheral impedance decreases. (Dawes, 1968).

The ratio of the foetal mass to the placental mass varies with gestational age, since the rate of growth of the placenta differs from the rate of growth of the foetus. This can be seen by comparing the graphs in Figure 2-5 and Figure 2-6.

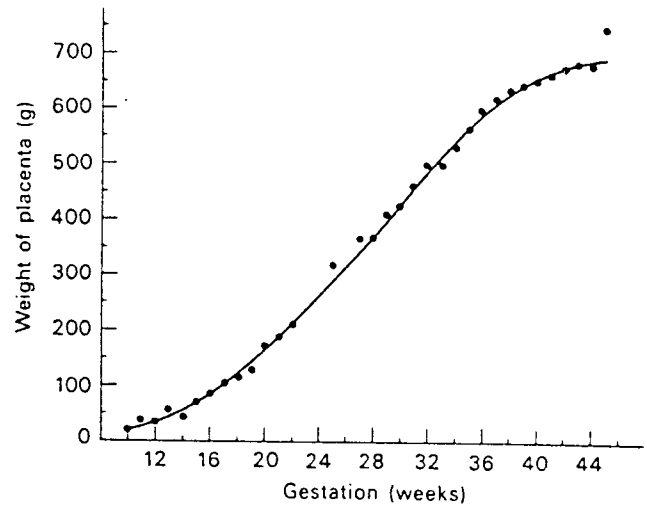

Figure 2-5 Placenta growth versus gestational age(Hytten & Chamberlain, 1991)

2.7 NORMAL GROWTH PATTERNS

The foetus has many circulatory and anatomical adaptations that enable it to tolerate its dependence on the maternal circulation for sustenance. In utero conditions are therefore optimised to facilitate the normal growth and development of the foetus. Figure 2-6 shows the normal growth rate of the foetus. Any foetus that falls below the 10th centile mass for its gestational age needs to be investigated for potential growth impairment.

Not every foetus below the 10th centile is growth-impaired, however, as some foetuses are just genetically disposed to a small size. The proportions of a naturally small-for-gestational-age foetus are normal, whereas those of a growth-impaired foetus are disproportionate,(Nicolaides et al, 1987). The rate of growth of the peripheral organs is lower than the rate of growth of the brain and heart in growth-impaired foetuses, as a result of blood flow redistribution.

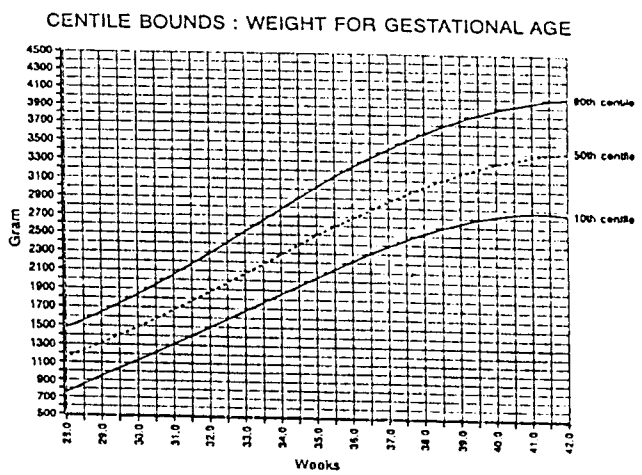

Figure 2-6 Normal foetal weights with respect to gestational age,(Theron & Thompson, 1995). Weight for gestational age given for an urban population of the Western Cape.

2.8 BLOOD FLOW WAVEFORM CHARACTERISATION

Foetal blood flow waveforms can be detected using Doppler ultrasound by the 15th week of gestation. The blood flow waveform is dependent on the impedance of the system into which the blood is pumped. For example, the greater the placental impedance, the less the blood flow to this area and the more pulsatile the waveform. The main contributors to the shape of the FVW are the peripheral outflow impedance, the cardiac flow output, the characteristics of the arterial walls and the blood viscosity,(Thompson et al., 1987).

Indices are used to quantify the shape of the blood flow waveform. This enables the waveform to be compared between foetuses and/or over time. Common indices which characterise the blood flow waveforms, are based on empirical observations and have no physical correlation. The benefit and predictive value of an index depends upon its sensitivity to the changes in shape of the blood flow waveform.

The umbilical artery maximum flow waveform is particularly simple in shape (Figure 2-7a). A normal pregnancy is characterised by forward flow throughout diastole, and an increase in end diastolic flow with gestational age. Lowered diastolic flows tending towards absent end diastolic flow have been shown to correlate with raised placental vascular impedance

and adverse perinatal outcome,(Rochelson, 1989). Abnormal umbilical artery waveforms correspond to vascular narrowing and obliteration of the small arteries in the placental villous bed,(Giles et al. 1985).

Two indices have been used in this study to characterise the shape of the maximum blood flow velocity waveform. These indices are the pulsatility index (PI) -(Gosling & King, 1975 cited in Evans et al. 1994) and the high resistance state index (HRSI) -(Szentkuti et al., 1993). The PI index is used extensively in umbilical circulatory models,(Thompson & (Trudinger 1990 , Maulik et al., 1991 , Mires et al, 1990), while the HRSI, is a relatively new index which is particularly sensitive in regions of absent end diastolic flow,(Szentkuti et al, 1993).

The pulsatility index is calculated from the systolic maximum (S), diastolic minimum (D) and the mean blood flow (M) during a cardiac cycle (Figure 2-7a), according to Equ 2-2.

$$PI = \frac{S - D}{M} \qquad \text{Equ 2-2}$$

The normal range of PI versus gestation is given in Table 2-2.

Gest. Weeks	Umbilical artery PI		
	5th	50th	95th
24	0.81	1.30	1.79
26	0.71	1.20	1.69
28	0.63	1.12	1.61
30	0.56	1.05	1.54

Table 2-2 Pulsatility Index 5th, 50th, 95th centile reference limits for different gestations, (Arduini et al., 1990)

The HRSI index is obtained from a curve called the Resistance Profile (RP) which is given by

$$RP(t) = \frac{S - X(t)}{S} \qquad \text{Equ 2-3}$$

X(t) is the value of the flow waveform at time t (Figure 2-7a).

For a given gestational age, a rectangular region of interest is defined as the area between the 95th centile RI value,(Pattinson et al., 1989) and the RI=1.0 line (RI -resistance index, (Porcelot, 1974 cited in Low 1991) as shown in Figure 2-7b. The area under the RP curve that falls into this rectangle is expressed as a percentage of the total area of the rectangle, and is labelled the High Resistance State Index HRSI. A HRSI >32% indicates a trend for more rapid foetal deterioration.(Szentkuti et al, 1993). The blood entire flow waveform is used to calculate the HRSI index.

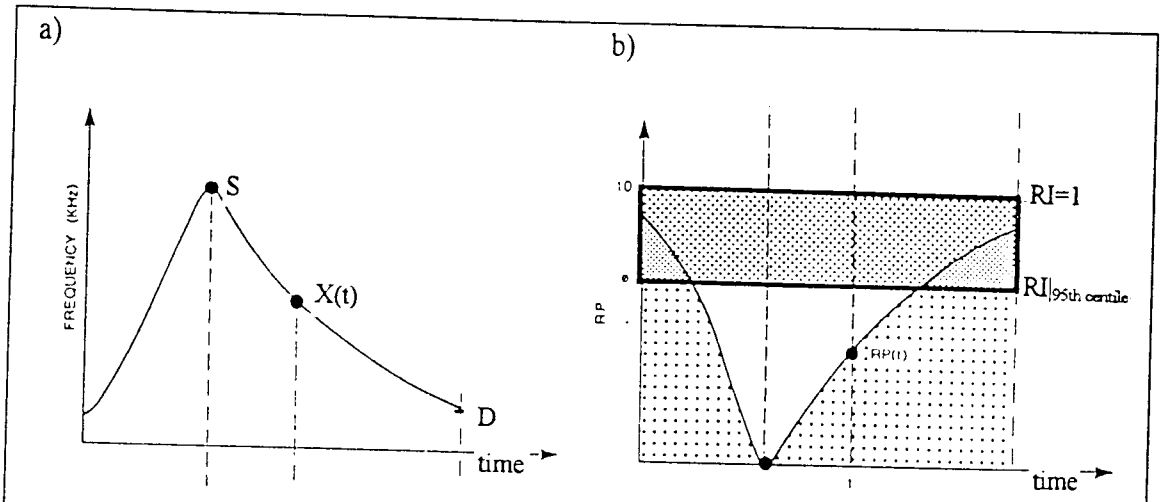

Figure 2-7 a Typical normal umbilical waveform with defined index parameters
b Resistance profile used to determine HRSI,(Szentkuti et al., 1993)
S - maximum systolic flow ; D - minimum diastolic flow

Indice approximations obtained from Doppler analysis have a finite range over which they can accurately represent blood flow with a vessel. Two factors need to be considered when using the PI and HRSI. Firstly, the comparative data available for verification of the HRSI is limited. Secondly, the PI during normal pregnancy decreases with advancing gestational age. An increase in the PI has been shown to correspond with an increase in placental impedance and to be indicative of foetal morbidity (Chudleigh & Pearce, 1986) found clinically that just prior to foetal death or during severe foetal morbidity the PI decreased.

This situation would arise if a further increase in peripheral impedance and a corresponding decrease in the amplitude of the systolic peak were to occur under absent end diastolic flow conditions. Consequently, there is a finite range over which some indices can provide clinically relevant information and it is important to determine this range.

2.9 FOETAL RESPONSE TO ADVERSE CONDITIONS

This chapter has focused on the normal foetal circulation and, in particular, the special anatomical and physiological adaptations used by the foetus to optimise its normal growth and development. However, regardless of any adaptations, the foetus is still entirely dependent on the mother for nutrients and gaseous exchange.

If, for foetal or maternal reasons, any of the adaptive mechanisms were to fail and the natural growth and development of the foetus were to be compromised the foetus would be forced to redistribute its resources and adapt in order to ensure its survival. The following chapter investigates the appropriate responses employed by the foetus when exposed to adverse conditions.

3. COMPROMISED FOETAL CIRCULATION.

3.1 INTRODUCTION

Foetal compromise occurs when the foetus is exposed to conditions that prevent it from growing and developing normally. This type of distress arises from the failure of the maternal, foetal or placental circulations to provide for the needs of the foetus.

At the start of the third trimester, the foetus is able to employ appropriate physiological mechanisms to compensate for the effects of potential adverse conditions. The foetal circulatory response to hypoxemia, for example, involves a centralisation of blood flow. This mechanism favours blood flow to the brain, heart and adrenals whilst sacrificing blood flow to most of the peripheral organs, in particular, the lungs and skin.

The foetal response to acute hypoxia however, is qualitatively similar but quantitatively different from the foetal response to chronic hypoxia. This chapter therefore considers the foetal response to both conditions, based on ovine foetal experiments.

3.2 ACUTE HYPOXIA

Acute hypoxemia can occur as a result of sporadic uterine contractions, umbilical cord compression or in some cases abruptio placentae. In each instance, the maternal provision of nutrients, gases and waste removal is interrupted for a short period. The corresponding foetal compensatory mechanisms alter the foetal blood pressure, FHR, peripheral impedance and cardiac tone in an appropriate manner to limit the effect of the absence of flow on the foetus. This section describes the variety of foetal responses to different causes of acute hypoxia.

3.2.1 SPORADIC UTERINE CONTRACTIONS

Repeated reductions in uterine blood flow occur more frequently as the foetus approaches term. The uterine contractions cause the oxygen saturation of the haemoglobin to fall and the plasma catecholamine concentration and the arterial blood pressure to rise. The foetal response under these conditions is to decrease the heart rate and peripheral blood flow which results in an increased foetal blood pressure. (Jensen et al 1985)

3.2.2 UMBILICAL CORD COMPRESSION

A reduction of arterial and/or venous blood flow causes a decrease in oxygen delivered to the foetus. The foetal response to an acute decrease in oxygen supply is an increase in arterial blood pressure and the combined ventricular output (Itskovitz et al 1982 , 1983 , 1987 cited in Jensen and Berger, 1991). A reduction in umbilical blood flow is accompanied by a redistribution of blood. The flow to the brain, heart and adrenals increases, whereas the flow to the peripheral organs does not change. The fraction of umbilical blood shunted through the ductus venosus increases by 30% when the umbilical flow is reduced by 75%,(Edelstone et al, 1980).

3.2.3 FOETAL HAEMORRHAGE

A reduction in the foetal blood volume causes a reduction in the heart rate, the arterial blood pressure and the cardiac output. Percentage blood flow to the head, heart and adrenals is maintained by a decrease in the impedance to blood flow in these organs. Flow to most of the peripheral organs however, including the placenta fall,(Toubas et al, 1981). Oxygen delivery to the upper body segments increases because the fraction of umbilical venous blood flowing through the ductus venosus increases.

From the three separate postulations recorded above, it can be seen that the foetus employs appropriate mechanisms in order to limit the impact of the hypoxic event upon itself. In each of these examples the flow distribution, blood pressure and FHR return to their normal levels when the hypoxic insult subsides.

3.3 CHRONIC HYPOXIA

Chronic hypoxia is usually less intense than acute hypoxia and occurs over longer periods. This pathology causes continuous stress to the foetus as the hypoxic conditions are persistent and do not subside. Chronic hypoxia is most commonly caused by a complication in the maternal respiratory or circulatory systems, or a decrease in the cross-sectional area of the maternal or foetal placenta over which gaseous and nutrient exchange occur.

3.3.1 GROWTH IMPAIRMENT

Chronic hypoxia can be modelled by prolonged maternal hypoxia or graded constriction of the utero-placental and foetal vessels. Regardless of the mechanism, however, chronic hypoxia results in foetal growth impairment. Reduced foetal growth is associated with a number of metabolic and endocrine changes. One such change is an increase in the concentration of catecholamines. Catecholamines are vasocontrictors which, as their concentration increases, cause a graded increase in the impedance to blood flow within the foeto-placental vessels (Howard et al., 1987). In severe cases, the increased placental vasoconstriction could result in an increase in blood pressure, (Koos et al., 1987).

Growth-impaired foetuses tend to have a slightly higher heart rate,(Robinson et al. 1983), although Kitanaka et al. (1989) and Alonso et al. (1989) report minimal changes in heart rate during chronic hypoxia. The chronic reduction in foetal oxygen delivery is compensated by a combination of an increased red cell volume, an increase in the transport capacity of oxygen and a decrease in oxygen consumption,(Robinson et al. 1983). Minor degrees of chronically reduced foetal oxygen delivery are not necessarily associated with major circulatory responses,(Block et al. 1990). However, major changes in chronically reduced foetal oxygen delivery cause a circulatory centralisation in favour of the brain and heart as shown in Figure 3-1,(Creasy et al. 1973 , Polin & Fox, 1992). This is reflected by a relative maintenance of the mass of central organs as compared to that of the foetal body in general.

(Robinson et al., 1983) investigated the response of growth impaired foetuses to acute hypoxemia and found that they develop acidemia faster than normal sized foetuses.

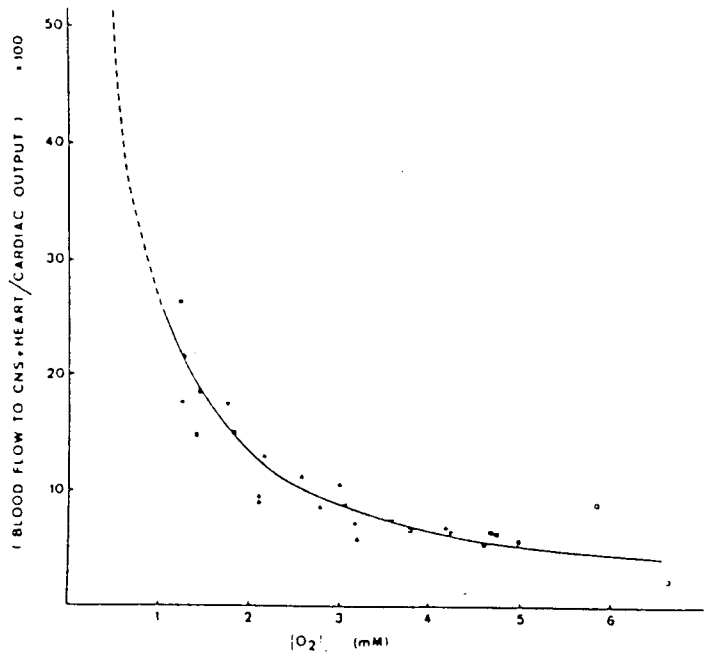

Figure 3-1 Redistribution of the combined ventricular output to the heart and brain. (Polin & Fox, 1992)

3.3.2 OXYGEN DELIVERY AND CONSUMPTION

Foetal oxygen consumption is kept constant over a wide range of blood flow through the uterine and umbilical circulation. This mechanism is possible due to the large reserve capacity of the foetal blood to transport oxygen, and the reserve capacity of the foetal organs to extract oxygen, (Itskovitz et al. 1987). When oxygen delivery to the foetus is reduced, the foetus can increase the amount of oxygen extracted from the blood across the utero-placental bed; the umbilical-placental bed; and the arterio-venous vascular bed of each individual organ, (Carter, 1989). The oxygen consumption of the whole foetus and individual organs will therefore remain constant over a wide range of changes in oxygen delivery. Oxygen consumption will only decrease when oxygen extraction is maximal and oxygen delivery is further reduced.

These conditions can arise due to prolonged hypoxemia which causes chronic blood flow redistribution,(Jensen et al, 1987). Under these circumstances, blood is shunted away from the peripheral organs towards more vital organs and oxygen consumption of peripheral organs becomes proportional to the peripheral blood flow,(Carter, 1989), Figure 3-2.

This important mechanism enables the foetus to conserve oxygen in the peripheral organs thereby maintaining oxidative metabolism in central organs. (Braems & Jensen 1991 , Cohn et al., 1974, cited in Jensen et al. 1991). This phenomenon, as seen in Figure 3-2 shows how oxygen delivery determines oxygen consumption in peripheral organs when oxygen is in short supply. This is a specialised foetal adaptation which does not occur post-natally,(Jensen et al. 1987). The compensatory mechanisms mentioned in this section cannot continue indefinitely and a point is reached were they fail. This is considered in greater detail in chapter five.

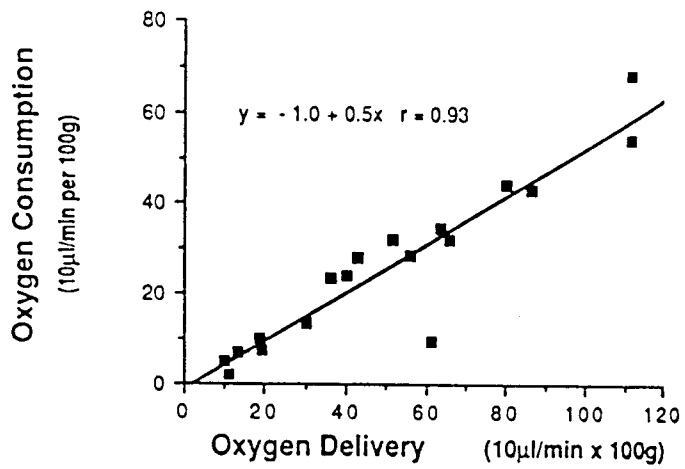

Figure 3-2 Correlation between oxygen delivery and oxygen consumption.(Jensen et al. 1991)

Behrman et al. (1970) found that prolonged hypoxia abolished the preferential streaming of ductus venosus blood across the foramen ovale and substantially increased the proportion of poorly oxygenated superior vena cava blood flowing across the foramen ovale. The oxygen content of the blood crossing the foramen ovale

therefore falls and oxygen delivery to the brain and heart has to be maintained by increasing the blood flow,(Itskovitz et al. 1987).

3.4 CARDIAC RESPONSE TO HYPOXIA

The foetal heart rate and its variability are dependent on the condition of the foetus. Chronic or prolonged hypoxia has been shown to cause little change in the foetal heart rate, but rather a rapid decrease in the stroke volume. The mean arterial pressure is reported to rise but not significantly. The flow from the right ventricle showed a triphasic response (primary maintenance, secondary depression and subsequent recovery), achieving a new lower steady state condition,(Alonso et al. 1989)

The foetal response to acute hypoxemia is more variable. Dawes et al.(1989), Spencer et al.(1986) and Morrow et al.(1989) cited in Bocking (1989) show chemo- and baro-receptor activity giving rise to bradycardia and a decrease in heart rate variability with acute hypoxia. This finding is not consistent in all studies; for example no significant heart rate changes were found by Arbeille et al. (1995) during hypoxia induced by cord compression.

3.5 SEVERE FOETAL HYPOXIA

The mechanisms discussed above are available to the foetus in order to compensate for the effects of acute or chronic hypoxia. These mechanisms have a limited range of influence and usually jeopardise or sacrifice some aspect of the natural growth and development of the foetus. Consequently, if the pathology causing acute hypoxia were to persist, or a chronically hypoxic foetus were to be exposed to an episode of acute hypoxia, the foetal condition would deteriorate rapidly.

Severe hypoxia is accompanied by rapid changes in both the foetal and the umbilical circulation. Under these conditions the heart rate, arterial oxygen content, pH, and combined ventricular output fall, whereas arterial blood pressure, PCO_2, and lactate concentrations rise rapidly,(Jensen et al. 1987). This foetal response indicates that the foetal circulatory reserve can become depleted and circulatory centralisation cannot be

maintained. There is a decentralisation of foetal blood as the impedance of peripheral organs decreases with a corresponding increase in the impedance of central organs. Umbilical impedance rises and placental flow falls. These changes are associated with severe metabolic compromise and severe foetal acidemia which will lead to foetal death unless immediate resuscitation occurs,(Jensen et al. 1987,, Block et al. 1990).

The fate of the foetus during severe hypoxia is determined by the degree of hypoxic damage and by the depletion of the cardiac glycogen stores. Agonal heart rate patterns, increasing cardiac failure and the resultant increase in central venous pressures precede foetal death,(Block 1990).

3.6 AETIOLOGY OF GROWTH IMPAIRMENT

The actual mechanisms involved in the reduction of foetal growth are not well understood. Maternal gestational proteinuric hypertension (GPH) is a major factor associated with foetal growth impairment and placental ischemia, (Davey & MacGillivray 1988). Approximately 60% of all growth impaired pregnancies present with maternal hypertension,(Dekker & van Geijn, 1994). Maternal hypertension is defined as a blood pressure greater than 140/90 mmHg.

In a normal pregnancy, the trophoblasts invade the placental bed and migrate down the entire length of the spiral arteries by about the 20th post menstrual week, (Brosens et al. 1967). The spiral artery is therefore stripped of its myometrial lining, which reduces the peripheral impedance and hence maternal blood pressure (Figure 3-3). If foetal trophoblasts do not penetrate the maternal spiral arteries sufficiently, the remaining myometrial portion of the spiral artery can still respond to autonomic humoral and neural control,(Brosens et al 1977). Maternal pathology resulting in a decreased blood supply to peripheral organs will result in decreased placental supply to the placenta, if the autonomic control of the spiral arteries has been maintained. Therefore, persistent blood flow shunting resulting from a condition such as chronic hypoxia, could result in placental ischemia if trophoblastic invasion is incomplete.

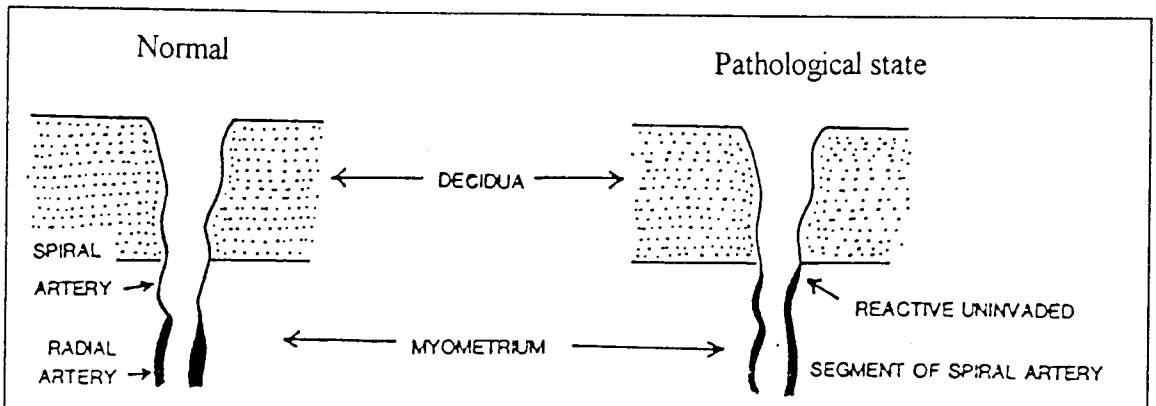

Figure 3-3 Diagrammatic representation of the trophoblastic invasion of the placenta. (Pearce 1988)

The inter-relationship between maternal hypertension, placental ischemia and growth impairment is an extremely complex field, which is presently being considered by many researchers,(Jensen et al. 1991 [Review] , Low, 1991) [Review]) One hypothesis notes placental ischemia to release, amongst other things, free radicals (lipid peroxide) into the maternal circulation. These free radicals are thought to bind to the lipid molecules of endothelial walls and compromise their permeability. Endothelial damage affects the balance of vasodilators and vasoconstrictors. Under normal conditions prostacyclin, a vasodilator, has a higher concentration than thromboxan which is a vasoconstrictor. This allows good perfusion and a reduced maternal blood pressure. If the endothelium is damaged, the existing prostacylins are lost, platelets are laid down and additional thromboxan is released. This further increases the concentration of thromboxan in the maternal circulation, causing extensive vasoconstriction, which ultimately results in an increased maternal blood pressure.

3.7 CLINICAL INTERVENTIONS

Perinatal outcome in GPH depends on the severity of the disease process, gestational age at delivery and the quality of neonatal care. Foetal delivery is advised under pathological conditions such as placental ischemia and severe GPH, and also due to a compromise in maternal health. Delivery before 28 weeks however, is associated with a low foetal survival rate. Consequently, clinical treatment protocols include

administration of steroids to increase the rate of development of the foetus. Several clinical trials have also investigated the effect of optimising the foetal environment in the period before delivery, through maternal hyperoxygenation. (Bertolizio et al, 1966 , Owens et al, 1987 , Nicolaides et al, 1988 , Arduini et al., 1989,1990 , Bekedam et al., 1992 , Meyenburg et al., 1992 , Battaglia et al, 1992 , Fruchter 1994 , Polvi et al., 1995).

Nicolaides reported that during maternal hyperoxgenation the foetal PO_2 rose from well below the 5th centile range to lie within the normal range. Five of the six foetuses in this uncontrolled study survived with little morbidity, whereas in a similar group of foetuses with absent end diastolic flow not receiving oxygen, 85% had severe neonatal complications, (Hackett et al. 1987). Owens et al.(1987) found that maternal hyperoxygenation, with a 50% enriched air mixture, increased the oxygen tension in growth-impaired foetuses to within a normal range. Owens cautioned, however, against using intermittent maternal hyperoxygenation as a form of therapy, as oxygen consumption by the growth impaired foetus was lower in post- than pre-hyperoxemic periods. Battaglia et al. (1992) found significant improvement in Doppler flow waveforms during the treatment of foetal growth impairment with maternal hyperoxygenation. Bekedam et al.(1992) found that maternal hyperoxygenation improved the heart rate variation of growth impaired foetuses, but had no effect on normal foetuses.

Not all investigators agree with the benefit of oxygen treatment. Polvi et al (1995) found a redistribution in the maternal circulation with no detectable effects on the foetus. Arduini et al (1990) found no significant change in the carotid PI index of 36 out of 45 SGA patients investigated. Meyenburg et al.(1992) found the blood flow velocity and blood volume of the foetal aorta to remain unchanged during oxygen administration.

3.8 CLINICAL ASSESSMENT WITH DOPPLER ULTRASOUND

Clinical assessment of growth-impaired foetuses is particularly difficult as the foetal size is not representative of the foetal gestation. Doppler analysis focuses on the

haemodynamic function rather than the foetal size and is thus able to identify the foetuses at risk. Doppler waveforms in any vascular region are related to impedance distal to the point of measurement. A large reduction or total absence of diastolic flow within the umbilical artery velocity waveform, is a distinctly abnormal finding. It identifies a high impedance foeto-placental circulation, rather than the normally low impedance condition

The development of the normal foeto-placental circulation depends on the proliferation and maintenance of small vessels in the secondary and tertiary villi. As the number of villi and vessels increase with gestational age, placental vascular impedance decreases and there is a relative increase in the diastolic component of the umbilical artery. End diastolic velocities are absent in young human foetuses and only appear at about 15 weeks,(Rochelson 1989).

In significant foetal or maternal disease, the small vessels of the placenta either fail to develop or are obliterated, and the end diastolic flow velocity remains low,(Giles et al. 1985 , Trudinger et al. 1987). The most extreme form of this pathologic condition results in the absence and potential reversal of diastolic flow velocity as seen in Figure 3-4 b and c.

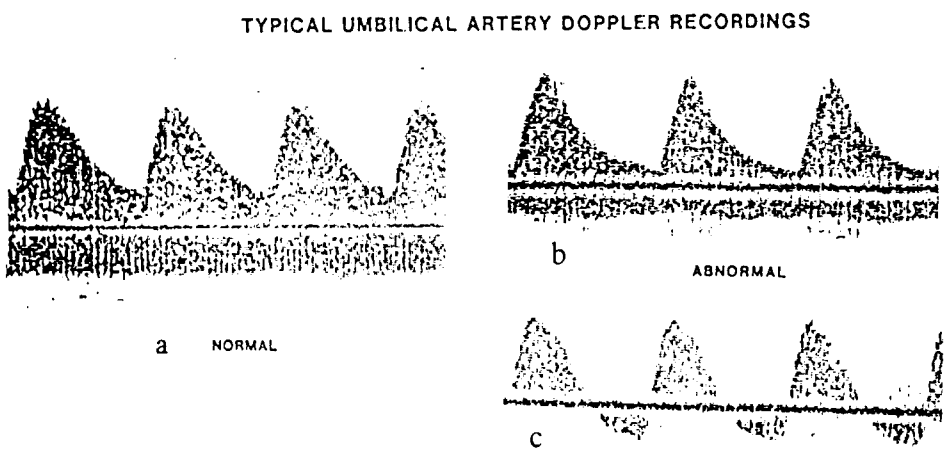

Figure 3-4 Absent end diastolic flow in the umbilical artery. Pearce (1988)

4. A MODEL OF THE FOETAL CIRCULATION

4.1 INTRODUCTION

This chapter presents a model in which the complex haemodynamic system of the foetus was reduced to a simpler functional equivalent. The aim of this model was twofold: firstly, to provide haemodynamic insight into the arterial circulation of a 28 week old foetus, and secondly, to gain an understanding of the physiological variables that affect the umbilical arterial blood flow velocity waveform.

Modelling of blood flow under different foetal conditions has been well substantiated with non-invasive Doppler measurements. The model presented in this chapter was based on anatomical and parametric data gathered by researchers such as Thompson & Trudinger (1990) who investigated pressure and flow in the placental circulation; Guiot & Todros (1992) who modelled the foeto-placental unit; Huikeshoven et al. (1985) for mathematical modelling of the foetal circulation; Mo et al. (1988) who investigated modelling using transmission line theory; and Jager et al. (1965) for modelling pulsatile flow in the arterial system.

This chapter describes a model that simplifies the foetal circulation into anatomically appropriate units. Each unit is modelled using electrical analogies in order to derive a single expression which characterises the arterial system.

4.2 FUNCTIONAL SIMPLIFICATIONS OF THE FOETAL CIRCULATION

Chapter two describes the normal foetal circulation in detail. The complex circulatory system shown in Figure 4-1a was simplified by dividing it into three functional units, namely the foetal heart, visceral vessels and the placenta.

A cross-sectional diagram of the foetal heart is shown in Figure 2-2a. The foetal heart could be simplified to a single flow source since the ductus arteriosus and the aortic arch have similar dimensions, and the two ventricles could be assumed to have equal output volumes and mean pressures, (Dawes , 1968 , DeMuylder et al. , 1984).

The foetal vasculature, Figure 4-1a, was reduced to a simplified equivalent consisting of several vessels branching off the aorta, Figure 4-1b. The vessels supplying blood to the cerebral and myocardial tissue were grouped into a single branch off the aorta labelled HAH (head and heart). Vessels supplying blood to the upper-body, thorax, abdomen and adrenal glands were simplified by three staggered branches off the descending aorta, labelled THR (upper-body and thorax), ABD (abdomen) and ADR (adrenals) respectively. The external iliac, superior gluteal and ischiadic arteries were grouped into a single vessel supplying the lower body (BODY), Figure 4-1b. Finally, the two umbilical arterial vessels which supply blood to the placenta were simplified by a single functional vessel labelled UMB (umbilical). This was considered an appropriate approximation since the umbilical vessels anastomose before branching into the radial arteries, (Thompson & Trudinger, 1990).

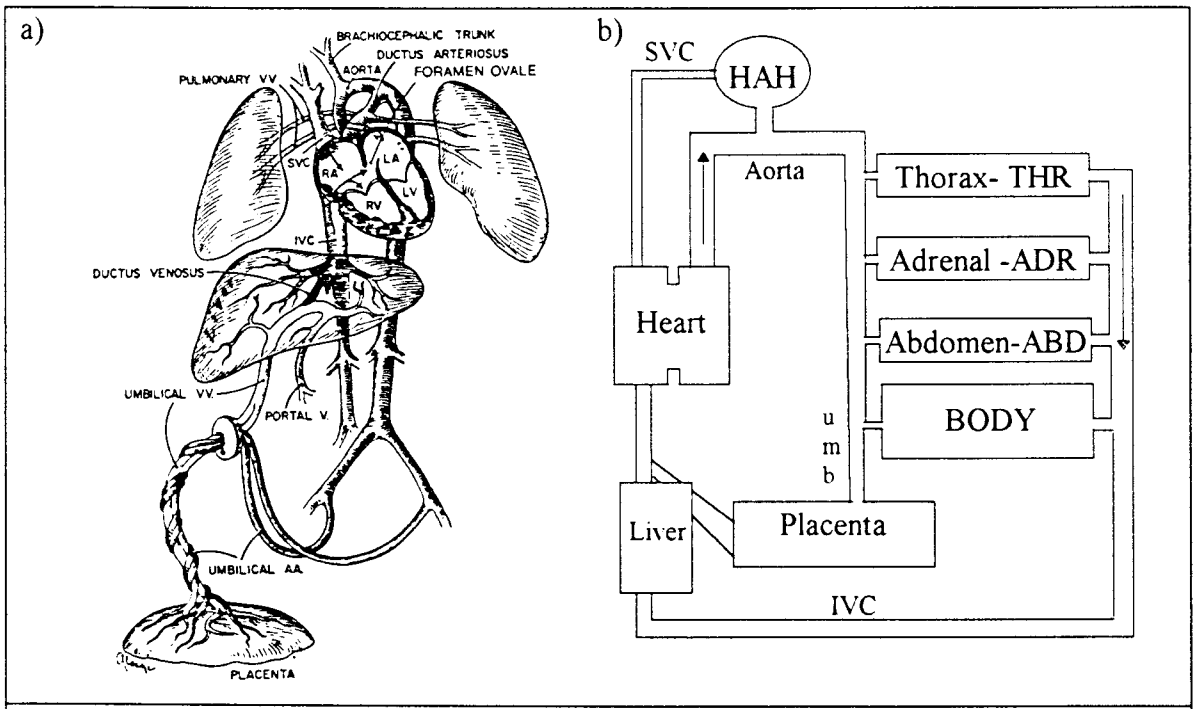

Figure 4-1 Arterial simplification of the foetal arterial system

The simplified arterial structure as shown in Figure 4-1b, was translated into its electrical equivalent, Figure 4-2, by substituting each functional unit with its electrical equivalent. The foetal heart was simplified by a single flow source and the visceral vessels and placenta approximated by appropriate impedance units.

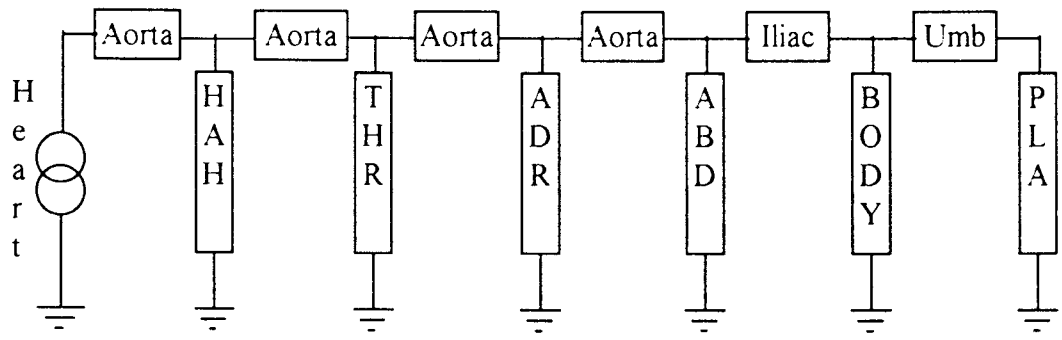

Figure 4-2 Electrical representation of the simplified foetal circulation.
LegendFlow ⊖ source - foetal heart
□ Impedance unit - visceral vessels and terminating placenta

4.3 AN ANALOGOUS ELECTRICAL MODEL

The researchers mentioned in the introduction have used various modelling techniques to approximate the foetal circulation. One of these techniques is the distributed parameter approach which has been used extensively in modelling the arterial system of the human leg (Skidmore et al., 1980), and more recently, has been applied to foeto-maternal circulation by Mo et al (1988) and Thompson & Stevens (1989).

An artery can be viewed as a continuous series of distributed units each consisting of inertive, conductive, compliant and resistive elements. These elements can be represented electrically by inductive (L), conductive (G), capacitive (C) and resistive (R) components respectively, illustrated in Figure 4-4. With this approach, the voltage and current in the electrical circuit is analogous to the blood pressure and flow in the arterial system. The advantage of using such a modelling technique, is that circuit and transmission line theory can be applied to the human vasculature.

Blood flow in the umbilical arteries can be considered analogous to current flow in an electrical transmission line, (Mo et al., 1988). Any change in pressure or flow along the arterial vessel can be described, using transmission line theory, as an analogous change in voltage or current along the transmission line.

The model presented in this chapter uses two types of vascular segments. The first, shown in Figure 4-4, models vessels that carry blood to the placenta. This category was found to account for the change in flow profile shape due to transmission effects, such as friction and compliance. The second vascular segment, shown in Figure C-2b, models a 'bleed-off' resistance which conducts blood away from the placenta to other organs. In this model individual organs were collectively grouped into regions for example the thorax (THR) and the abdomen (ABD). The magnitude of the bleed-off resistance was determined from the proportion of the total cardiac output supplied to that region. The larger the resistance, the less the percentage cardiac output conducted to that region. This modelling technique

enabled preferential blood flow shunting to be investigated by suitably adjusting the size of the bleed-off resistances. This technique is considered in greater detail in Appendix F.

The electrical approximation of the foetal circulation enabled circuit simplification techniques to be used. These techniques allowed the branching arterial structure to be reduced to an equivalent circuit representing all the characteristics of the arterial system. The circuit analysis technique particularly suited to this type of modelling is two port analysis, which enabled all the vascular units to be cascaded into a single expression.

4.3.1 AN ELECTRICAL EQUIVALENT OF A SHORT SEGMENT OF VESSEL

If the radial dimensions of a vessel are small compared with the minimum wavelength travelling down the vessel and the vessel has thin elastic walls it is possible to assign equivalent electrical properties to a short section along the vessel axis,(Bunn ,1980). These conditions specified by Bunn are valid when approximating foetal arterial vessels, inferring that the resistive, inertive, compliant and conductive components of the vessels can be described in terms of their electrical properties.

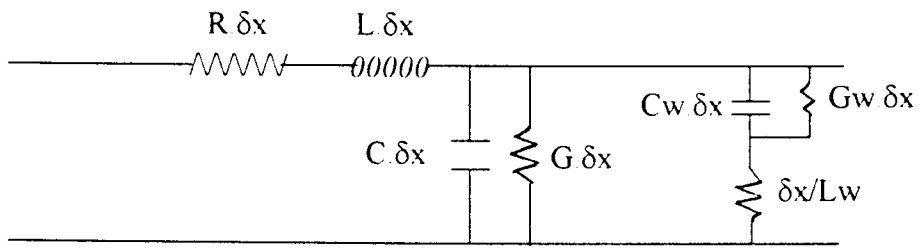

Figure 4-3 Analogous electrical circuit for vessel segment of length δx.

The circuit in Figure 4-3 can be reduced to the simplified but mathematically equivalent form shown in Figure 4-4. The electrical analogous terms used to describe each of these segments are defined in Table 4-1.

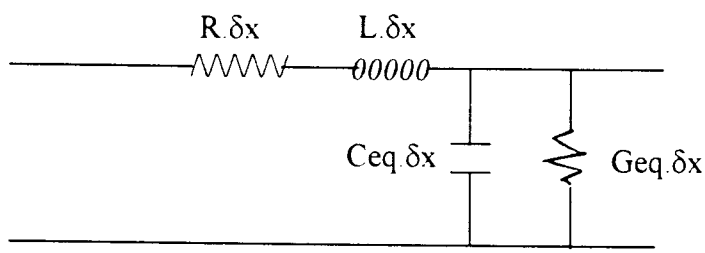

Figure 4-4 Equivalent electrical circuit for vessel segment of length δx

Table 4-1 Electrical definitions of flow parameters

x-	Length along vessel axis
R-	Frictional resistance to longitudinal fluid motion / unit length
L-	Longitudinal inertance/unit length of blood in the vessel
G-	Leakage conductance/unit length of blood in the vessel
C-	Volume compliance/unit length of blood within the vessel
Gw-	Leakage conductance in the wall/unit length of vessel
Cw-	Volume compliance/unit length of the vessel wall
1 Lw-	Reciprocal inertance per unit length of the tube wall
Geq-	Equivalent leakage conductance/unit length of blood in the vessel and the wall
Ceq-	Equivalent volume compliance/unit length of vessel wall

The resistive, inductive, capacitive and conductive parameters used to define an electrical analogous circuit are mathematically described below.

1. **Resistance** results from friction against the vessel walls and viscosity of the fluid. Under steady state conditions, when parabolic flow can be maintained, the resistance per unit length(R) is defined by Poiseuille's equation.

$$R = \frac{8.\mu}{\pi.r^4} \qquad \mu \text{ - fluid viscosity} \qquad \text{Equ 4-1}$$

2. **Inductance** - represents the axial blood inertance (L) in the vessel and transverse inertance (Lw) of the pulsating wall. Inertance is defined as the ratio of mass to area^2. Under steady-state parabolic flow conditions, Equ 4-2,3 describe the per unit length axial and transverse inertances respectively.

$$L = 1.35\frac{\rho}{\pi . r^2}$$ ρ - fluid density Equ 4-2

$$Lw = \frac{\rho . h}{2\pi . r} + \frac{\rho}{8\pi}$$ h - vessel wall thickness Equ 4-3

3. **Capacitance** - represents the per unit length volume compliance of the blood (C) and the vessel wall compliance (Cw). Capacitance is defined as the ratio of volume to bulk modulus (Kb) and can be described by Equ's 4-4,5 under steady state flow conditions.

$$C = \frac{\pi . r^2}{\mathrm{Kb}}$$ σ - Poisson ratio - wall Equ 4-4

$$Cw = \frac{2 . \pi . r^3 . \left(1 - \sigma^2\right)}{E . h}$$ E - Young's Modulus Equ 4-5

4. **Conductance** (G) depends on hysterisis losses in the vessel wall. Scaling factor k depends on the extent of the hysterisis losses.

$$G = k . 2\pi . f$$ Equ 4-6

Wall inertance (Lw), compliance (Cw), fluid compliance (C) and conductance (G) can be mathematically reduced to an equivalent compliance (Ceq) and conductance (Geq). Bunn (1980)

$$Ceq = \left[\frac{Cw . \left(1 - \omega^2 . Lw . Cw\right) - G^2 . Lw}{\left(1 - \omega^2 . Lw . Cw\right) + G^2 . \omega^2 . Lw^2} + C\right]$$ Equ 4-7

$$Geq = \left[\frac{G}{\left(1 - \omega^2 . Lw . Cw\right) + G^2 . \omega^2 . Lw^2} \right] \qquad \text{Equ 4-8}$$

The electrical parameters Equ 4-1 to 4-8 are defined per unit length and need to be multiplied by the actual length of each segment in order to determine the absolute value of each electrical parameter. The length of these segments are determined in Appendix A, from the wavelength present in the vessel.

4.3.2 NON-PARABOLIC BLOOD FLOW CONSIDERATIONS

The calculation of flow resistance as derived by Poiseuille (Equ 4-1) depends on steady parabolic flow. In arteries close to the heart, however, it is not possible to maintain this condition as flow is periodically disturbed by a heart beat and time is required to re-establish parabolic flow conditions. Blood flow is therefore not parabolic during the entire cardiac cycle and it is necessary to accommodate this factor when assessing resistance to flow in arteries.

Wormersley (1957), cited in McDonald (1974), solved a linearised form of the Navier-Stokes equations to derive a mathematical expression for the relationship between flow and pressure gradient of non-parabolic flow in an elastic tube. He introduced a frequency dependent dimensionless parameter alpha (α) which describes the flow profile within the vessel and is considered in greater detail in Appendix E.

$$\text{alpha } (\alpha) = r \sqrt{\frac{\omega}{\nu}} \qquad \text{Equ 4-9}$$

Alpha is a function of vessel radius (r), fundamental frequency (ω) and kinematic viscosity* (ν). Normalised flow resistance and fluid inertance are graphed against alpha in Figure 4-5.

* Kinematic viscosity - ratio of viscosity μ and blood density ρ in units of Stokes ($cm^2.sec^{-1}$).

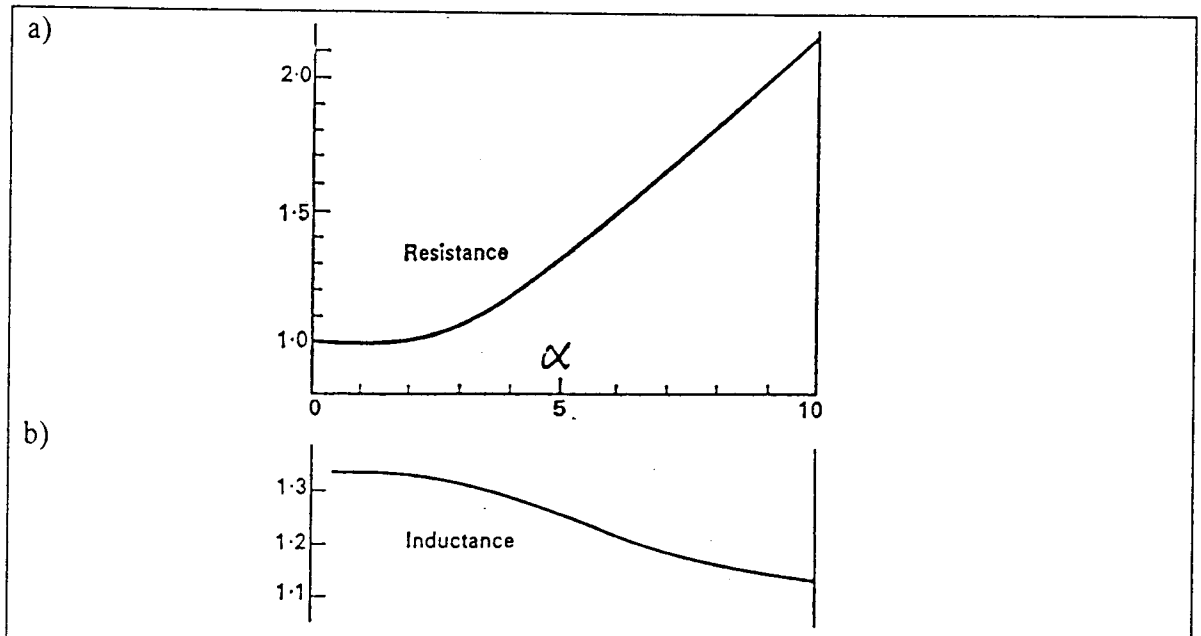

Figure 4-5 Resistance and inductance scaling factors for different alpha values. McDonald (1974)

When the profile in the vessel is approximately parabolic, alpha is small and the effect on the flow resistance is negligible. The further the profile tends towards plug flow the higher the alpha value and the greater the effect on the flow resistance. This is shown in Figure 4-5a. The inertance decreases to a constant level as the pulsatility of the waveform increases, as shown in Figure 4-5b.

4.3.3 THE APPROXIMATION FOR THE FOETAL HEART

The average mass of a human foetus aged 28-30 weeks is 1.1(±0.2)kg (Sabbagha et al.(1989), Theron & Thompson ,1995). The foetal cardiac output according to Polin & Fox (1992), is approximately 330 $ml.min^{-1}\ kg^{-1}$ for a normal foetus and thus the average cardiac output was calculated as $360ml.min^{-1}$ or $6cm^3.sec^{-1}$. The volume ejected from the heart on each heart beat, known as the stroke volume, is given by

$$\text{Stroke Volume} = \frac{\text{total cardiac output}}{\text{number of heart beats}} \qquad \text{Equ 4-10}$$

The stroke volume, for an average heart rate of 140bpm was therefore about 2.6ml.

Veth (1976) and Raymond & Whitfield (1987) give the mean systolic time interval (STI) as approximately 0.2sec for a normal foetus of 28 weeks. Blood flow resulting from myocardial contraction occurs during only this time. Therefore, the average flow expected during contraction in the proximal aorta is approximately $13cm^3.sec^{-1}$.

The exact flow profile in the proximal aorta is unknown. A profile approximation was determined from the flow information given above by assuming the systolic rise time to be a quarter of the systolic time interval.

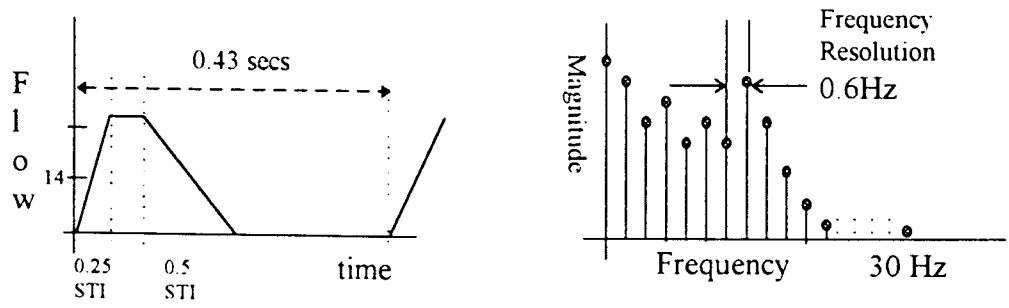

Figure 4-6 Proximal aorta flow profile and corresponding frequency spectrum.

The flow profile consists of a number of frequencies which can be calculated using the FFT. The aortic blood flow waveform and its frequency domain equivalent are shown in Figure 4-6. When this signal is used as an input to the analogous frequency model, each frequency present has to be considered independently because of the frequency dependence of the vascular segments. The resultant output flow waveform can be determined from the sum of model outputs caused by each of the individual input frequencies,(Skidmore et al , 1980).

4.3.4 PLACENTAL VASCULAR APPROXIMATION

This model based its approximation of the placenta on the representation used by Thompson & Trudinger (1990). They considered the placenta as a lumped equivalent circuit with the electrical parameters being calculated from the dimensions and characteristics of the placental vessels.

This model used the same simplification technique and approximated the multi-level branching of the placenta, as seen in Figure 2-4, by separate parallel vascular units. The umbilical artery was assumed to branch into N separate vascular units or lobes, with each lobe consisting of M smaller tertiary stem villi (TSV). The total number of terminating placental villi is therefore equal to the product of M and N. The approximated branching structure of the placental bed is shown in Figure 4-7a.

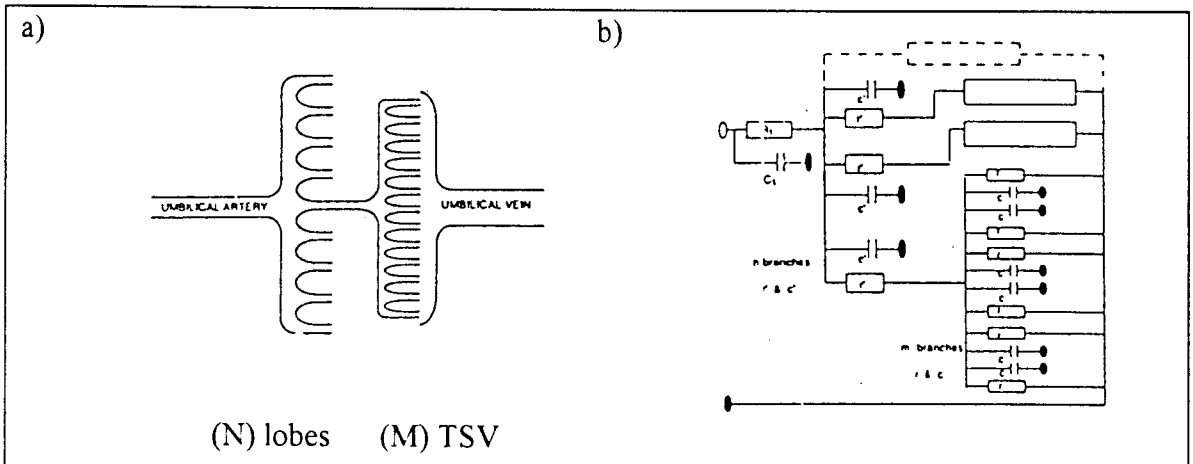

Figure 4-7 Schematic representation of the placental branching structure and equivalent circuit (Thompson and Trudinger 1990).

Placental lobes and the corresponding TSV were represented purely by resistive and capacitive units as blood flow in the umbilical arteries was determined to be quasi-steady, Figure 4-7b. Quasi-steady flow describes the state where the flow velocity profile in an artery remains parabolic, (Thompson & Stevens, 1989). Under these conditions flow is thought to be dominated by viscous, rather than inertial, forces. The inertive component is thus ignored, (McDonald, 1974).

The compliance and resistance of the placental lobes and tertiary stem villi are calculated according to Equ 4-11 and 4-12. Rp is the equivalent resistance of the placenta as a result of vessel branching and is described by

$$Rp = \frac{R + \frac{r}{M}}{N} = \frac{(R.M + r)}{M.N} \qquad \text{Equ 4-11}$$

Rp = placental resistance

R = primary stem villi resistance

r = tertiary stem villi resistance

Similarly Cp is the equivalent compliance of the placenta and is described by

$$Cp = N.C + N.M.c \qquad \text{Equ 4-12}$$

Cp = placental compliance

C = primary and secondary stem villi compliance

c = tertiary stem villi compliance

The placenta is the final component of the model and is represented by it's equivalent circuit in Figure 4-8.

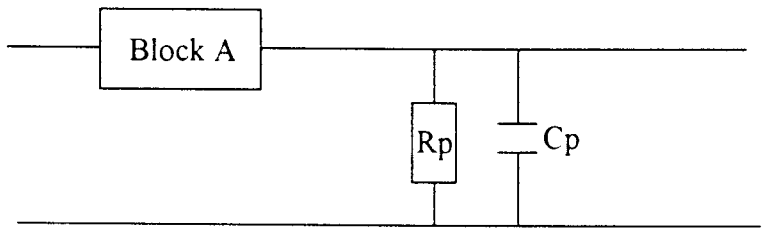

Figure 4-8 A lumped parameter equivalent circuit representing the placental vessels. (Thompson and Stevens, 1989).

Block A represents the combined resistance, compliance, conductance and inertance for the umbilical and radial arteries. Each lobe corresponding to primary or secondary stem villi is represented by a resistance (R) and compliance (C). Each lobule has M smaller TSV consisting of resistance (r) and compliance (c) terms.

4.4 TWO PORT ANALYSIS

Two port parameters, as defined in Appendix C, were used to replace each of the electrical circuits in Figure 4-4 and Figure C-2a. The advantage of this analysis technique, is that once each block has been described in terms of its A parameter matrix, successive blocks can be cascaded by matrix multiplication of their corresponding A parameter matrices.

The cascade parameters are described in their matrix format below. In this format, it is possible to cascade successive blocks since the voltage and current output of one block can be viewed as the voltage and current input of the adjacent block. For each successive block, the product of the two cascade parameter matrices results in a combined 2x2 cascade matrix representing all the segments cascaded thus far.

$$\begin{bmatrix} Vin \\ Iin \end{bmatrix} = \begin{bmatrix} A_{11} & A_{12} \\ A_{21} & A_{22} \end{bmatrix} * \begin{bmatrix} Vout \\ -Iout \end{bmatrix} \qquad \text{Equ 4-13}$$

By applying two port analysis to the arterial vessels, it was possible to define a current or analogous flow transfer function dependent only on the characteristics or dimensions of the arterial vessels This function, $1/(A_{21}.Z_{placenta}^{*} + A_{22})$, defined in Appendix C made it possible to alter both the input flow waveform from the heart, and the dimensions and characteristics of the arterial vessels, in order to observe their effect on the umbilical blood flow waveform.

* Placental impedance

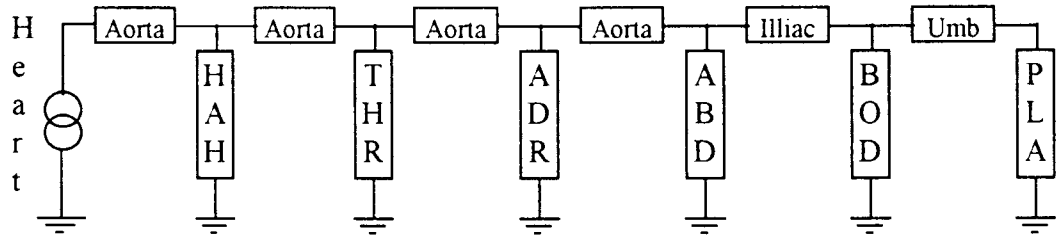

$$\begin{bmatrix} A_{11} & A_{12} \\ A_{21} & A_{22} \end{bmatrix} = [A_{Aorta}]*[A_{HAH}]*[A_{Aorta}]*[A_{Thorax}]*[A_{Aorta}]*[A_{Adrenal}]*[A_{Aorta}]*$$

$$[A_{Abdomen}]*[A_{Illiac}]^2*[A_{Body}]*[A_{Umbilical}]^8*[A_{Placenta}]$$

Figure 4-9 Two port analysis parameter for the foetal arterial forward flow transfer function (A_{22}).

Figure 4-9 shows how the electrical approximations of the foetal arterial vessels were simplified by the sequential multiplication of their corresponding A parameter matrices. A long vessel, for example the umbilical artery, is represented by several impedance units.

4.5 TRANSFER FUNCTION ANALYSIS

The transfer function of any system can be determined by investigating the relationship between the system's input and the system's output at discrete frequency increments. A comparison of the input and output signals describe the attributes of the system through which the input signal has been passed.

The flow transfer function of the arterial vessels was represented by the two port parameter $1/A_{22}$ (Equ4-9) which incorporated all the frequency dependent terms approximating vessel resistance, inertance, capacitance and conductance. The vessel transfer function was determined for a range of frequencies (0-30Hz) in increments of 0.6Hz.

The Fast Fourier Transform (FFT) was used to determine the frequency spectrum of the input pulse from the heart (Figure 4-6). A sampling frequency was chosen to ensure 256 samples in any one cardiac cycle with a normal frequency of 140 beats per minute. The input waveform could subsequently be transformed (Appendix D) to its frequency equivalent with a resolution of 0.6Hz.

The output spectrum of the system was determined from the product of the input spectrum and the arterial transfer function for each successive frequency increments of 0.6Hz. Hoskins et al.(1991) and Skidmore et al. (1980) demonstrated that the conditions required for system linearity were maintained for periods longer than that of the heart beat, consequently the output spectrum could be assumed as a linear sum of the individual input spectrums.

As a result of system linearity, the Inverse Fourier Transform (IFT) was determined to calculate the time equivalent output waveform. The details of the spectral analysis are dealt with in Appendix D. A flow diagram illustrating how the output waveform was obtained is shown Figure 4-10.

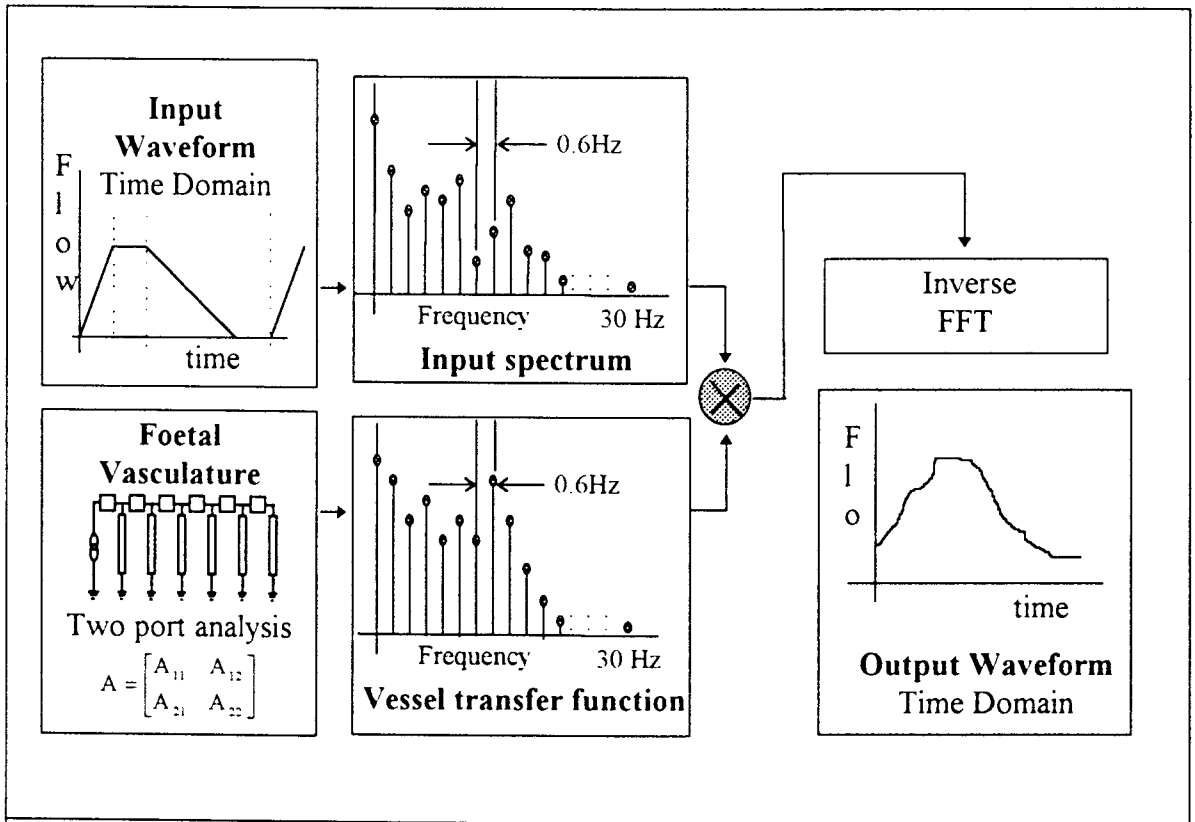

Figure 4-10 Flow diagram of the output flow waveform generation.

Figure 4-10 illustrates how the input waveform was Fast Fourier transformed (FFT) into the frequency domain with a frequency resolution of 0.6Hz and a maximum frequency component of 30Hz. The current transfer function of the foetal vasculature was determined using two port parameter analysis, also with a frequency resolution of 0.6Hz and a maximum frequency component of 30Hz. Each set of corresponding frequency components were multiplied together before being Inverse Fast Fourier transformed (IFFT) back into the time domain. The resultant waveform was a function of the input signal from the heart and the characteristics of the foetal vasculature.

4.6 NORMAL DATA RANGES AND VESSEL DIMENSIONS

Data in the following tables was used in the equations described in this chapter, to determine all the parameters needed to model the foetal circulation. All constants are given in the symbols list and abbreviations on page xv.

FOETAL DATA

Gestational age	- 28 weeks
Foetal weight	- 1.1 kg
Heart rate	- 140bpm
Cardiac output	- 330ml/min/kg

MODEL CONSTANTS

μ	- 0.03 dyne.s/cm^2
Kb	- 8 x 10^7 dyne/cm^2
ρ	- 1.06 g/cm^3
σ	- 0.47
k	- 0.15

VESSEL DIMENSIONS

The frequency response of the arterial system is assumed to depend only on the vessel parameters described below because arterial stiffening or disease is assumed absent in normal foetuses. Normal, human foetal vessel dimensions were gathered from Chen et al. (1988) and from post mortem studies Wright (1994).

Table 4-2 Vessel dimensions of relevant foetal arterial vessels for normal foetuses of 28-30 weeks gestation. These values were used in Table A-1 to determine the segment lengths.

Vessel	Aorta	Common iliac artery	Umbilical artery
radius (cm)	0.32	0.14	0.11
length (cm)	7.5	1.2	19.1
vessel thickness(cm)	0.028	0.006	0.001
Young's modulus (dyn.cm^{-2})	1E7	1.3E7	1E7

PLACENTAL APPROXIMATIONS

Table 4-3 Properties and dimensions of a normal placenta (Thompson & Stevens 1989).

Vessel	Primary and secondary stem villi (N)	Tertiary stem villi (M)
radius (cm)	0.02	0.001
length (cm)	4	1
vessel thickness(cm)	0.01	0.008
Young's modulus(dyn.cm^{-2})	5E6	5E6

Table 4-4 Ranges used for lobes and TSV of the placenta.

	Small Placenta	Large Placenta
Number of lobes (N)	10	20
Number of TSV (M)	50	200

ARTERIAL PRESSURE INPUT

Systolic blood pressure - 80mmHg

Diastolic blood pressure - 50mmHg

Average blood pressure - 60mmHg

4.7 FOETAL MODEL

Using the electrical representation of the vessel segments, an equivalent circuit has been described for the foetal circulation. The normal values shown in Table 4-2,3,4 were substituted for Equ's 4-1,8 and the actual vessel parameters calculated. With this representation, the normal flow waveform in the umbilical artery could be calculated. In the next chapter the normal flow waveform is validated, and the effect of changes in the normal foetal circulation investigated.

5. SIMULATIONS OF FOETAL BLOOD FLOW UNDER HYPOXIC CONDITIONS

5.1 INTRODUCTION

Doppler analysis makes non-invasive determination of the umbilical arterial blood flow waveform possible. The flow waveform has a characteristic shape that can be characterised clinically by the pulsatility index (PI). Foetal compromise causes a change in the umbilical blood flow and hence, a change in the associated pulsatility index. Monitoring of the PI, and other indices that characterise the waveform shape, has therefore been proposed as a method for screening high risk foetuses.

Contractility of the foetal heart, morphology of the arterial system, impedance to flow within the placenta and redistribution of blood flow are some of the factors that could influence the shape of the flow waveform. Many of these factors have been investigated clinically or using animal models. It is, however, difficult to perform the necessary experiments in this way. The use of an equivalent model provides a very effective and flexible tool to isolate and investigate individual factors which affect the umbilical flow waveform.

The model described in chapter four is a functional electrical analogous model of the foetal circulation which is based on the average arterial dimensions and blood flow rates present in a 28 week old foetus. This chapter describes simulations performed with the model, firstly to calculate the PI for normal foetuses and, secondly to investigate how the PI is affected by changes to the model parameters.

5.2 METHODS

5.2.1 MODEL VALIDATION FOR A NORMAL 28 WEEK OLD FOETUS

The model, configured for a normal 28 week old foetus, was used to simulate the umbilical blood flow over a time period corresponding to a single cardiac cycle. This flow-versus-time-waveform, generated by the model, was processed by an algorithm to calculate the PI. The PI value was then compared with clinical measurements of the umbilical PI on a population of healthy foetuses.

5.2.2 THE EFFECT OF NON-PARABOLIC FLOW ON THE UMBILICAL PI.

The purpose of this experiment was to estimate the effect of the flow profile on the umbilical PI. The effect of non-parabolic flow was assessed by substituting the steady state impedance and inertance terms defined in Equations 4-1,2, with their non-parabolic flow equivalents given in Equations E-1,2. In this way, waveforms generated using a mathematically complex, non-parabolic flow model could be compared to waveforms generated using a simpler parabolic flow model.

5.2.3 THE EFFECT OF HEART PULSATILITY ON THE UMBILICAL PI

The pulsatility of the blood flow waveform from the heart was characterised by three parameters: (i) the high frequency components (ii) the flow profile shape and (iii) the systolic rise and diastolic fall times.

5.2.3.1 WAVEFORM FILTERING OF HIGH FREQUENCY COMPONENTS

Several input waveforms are shown in Table 5-2. Graph (a) is used in the model as the heart input flow pulse; it has a systolic interval of 0.18 sec, a period of 0.43sec and a peak flow of 20 $cm^3.sec^{-1}$. The effect of high frequency components was investigated by increasing the degree of input waveform filtering. A range of cut-off frequencies (15-6Hz)

was chosen to filter this flow waveform, thereby removing the higher frequency components.

5.2.3.2 HEART FLOW PROFILE

Four piece wise linear[1] approximations of the foetal heart flow pulse are shown in Table 5-3. All proposed waveforms had equal stroke volumes and equal systolic time intervals (STI) as these were assumed constant. The waveforms ranged from a step input function to triangular function, which has a steep systolic rise time (33% STI) and a slower falling diastolic interval (66% STI). The two centre waveforms are extrapolated from these two extremes by adjusting the magnitude and period of peak flow. The umbilical PI for each input waveform shown in Table 5-3, was compared to investigate the indices' dependence on the cardiac flow waveform.

5.2.3.3 SYSTOLIC AND DIASTOLIC TIME INTERVALS

The peak flow of the cardiac waveform was moved in time increments of 0.1STI from 0.1STI to 0.5STI as shown in Table 5-4. By adjusting the fraction of the cardiac cycle during which systolic flow occurs, the effect of systolic rise and diastolic fall times on the umbilical PI was investigated.

5.2.4 THE EFFECT OF PLACENTAL BLOOD DISTRIBUTION ON THE PI

Chronic foetal hypoxia can result in a decrease of the placental cross sectional area over which oxygen and nutrient transfer can take place. This exchange occurs predominantly within the terminating villi of the placenta. Processes such as vessel constriction and embolisation reduce the placental cross sectional area available for exchange. The aetiology and inter-relationship of each of these processes are currently under investigation (section 3.4). Regardless of the actual patho-physiological processes involved, however, the impedance to placental blood flow increases, and the corresponding vessel compliance decreases, when the placental cross sectional area is reduced.

The placenta consists of a number of parallel branching networks of arteries which form separate vascular units. For this study, the complex multiple branching of the placental vessels was simplified, in the same way as Thompson & Trudinger (1990), by modelling the placenta with N lobes which each branch into M lobules, shown in Figure 4-7.

Scaling factor N, represents the number of lobes or primary and secondary stem villi within the placenta, and factor M, the number of tertiary stem villi (TSV) contained within each lobe. The total number of terminating villi in the model is therefore equal to the product of M and N. This model investigated the effect of an increase in placental impedance by decreasing the number of terminating villi of the placental vasculature.

The model assumed a normal number of lobes (N=74) and set the placental size according to the number of lobules per lobe. A large placenta has approximately 200 lobules per lobe, a normal placenta 120-140 lobules/lobe whereas, a small placenta has approximately 80 lobules per lobe.

The effect of small vessel obliteration on the umbilical blood flow waveform was investigated for different placental sizes. In order to simulate five different sized placentae, the number of lobules/lobe were reduced from 650 down to 240, in decrements of 180. For each placental size the number of terminal villi (MxN) available to conduct flow were decreased until only 3% remained. The umbilical blood flow waveform was extracted from the model for each iteration, and the PI calculated from this waveform.

5.2.5 PREFERENTIAL BLOOD FLOW SHUNTING ON THE UMBILICAL PI

The foetal circulation has a large reserve capacity to carry and extract oxygen. If the foetus is exposed to conditions that deprive it of oxygen, it will utilise this reserve capacity in an attempt to maintain normal oxygen delivery. Chronic exposure to such conditions depletes this reserve and physiological development of the foetus is impaired. A foetus in

[1] Any complex waveform can be approximated by successive straight line sections. The shorter the line

this condition has to employ appropriate physiological responses to overcome the resulting hypoxic conditions.

Blood flow shunting is one such response which occurs in the presence of extensive placental insufficiency. By suitably adjusting the impedance of the peripheral and central organs, the foetus is able to augment blood flow to the brain, heart and adrenals, whilst blood flow to the gut, kidneys and carcass is reduced. A threshold level is reached, however, where physiological mechanisms cannot maintain oxygen delivery to the heart and brain, and compensation fails,(Field et al. 1990).

This study used the results of investigations into the circulation of foetal sheep, to assess the effect of blood flow shunting, and its failure, on the umbilical blood flow waveform.

sections used. the more accurate the approximation.

5.3 RESULTS

5.3.1 UMBILICAL BLOOD FLOW FOR A NORMAL 28 WEEK OLD FOETUS

Figure 5-1 shows, on common axes, a simulated maximum umbilical flow waveform and a clinical umbilical sonogram for a normal 28 week old foetus. The simulated maximum umbilical flow waveform corresponds well with the clinically obtained sonogram for a normal foetus. The PI calculated from the simulated waveform (PI=0.94) was well within the standard deviation of the normal population, as seen in Table 2-2, when compared to the PI of the clinical waveform (PI=1.3±0.3),(Reed et al. 1987).

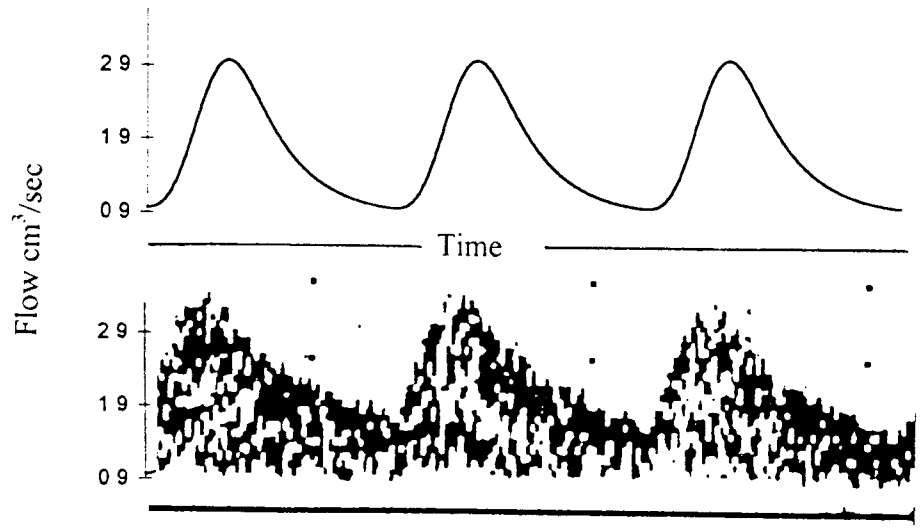

Figure 5-1 Measured and modelled umbilical flow waveforms. Reed et al. (1987)

5.3.2 THE EFFECT OF NON-PARABOLIC FLOW ON THE UMBILICAL PI.

The flow distribution percentages given in Table 5-1 are taken from Block et al. (1984). They represent a range of flow conditions, beginning with normal flow and tending towards obstructed flow due to increased placental impedance

Regardless of whether the non-parabolic flow equations E-1,2 or the parabolic flow equations 4-1,2 were used, the PI increased with a deterioration in foetal condition. The

relative difference between the PI for non-parabolic flow and the PI for parabolic flow also increased when the foetal condition deteriorated. This fractional change (less than 1%), is insignificant, however, when compared to the normal PI ranges (Table 2-2). The complex mathematical model that accommodates non-parabolic flow is therefore unnecessary and can, according to the simplifications and assumptions of this model, be replaced by its simpler parabolic equivalent.

Table 5-1 Comparison of PI when including or neglecting non-parabolic flow.

PERCENTAGE FLOW DISTRIBUTIONS							PI	PI
	HAH %	PLAC %	THOR %	ABD %	ADR %	BODY %	parabolic flow	non-parabolic flow
1	4.9	40.0	8.0	8.7	0.1	38.4	1.351	1.351
2	9.8	45.2	6.0	7.7	0.2	35.6	1.024	1.026
3	9.8	31.2	6.6	11.6	0.2	41.7	2.065	2.068
4	17.2	32.2	4.5	10.4	0.4	35.6	1.965	1.970

5.3.3 THE EFFECT OF HEART PULSATILITY ON THE UMBILICAL PI.

In this section three simulations permitted the effect of different heart parameters on the umbilical PI to be investigated. Each simulation was conducted under normal and hypoxic flow conditions obtained from the distributions measured by Block et al.(1984), condition number 4 in Table 5-1.

5.3.3.1 HIGH FREQUENCY CONTENT OF THE HEART FLOW WAVEFORM

Table 5-2 shows the filtered flow waveforms, cut-off frequencies and corresponding PI indices for normal and hypoxic flow conditions.

2nd order low pass Butterworth filtering of the input waveform

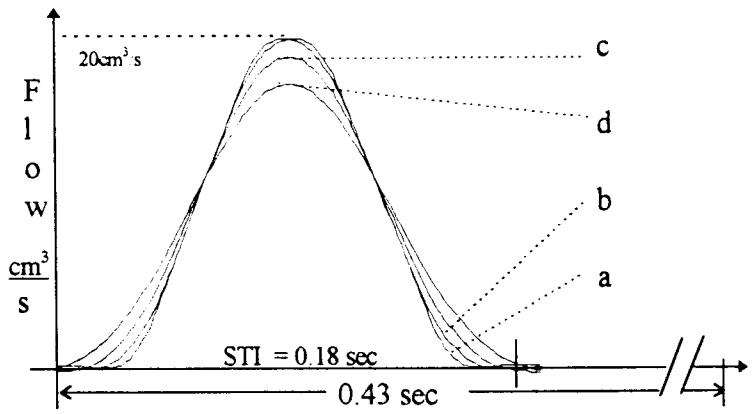

	C/O freq (Hz)	PI Norm	PI Hypo
a	15	0.85	1.40
b	12	0.84	1.40
c	9	0.83	1.37
d	6	0.80	1.32

Table 5-2 Smoothing of the heart flow waveform

Norm - Normal circulatory conditions; Hypo - hypoxic circulatory conditions;
C/O freq - Filter cut-off frequency

As the cut-off frequency of the second order filter was decreased in 3Hz decrements from 15Hz to 6Hz, the total change in PI was 5.8% and 5.7% respectively for normal and hypoxic flow. These small changes showed the umbilical PI to be insensitive to the high frequency content of the heart flow waveform, regardless of the foetal condition.

5.3.3.2 HEART FLOW WAVEFORM SHAPE

Table 5-3 shows the approximations to the heart waveform shape and their corresponding umbilical PI's for normal and hypoxic flow conditions.

Piece wise linear approximations to the heart flow pulse

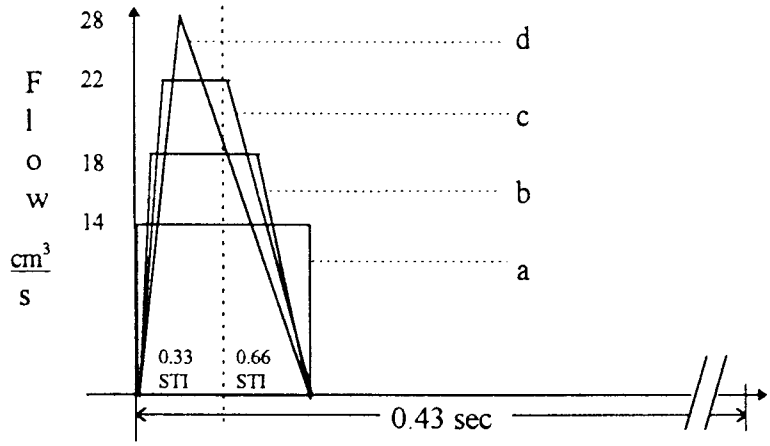

	PI Norm	PI Hypo
a	0.77	1.34
b	0.83	1.47
c	0.85	1.50
d	0.84	1.49

Table 5-3 Input waveform profile and corresponding PI's

Waveforms (a) - (d) are a range of physiologically appropriate heart flow waveform shapes. The actual heart flow shape would best be approximated by waveform (b) or (c) as the sharp decrease of flow in (a) and the instantneous increase of flow in (d) would not be physically realisable. The change in PI was found to be small with respect to the changes which result from hypoxia.

5.3.3.3 SYSTOLIC AND DIASTOLIC TIME INTERVALS

Table 5-4 compares the PI with the fraction of the STI required for the systolic blood flow peak to be reached. In graph a) the systolic rise time is equal to 0.1STI, as compared with graph e) which has a systolic rise time equal to 0.5STI.

Variable systolic rise and diastolic fall times of the heart flow profile

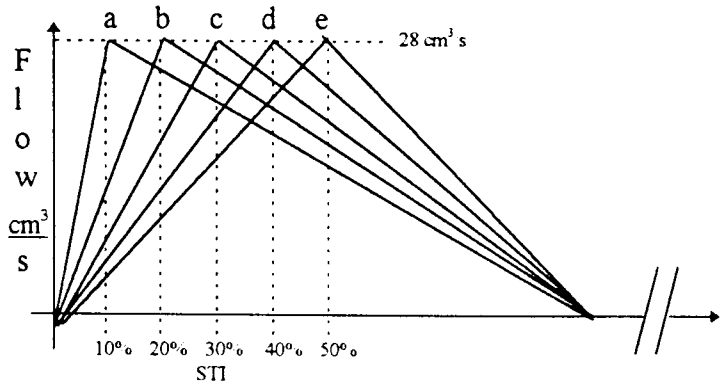

	PI Norm	PI Hypo
a	0.85	1.41
b	0.84	1.39
c	0.83	1.36
d	0.83	1.35
e	0.82	1.35

Table 5-4 Systolic time intervals versus umbilical pulsatility index.

Adjusting the systolic peak from 10% to 50% of the STI decreased the umbilical PI by 0.03 and 0.06, for normal and hypoxic flow conditions respectively. This change in PI is once again negligible in comparison to the normal range of PI.

The results of these simulations indicate that the pulsatility and shape of the input waveform do not significantly affect the umbilical PI when investigating foetal hypoxia.

5.3.4 THE EFFECT OF PLACENTAL BLOOD DISTRIBUTION ON THE UMBILICAL PI.

Giles et al.(1985) determined that the placental impedance was determined predominantly by the number of terminating placental villi. Figure 5-2 graphs the effect on the umbilical PI of a range of terminating villi for various placental sizes. This figure also shows the 95th, 50th and 5th centile PI values for a healthy population of 28 week old foetuses, (Arduini & Rizzo, 1990).

Figure 5-2 shows the placental reserve capacity to accommodate increased degrees of terminal villi obliteration. From this it can be seen that a normal placenta (M=130) can tolerate a decrease in the total number of terminating villi of 85% before the corresponding PI of the umbilical blood flow waveform increases above the 95th centile. The PI of a waveform flowing to a smaller placenta, with fewer lobules (M=40), can tolerate a smaller percentage decrease in the number of terminating villi before reaching the 95th PI (33%). Conversely, PI for flow to a larger placenta (M=190), only reaches the 95th centile with a decrease in the number of terminating villi of 93%, thereby indicating a larger reserve capacity.

The curve corresponding to M=40 in Figure 5-2 shows that it is possible for the PI to decrease with increasing terminal villi obliteration, after a critical level of obliteration has been reached. This finding was investigated further in Figure 5-3, where less lobules per lobe were considered. The resultant graphs in Figure 5-3 all reached a maximum after which the PI decreased for an increase in terminal villi obliteration. The point at which the maximum PI occurred, however, depended on the placental size. The smaller placentae reached the maximum at lower degrees of terminal villi obliteration.

The overall trend in Figure 5-2 shows how a decrease in the number of terminating villi causes a corresponding increase in the umbilical PI. The rate of increase is, however,

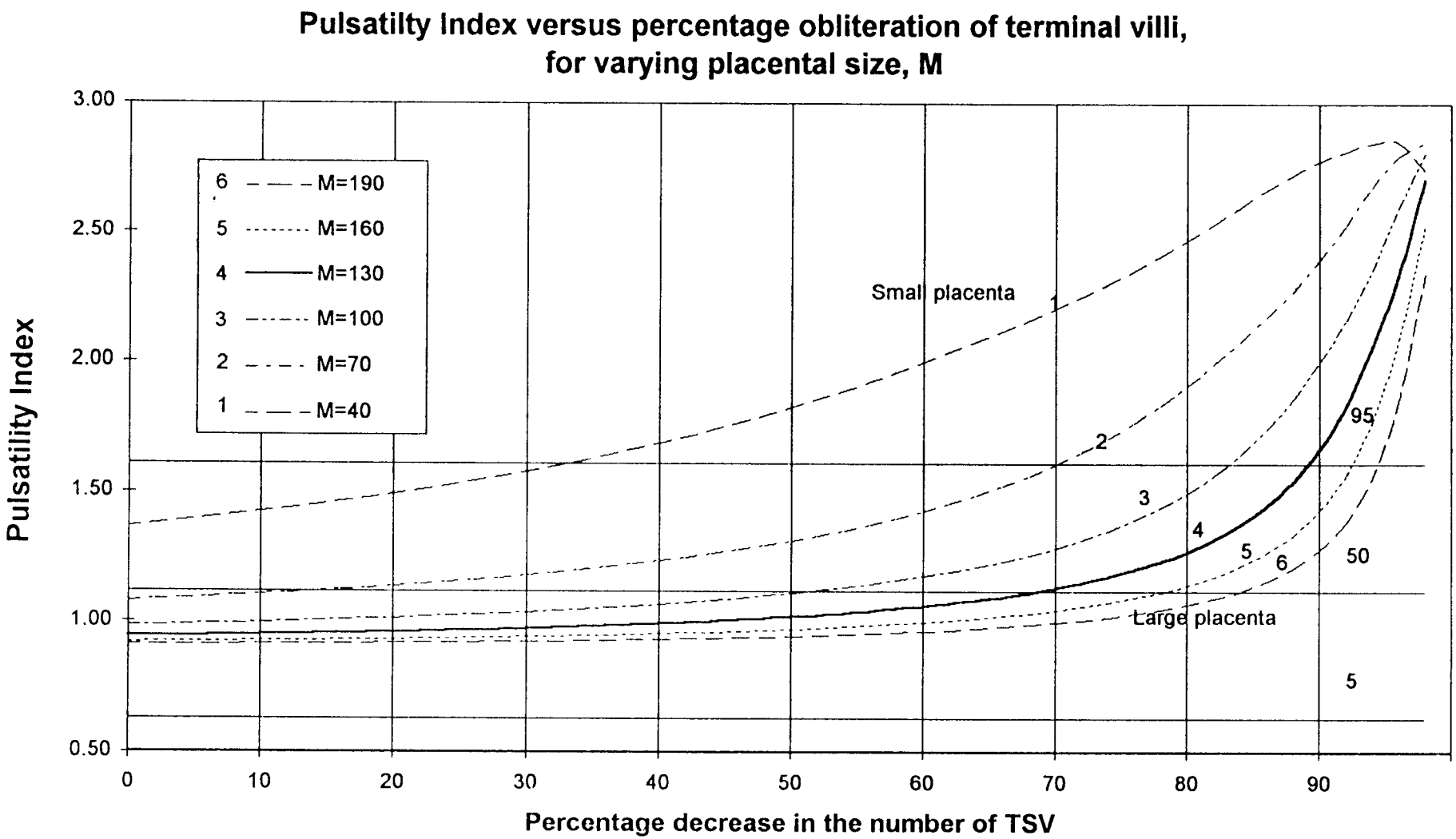
Pulsatilty Index versus percentage obliteration of terminal villi, for varying placental size, M
Pulsatility Index
3.00
2.50
2.00
1.50
1.00
0.50
0
10
20
30
40
50
60
70
80
90
Percentage decrease in the number of TSV
6 M=190
5 M=160
4 M=130
3 M=100
2 M=70
1 M=40
Small placenta
Large placenta
1
2
3
4
5
6
95
50
5

Figure 5-2

dependent on the size of the placenta. Irrespective of the placental size, a rapid increase in the PI index occurs when the total number of terminating villi have been reduced by more than 90%.

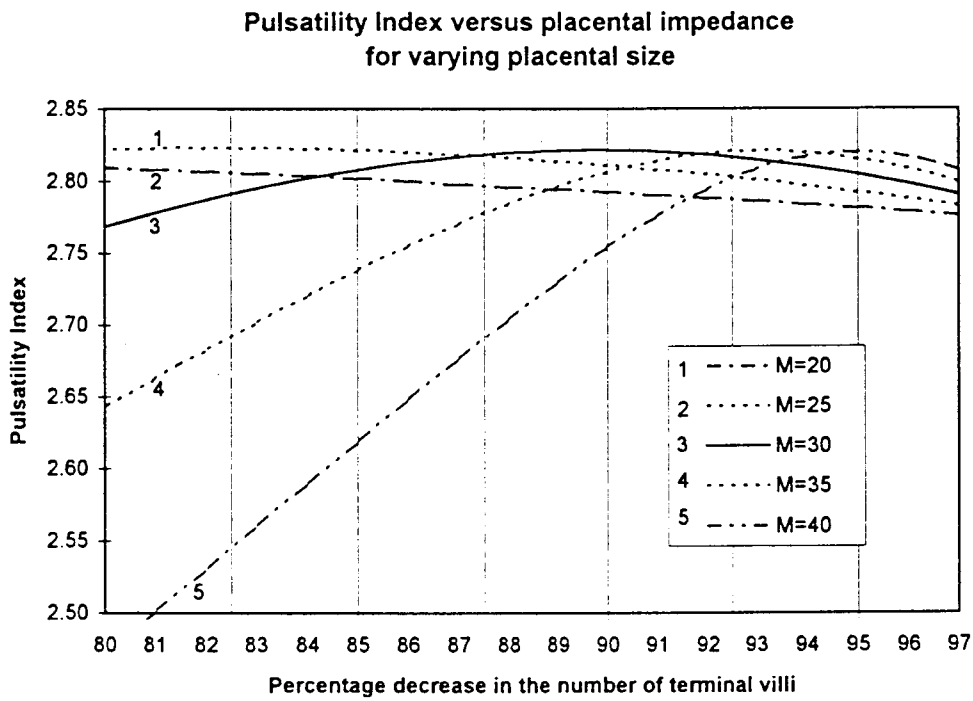

Figure 5-3 Extreme placental impedance and obstruction of umbilical blood flow.

5.3.5 BLOOD FLOW SHUNTING

Table 5-5 reflects in summary the results of several blood flow distributions resulting from a range of different foetal conditions. Each blood flow distribution affects the haemodymanics of the foetal circulation and influences the shape of the umbilical blood flow waveform. The PI index is calculated for each distribution to determine the extent of the waveform change. The regional percentage blood flows, as measured by isotope labelling, are given for the vascular regions of the head and heart (HAH), placenta (PLA), thorax (THR), abdomen (ABd), adrenals (ADr) and the remainder of the body (BODY).

Each of these studies used ovine foetuses between 110-120 days gestation.

Authors	Clinical Complication	Regional Percentage blood flow						Umb PI
		HAH	PLA	THR	ABd	ADr	BODY	
Rudolph & Heymann	Normal (1967)	6.9	42.7	5.9	9.4	0.1	35.0	**1.17**
	Normal (1970)	9.5	41.0	4.4	10.0	0.1	35.0	**1.28**
Block et al. (1984)	Control	4.9	40.0	7.9	8.7	0.1	38.4	**1.35**
	Hypoxic control	9.8	45.2	6.0	6.2	0.2	32.6	**1.02**
	Basal embolised	9.8	31.2	6.6	10.5	0.2	41.7	**2.06**
	Hypoxic embolised	17.2	32.2	4.5	10.1	0.4	35.6	**1.96**
Field et al. (1990)	Controlled hypoxia	6.4	33.9	9.9	10.4	0.1	39.3	**1.81**
	Hypoxia- group 1	14.6	41.5	3.6	8.7	0.8	30.8	**1.25**
	Hypoxia- group 2	18.2	40.4	4.9	6.1	1.2	29.2	**1.32**
Toubas etal. (1981)	Control	4.7	44.0	6.9	9.2	0.2	35.0	**1.09**
	15% haemorrhage	6.7	42.0	4.5	15.4	0.4	31.0	**1.21**
Itskovitz etal. (1987)	Control	6.2	46.0	8.0	7.5	0.3	32.0	**0.98**
	-25%umbilical flow	7.5	37.0	7.6	8.4	0.5	39.0	**1.56**
	-50%umbilical flow	10.7	28.0	5.4	10.4	1.0	44.5	**2.40**
Block et al. (1990)	Control	4.8	34.0	7.5	7.8	0.1	45.8	**1.80**
	Hypoxemia	9.3	36.7	5.0	5.8	0.2	43.0	**1.59**
	Hypoxemia with severe acidosis	18.0	28.6	12.1	7.0	0.3	34.0	**2.52**
	Agonal heart rate	11.0	7.8	6.9	6.0	0.3	68.0	**2.88**

Table 5-5 Effect of clinical blood flow shunting on the umbilical PI

Block et al.(1984) investigated acute hypoxemia in growth impaired foetuses secondary to placental embolisation. Initial maternal hypoxia induced by decreasing the inspired PO_2, increased the blood flow to the head (100%) and placenta (12%) at the expense of the periphery. Embolisation also increased the flow to the head and heart (100%) but,

predictably, limited the flow to the placenta. A hypoxic insult with placental embolisation resulted in a large increase in flow to the head and heart (75%) at the expense of the foetal body. Appropriate foetal shunting resulted in an increased placental flow which caused a decrease in the PI of 24%. However, after placental embolisation, the flow to the placenta was not able to increase as dramatically, and shunting of blood only resulted in a 5% decrease in the umbilical PI.

Field et al.(1990) induced acute foetal hypoxia by limiting flow in the uterine arteries for up to 90 minutes. The foetuses were categorised into group one if their ascending aortic oxygen content was greater than 1.0mmol/l, and into group two if it was less. Group two foetuses were severely hypoxic and suffered from metabolic and respiratory acidemia. In both cases of hypoxemia, the blood flow to the brain, heart and placenta increased at the expense of the periphery. Blood flow shunting increased the percentage cardiac output to the placenta which reduced the PI by 30% in group one and 27% in group two. Under these conditions, an increase of blood flow to the body is an ominous finding as shown by Block et al. (1990), who found it to be associated with an agonal heart rate pattern.

Toubas et al (1981) investigated a reduction in oxygen delivery by a reduction in foetal blood volume. A reduction in blood volume of 15% is accompanied by a reduction in blood pressure and cardiac output. The proportions of blood conducted to any one region were retained and, although the umbilical PI increased by 11%, it was still within the normal PI range as defined in Table 2-2.

Itskovitz et al.(1987) partially occluded the umbilical arteries and illustrated the dependence of the pulsatility index on the umbilical blood flow. A decrease in the flow to the placenta caused a rapid increase in the umbilical PI whilst maintaining blood flow shunting to the head and heart. The shunting effect was more pronounced for greater reduction in umbilical arterial flow, 21% and 73% for decreases of 25% and 50% respectively.

Block et al.(1990) considered chronic hypoxia through uterine arterial occlusion and maternal hypoxemia. Initial hypoxemia elicited an appropriate increase (93%) in blood flow to the foetal head and heart. This change caused a decrease in umbilical PI of 11% whilst maintaining flow to other regions. Continued hypoxia with uterine occlusion resulted in hypoxemia with severe acidosis. Under these conditions, blood flow to the head and heart is maintained at the expense of the placental and peripheral organs. Finally, due to severe foetal hypoxia and acidemia, the compensatory mechanisms failed. The blood flow to the head and heart fell, with an ominous increase in the peripheral flow. This condition was found to be associated with agonal heart rate patterns.

Simulated maximum flow waveforms from Block et al.(1984) are shown in Figure 5-4. As the foetal condition deteriorates (1 to 4), the waveform becomes more pulsatile, the pulsatility index increases and there is a tendency towards absent end diastolic flow.

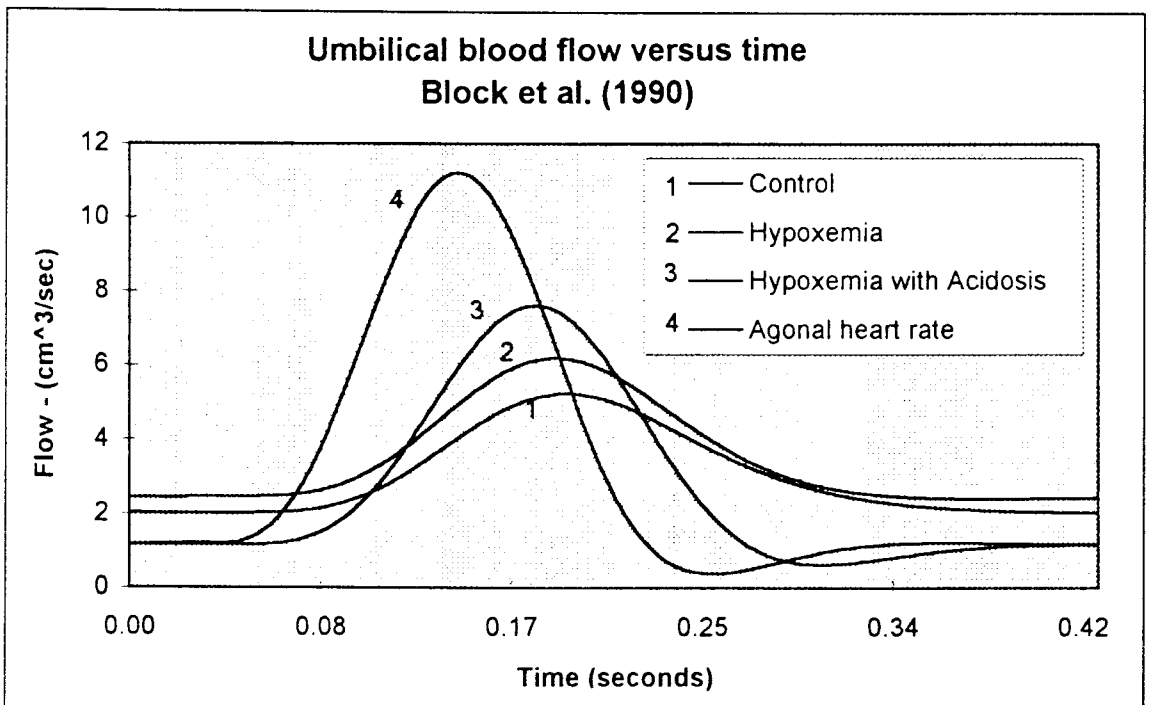

Figure 5-4 Simulated maximum flow waveforms under severely hypoxic conditions

5.4 DISCUSSION

The advantage of modelling and simulating any physiological event is that experiments can be performed non-invasively to ensure that the physiological mechanisms being observed are not disturbed. The usefulness of the results obtained, however, depends on the integrity and accuracy of the model.

5.4.1 VALIDATION

The electrical analogous flow model of the foetal vasculature was investigated, under normal and hypoxic flow conditions, to ensure that it was representative of the foetal circulation. This modelling technique cannot be used for all flow conditions, but was considered appropriate for this study as, under quasi-steady flow conditions, the non-Newtonian effects of blood can be neglected and system linearity assumed.

This model used typical ovine blood flow distributions to approximate the distribution in the human foetus. The ovine foetal flow distribution has been shown to correspond well with that of the human foetus except for the difference in the percentage cardiac output distributed to the head. In an ovine foetus this percentage is approximately 4%, whereas in a human foetus the percentage is approximately 10%(Rudolph , 1984). For this model, the maximum umbilical flow waveform shape and corresponding PI were found to depend predominantly on the distribution to the placenta and only marginally on the distribution to the head and heart region as shown in Table 5-6. Comparing case two and three, a 10% change in placental distribution resulted in a 60% change in PI, whereas a 9% change in head and heart blood flow resulted in 6% change in PI for case one and two. The distribution to the heart was assumed to be half that to the head.

	HAH %CO	PLA %CO	THR %CO	Abd %CO	Adr %CO	BODY %CO	**PI**
case one	6	45	6	6	0.2	36	**1.09**
case two	15	45	6	6	0.2	28	**1.04**
case three	15	35	6	6	0.2	38	**1.64**

Table 5-6 Experimental flow distributions (%CO - percentage cardiac output)

The error incurred, firstly, from grouping the distribution to the head and heart, and secondly, using the ovine blood distribution was therefore considered acceptable in comparison to the change in PI resulting from foetal compromise.

Investigation into the impact of assumptions regarding the heart input resulted in a finding that the effect of normal input flow-waveform harmonics and varying systolic time intervals, on the umbilical PI, was negligible. The umbilical flow waveform shape and pulsatility were shown to have very little effect on the resulting umbilical PI, and the inclusion of non-parabolic flow parameters was shown to be unnecessary. The electrical analogous flow model made it possible to approximate the heart as a current source and the blood flow waveform as a current pulse propagating along the electrical network.

Thus within the physiological limits present, this model and its assumptions were found to be representative of the foetal circulation. This model could consequently be used to investigate different foetal conditions, in particular the progression of chronic foetal hypoxia.

5.4.2 PLACENTAL IMPEDANCE

Foetal hypoxia results from a decrease in the placental cross-sectional area available for gaseous exchange. A decrease in the placental cross-sectional area, through terminal villi embolisation and/or vasoconstriction, results in an increased impedance to placental blood flow.(Adamson & Langille 1991). The mechanism through which this occurs is still under investigation, but, irrespective of the aetiology, it has been established that a sustained increase in the flow impedance within the placenta will result in foetal hypoxia.

The results given in Figure 5-2 of investigating the effect of placental terminal villi, correspond well with the results obtained for a similar experiment by Thompson & Trudinger (1990). Data obtained from their work is presented in Figure 5-5.

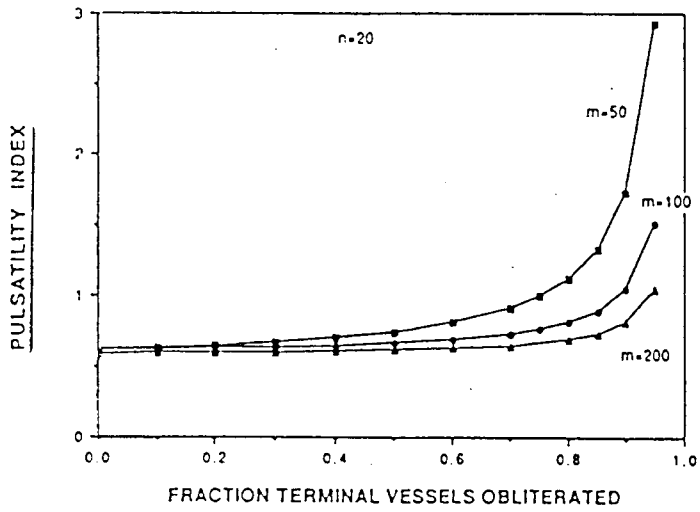

Figure 5-5 PI versus the number of terminating villi, Thompson & Trudinger (1990).

Figure 5-2 & Figure 5-5 illustrate the ability of the placenta to tolerate high degrees of terminal vessel obliteration. A normal foetus can tolerate a 45% decrease in the total number of placental terminating villi before a change of 10% in the umbilical flow waveform PI occurs. Although the placenta seems to have a high degree of redundancy, this reserve capacity is required to sustain the foetus through periods of adverse conditions when the blood flow to the placenta is limited or absent. Any decrease in the number of placental vessels increases the placental impedance and places the foetus at extreme risk when the foetal demand on the placental supply becomes critical.

Chudleigh & Pearce (1986) associated a decrease in the PI in severely growth-impaired foetus with foetal morbidity. Simulations to investigate the effect of a change in placental impedance also disclosed a decrease in PI for a continuing increase in impedance (Figure 5-3), for levels of extreme placental impedance. This phenomenon is contrary to the normal case where PI decreases with an improvement in the foetal condition, which was investigated in Figure 5-6.

Figure 5-6 illustrates, in a 3-dimensional plot, the effect of increasing impedance to placental blood flow on the umbilical maximum flow waveform. This figure plots flow magnitude (z-axis) versus an increasing degree of placental flow impedance (x-axis) for a complete cardiac cycle (y-axis). Figure 5-6 shows how, for extreme degrees of placental impedance, the systolic peak reaches a maximum (S), after which a further increase in placental impedance causes a decrease in the systolic peak. A similar effect on the diastolic minimum causes it to increase after having reached a minimum (D). The PI is defined, in Equation 2-2, as the difference in systolic and diastolic flow divided by the mean flow over the cardiac cycle. Figure 5-6 shows how the systolic to diastolic flow difference decreases more rapidly than the corresponding mean flow, thereby resulting in an apparent decrease in the PI, with a continued increase in placental impedance.

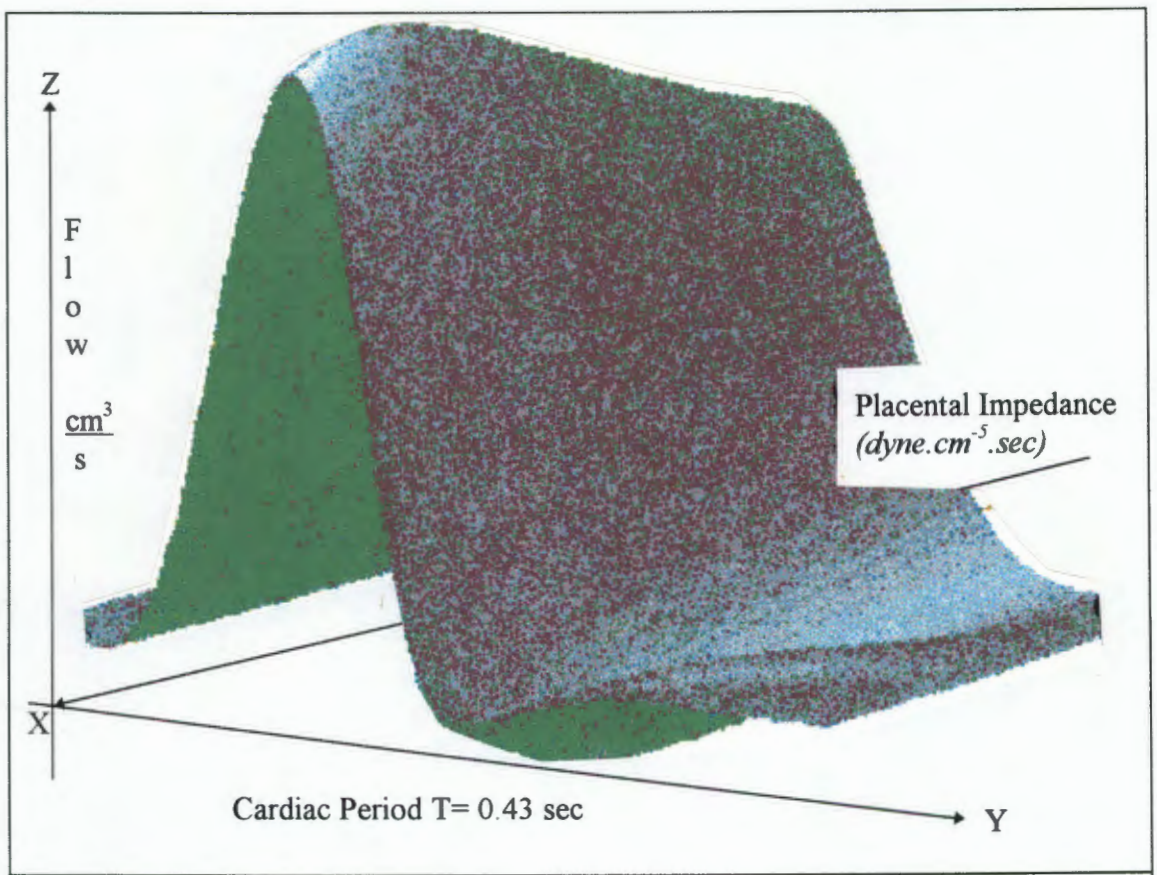

Figure 5-6 3-dimensional plot of placental impedance vs umbilical flow magnitudes

5.4.3 BLOOD FLOW SHUNTING

Blood flow shunting allows the foetus to shunt oxygenated blood preferentially to vital organs (head, heart and adrenals) at the expense of the peripheral supply, section 3-4. This is not the only compensatory mechanism that the foetus can employ to alleviate hypoxic conditions, but it is reported to precede other mechanisms, for example changes in heart rate and blood pressure, (Schulman et al., 1989).

Rudolph & Heymann (1967), were amongst the first investigators to inject isotope-labelled microspheres into the foetal circulation. This technique enabled localised blood flow to be calculated without interference to the normal foetal circulation. The normal flow distributions determined by Rudolph & Heymann (1967,1970) correspond well with the normal flow distributions given by Itskovitz et al. (1987), Toubas et al. (1981) and Block et al. (1984).

This foetal circulatory model does not include the effect of autonomic control mechansims, but rather institutes these manually. Consequently, the PI corresponding to a decrease in blood volume, as investigated by Toubas et al.(1981), is not an accurate representation of the foetal response, since changes in stroke volume and peripheral resistance were not supplied and therefore could not be accommodated. Giles et al.(1986) illustrated that umbilical artery flow velocity waveform analysis is not sensitive to changes in blood volume.

The effect of blood flow shunting and other circulatory compensation mechanisms, which limit the effect of hypoxia on the foetus, can be seen in the data obtained by Block et al.(1984,1990) and Field et al.(1990). The decrease in PI is not due to the maternal hypoxic conditions but rather as a result of the increased percentage blood flow to the head, heart and placenta. This finding is confirmed in work done by Maulik et al.(1992) who found that for peripheral haemodynamics, the indices reflect the changes in the peripheral impedance.

The foetal response to hypoxia seems to depend on the initial state of the foetus. Data from Block et al.(1984) indicated that blood flow shunting was more pronounced for normal, than embolised, foetuses. Similarly, the data from Field et al. (1990) showed how the same degree of uterine artery occlusion resulted in different degrees of blood flow shunting. Field et al. (1990) indicated that the discrepancy was dependent on the foetal oxygen concentration in the ascending aorta. When the oxygen content of the ascending aorta fell below 1mM, the cerebral oxygen consumption was no longer maintained but rather decreased linearly with oxygen content. This threshold level as illustrated in Figure 5-7, shows how the preferential blood supply to the head and heart is dependent on the state of the foetus. The compensatory mechanisms which alleviate stress imposed on the foetus are thus only effective over a limited range and cannot be employed indefinitely.

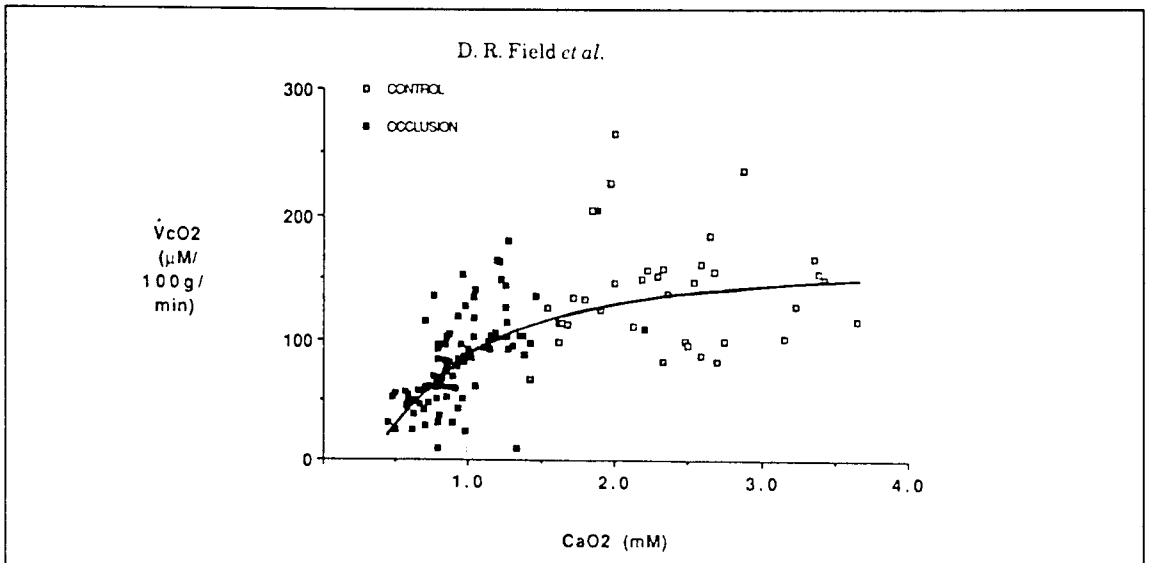

Figure 5-7 Cerebral oxygen consumption versus ascending oxygen content(Field et al. 1990)

5.5 CONCLUSION

The model used in this investigation was determined to be representative of the foetal circulation and gave predictable results when simulating normal conditions. It produced similar results to those determined in the literature for different degrees of placental impedance.

The PI accurately represents changes in the umbilical blood flow waveform over a finite range. Under extreme pathological conditions, when the impedance to blood flow exceeds a threshold level, the PI is unable to characterise changes in the umbilical blood flow waveform shape.

Blood flow shunting is able to assist foetal survival only for a limited period, since once a lower limit in arterial oxygen content has been reached, blood is no longer shunted to the vital organs. This event corresponds to a failure in the foetal compensatory mechanisms and unless the condition is circumvented it will result in severe foetal morbidity.

6. THEORETICAL AND PRACTICAL ASPECTS OF DOPPLER ULTRASOUND MEASUREMENTS.

6.1 INTRODUCTION

It is possible to perform a non-invasive measurement of the velocity of blood cells within a vessel by insonating the vessel with ultrasound and measuring the Doppler shift of the reflected beam. Since frictional, viscous and flow effects cause blood cells to travel at different velocities, the reflected beam contains a spectrum of Doppler shift frequencies. A sonogram is a useful two-dimensional method of displaying the Doppler shift spectrum. It displays the range of Doppler shift frequencies at each instant in time, where the power at any particular frequency is represented either by the intensity or the shade of the corresponding point. A single vertical line of a sonogram corresponds to a single power spectrum and provides the flow profile of all the particles moving within the sample volume at a specific time. The flow spectrum and sonogram are considered in detail in Appendix H.

Several techniques can be implemented to quantify the information contained within the sonogram. For example, the maximum flow follower reduces the power spectrum to a single representative frequency, for each short time interval. These representative frequencies, which make up the flow velocity waveform, are stored sequentially for each complete cardiac cycle.

The estimation of the flow velocity waveform in this way has several limitations that arise either practically from the measurement or inherently from ultrasound analysis. This chapter will consider these limitations, in particular those which arise when performing measurements on growth-impaired foetuses, since the ability to extract relevant obstetric information from the umbilical blood flow waveform is limited by the foetal state of health.

This investigation focused on the flow conditions which arise in foetuses who are small for gestational age (SGA) and who have absent end diastolic flow (AEDF).

Clinical waveforms obtained under these conditions are sometimes difficult to interpret. The purpose of this study was therefore to investigate, by means of a flow phantom (Figure 6-1), conditions which can occur when using Doppler ultrasound to assess SGA foetuses. Factors which have been recognised to compromise flow signals are: (i) reversed flow during diastole, (ii) opposite flow in adjacent vessels and (iii) movement of the vessels within the sample volume.

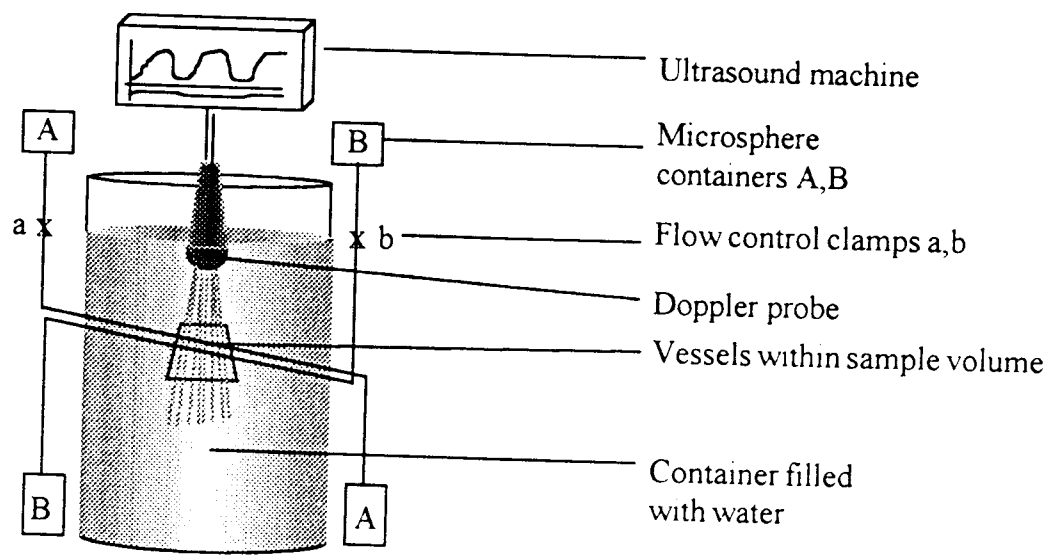

Figure 6-1 Flow phantom to investigate the factors affecting the acquisition of the MFW

Reverse flow during diastole

The MFW is a representation of the fastest moving particles in the sample volume at each instant in time. Positive and negative flow directions are represented by positive and negative frequencies on the sonogram respectively. In instances of extreme foetal compromise, flow at the end of diastole is absent (AEDF) and can reverse direction. Flow velocities under these conditions are of the same order of magnitude as the vessel wall,

and are thus attenuated by the low pass wall filter. This filter, which is essential to minimise the effect of wall movements on the flow spectrum, limits the range over which the maximum velocity waveform can represent the flow in the vessel.

Opposite flow in adjacent vessels

In the umbilical cord, the umbilical arteries and vein are in close proximity and helix around one another. To insonate a single vessel in the umbilicus is difficult, and it is quite possible that at some stage, the vein and the artery will be insonated simultaneously. Under normal conditions the flow velocity in the artery is always greater than that in the vein and concurrent insonation does not affect the MFW. However, under adverse foetal conditions the flow in the artery decreases during diastole to the extent that the flow velocity in the forward direction becomes less than the velocity of returning blood in the vein. Under these conditions, the MFW will be a representation of the flow velocity in the vein during part of the cardiac cycle, rather than the desired low flow velocity in the artery.

Vessel movement

Relative motion between the insonated vessel and the Doppler probe influences the flow profile extracted from the vessel. When the sample volume only partially insonates the vessels the resulting flow sonogram does not represent the flow profile. Any factor that would result in relative motion between the vessel and the sample volume must therefore be considered as a potential source of artefact. Movement of the vessel within the sample volume is more pronounced in growth impaired foetuses, since the reduced liquor volume surrounding the foetus cannot buffer it from maternal movement. Under these conditions any maternal movement is transferred directly to the foetus and Doppler probe. This results in a pronounced displacement of the vessels relative to the probe.

This analysis uses a flow phantom to approximate blood flow in the umbilicus so that several experiments could be performed under controlled conditions.

6.2 MATERIALS USED FOR THE FLOW PHANTOM

Figure 6-1 shows two narrow, thin-walled silicon tubes (inner/outer diameter 2.4mm/ 3.7mm) which were immersed in a container of water. Microspheres were mixed with water to achieve an equivalent 30% haematocrit level. This mixture was passed through the tubes under gravity where pulsatile flow was produced by clamping the tubes.
A SIEMENS SL 2 Duplex Doppler ultrasound machine was used to obtain the flow sonogram and representative maximum flow waveform (MFW).

6.3 METHODS

The following experiments were performed :

6.3.1 INVESTIGATION OF THE EFFECT OF CHANGING DOPPLER GAIN

SGA foetuses have lower blood volumes and smaller percentage placental blood flows than AGA foetuses and hence the Doppler signal strength received from the former is weaker. To compensate for this weaker signal the Doppler gain can be increased. This investigation assessed the effect of increasing the Doppler gain on the MFW. The Doppler gain was increased in increments of 5dB's from 20-30dB during one complete sonogram cycle and the resultant effect on the sonogram and the maximum flow waveform recorded.

6.3.2 REVERSE FLOW DURING DIASTOLE

Doppler analysis depends on a wall filter to remove the influence of the slow moving vessel wall on the received Doppler signal. The wall filter setting was fixed at 100Hz by the Doppler machine, and the effect of the wall filter and alternating flow on the MFW was investigated. Two flow conditions were considered : firstly, strong flow which changed direction rapidly, and secondly, weaker flow that changed direction over a longer period of time.

6.3.3 OPPOSITE FLOW IN ADJACENT VESSELS

Two tubes were arranged adjacent to one another with equal volumetric flow being conducted in opposite directions under gravity. Five flow configurations were considered, the first two to investigate laminar and pulsatile flow being conducted concurrently in both tubes but in opposite directions. The following three investigations approximated the effect of progressive deterioration in the condition of the foetus according to relative pulsatile and laminar flow configurations. In each of these investigations the pulsatile flow component during diastole (simulating arterial flow) was gradually reduced until reverse flow occurred. The sonogram and maximum flow waveform were determined for each configuration.

6.3.4 MATERNAL BREATHING

This investigation studied the effect of maternal breathing on the MFW. Clinically, maternal breathing was found to cause relative motion between the Doppler sample volume and the umbilical vessels. In this flow phantom, the equivalent effect of vessel movement was achieved by tilting the ultrasound transducer from 0-3 degrees at a rate of 14-16 times per minute. This tilting moved the sample volume 0.5cm relative to the vessels conducting laminar and pulsatile flow in opposite directions (Figure 6-1). The tilting moved the sample volume over the vessels and enabled the investigation of partial insonation on the MFW.

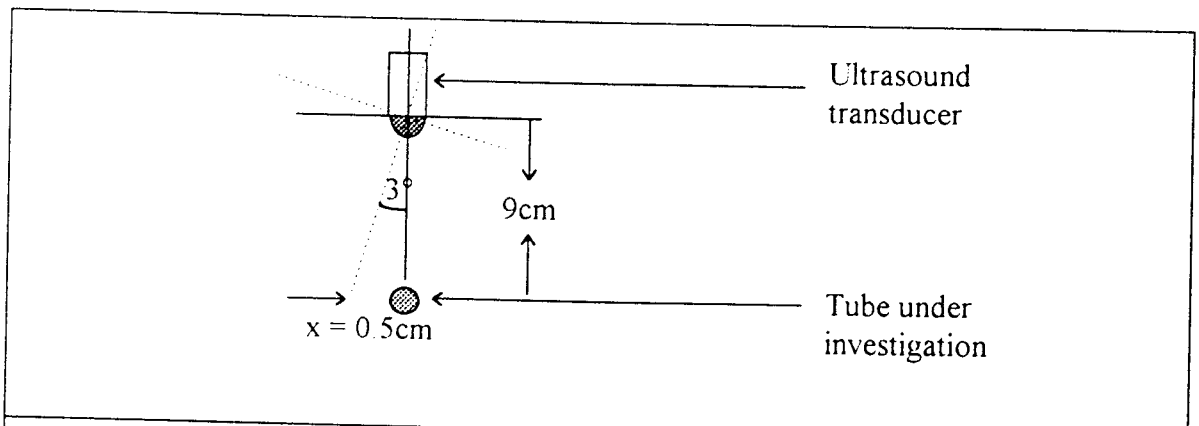

Figure 6-1 Relative movement of sample volume with respect to the insonated vessels.

6.4 RESULTS

Each figure given in the results below was obtained from the Doppler ultrasound machine via a SONY CN24 thermal printer. The top diagram represents the MFW and the lower, the sonogram. The horizontal axis represents time and the vertical axis blood velocity.

6.4.1 DOPPLER GAIN

When the gain was increased from 20-30dB's the intensity or shade of the sonogram increased, as the backscattered signal strengthened. An increase in gain caused a corresponding increase in the amplitude of the noise until a threshold level was reached. Further increases in the Doppler gain caused the maximum frequency follower to interpret the noise as a valid signal. The resulting MFW has spurious noise signals superimposed on the small laminar flow signal.

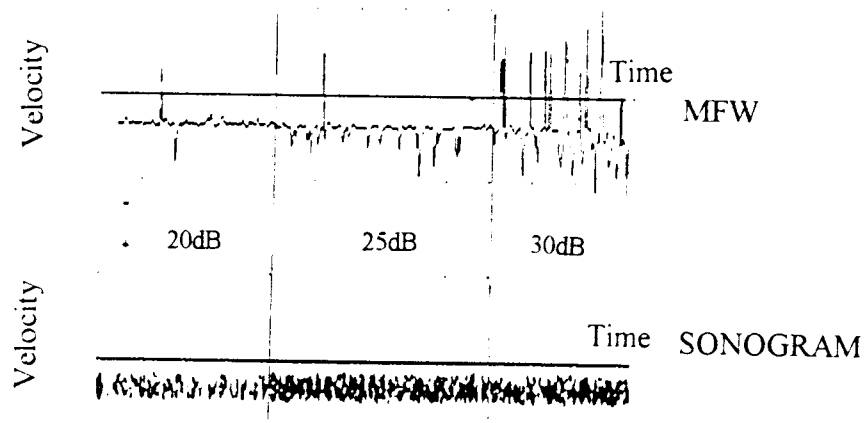

Figure 6-2 Increasing Doppler gain

6.4.2 REVERSAL OF FLOW WITHIN A VESSEL

The effect of the wall filter is represented on the sonogram by a band (as indicated between arrows in Figure 6-3a), centred around the zero flow level, where the amplitude

of the frequency shifted components, caused by low velocity particles, is attenuated. The width of this attenuating band depends on the minimum velocity threshold level. In Figure 6-3 the wall filter is set at 100Hz which corresponds to a minimum velocity threshold level of approximately 2.5cm/sec along the beam.

The MFW is particularly susceptible to artefact generated by the combined effect of the Doppler wall filter and periodic reversal in flow direction. Figure 6-3a shows the effect on the MFW of a rapid change in flow direction from negative to positive flow (indicated by section i) and a more gradual change in flow direction from positive to negative flow (as indicated by section ii). Figure 6-3b illustrates, schematically, how the resulting MFW under these conditions does not represent the actual flow in the insonated vessel.

The wall filter attenuates the signal received from particles travelling slower than the minimum velocity threshold level. The corresponding MFW is discontinuous, dropping or rising steeply as the particle velocity increases above, or falls below, this minimum threshold velocity. Figure 6-3a and 6-4b shows the resulting discontinuity to be less pronounced when the flow is changing direction rapidly (section i) as opposed to changing direction slowly (section ii).

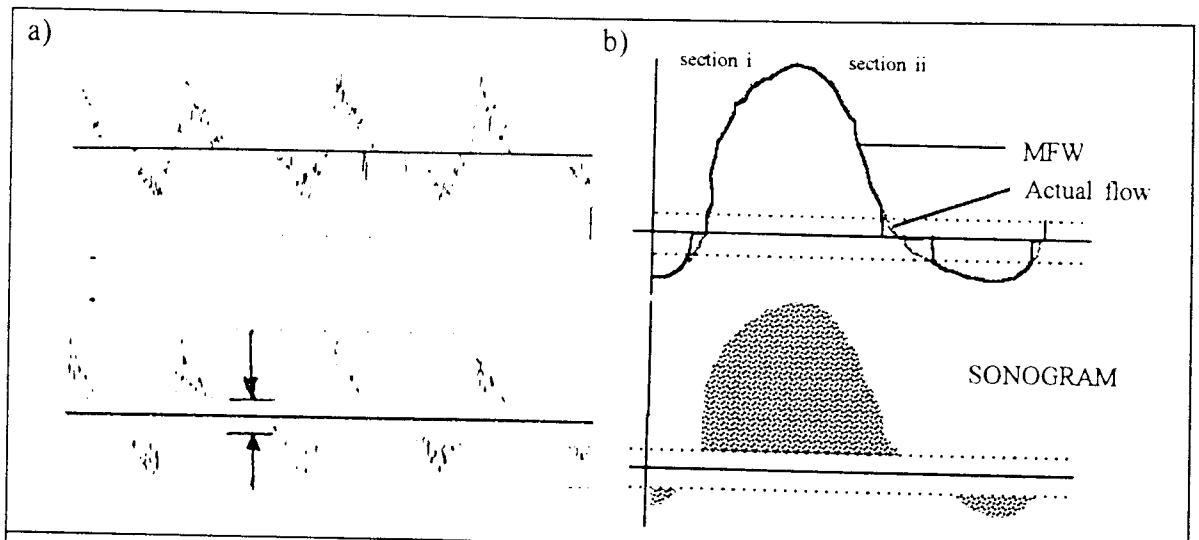

Figure 6-3 The effect of flow reversal on the MFW

6.4.3 FLOW IN OPPOSITE DIRECTIONS

Figure 6-4a reflects the simultaneous insonation of two vessels conducting laminar flow in opposite directions with approximately equal flow velocities. The resulting MFW is not representative of flow in either vessel, since the MFW continually oscillates between both vessels, determining the maximum flow for each time interval. The sonogram in Figure 6-4b shows the vessels conducting pulsatile flow in opposite directions. The MFW algorithm determines the maximum flow for each time instant and cannot differentiate between the origins of the signals. In the sonogram of Figure 6-4b the two individual flows can be identified, as the backscattered signal received from one is stronger than the other. The resulting MFW is a combination of the two flow profiles and is therefore representative of neither.

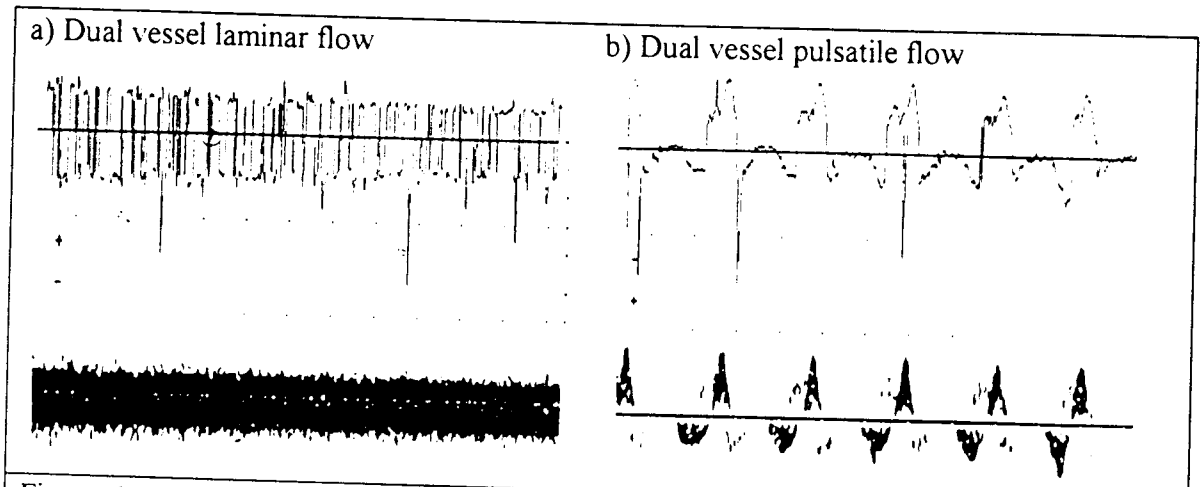

Figure 6-4 Dual flow for laminar and pulsatile flow conditions.

Figure 6-5a to 6-6c depict combinations of laminar and pulsatile flow occurring within two concurrently insonated vessels and the effect of their relative flow magnitudes on the MFW. The progression of waveforms a-c simulate three stages in the deterioration of the foetal circulation. In each of the figures, laminar flow represents the umbilical vein and pulsatile flow the umbilical artery. Figure 6-5a shows a typical umbilical blood flow waveform with decreased diastolic flow; Figure 6-5b shows the effect on the MFW as the flow during diastole reverses but is lower than the flow velocity in the vein which is

constant; finally, Figure 6-5c shows the response of the MFW when reverse flow is pronounced and the venous flow varies with time.

The MFW is able to represent accurately the blood flow in the umbilical arteries until the flow magnitudes within the arteries become comparable with those in the vein. This phenomenon is clearly illustrated in Figure 6-5a where the MFW accurately tracks the systolic part of the simulated arterial flow until the arterial flow velocity drops below that of the vein. At this stage the MFW oscillates between the two signals as it follows the maximum flow.

In Figure 6-5b the simulated diastolic flow has reversed but is still smaller than the simulated venous flow. The MFW follows the simulated arterial signal until the arterial signal is smaller than that from the simulated vein. The MFW then changes rapidly to follow the simulated venous signal. The resulting MFW is totally unrepresentative of flow in either of the vessels and without the sonogram, could not be interpreted accurately.

The resultant MFW shown in Figure 6-5c is not only unrepresentative of the flow waveform in either vessel, but also shows how a gradual change in the simulated venous signal could be mistaken for a fluctuating zero flow baseline. Once again, only with the aid of the sonogram could the origin of the discontinuities and rapid changes in the MFW be interpreted accurately.

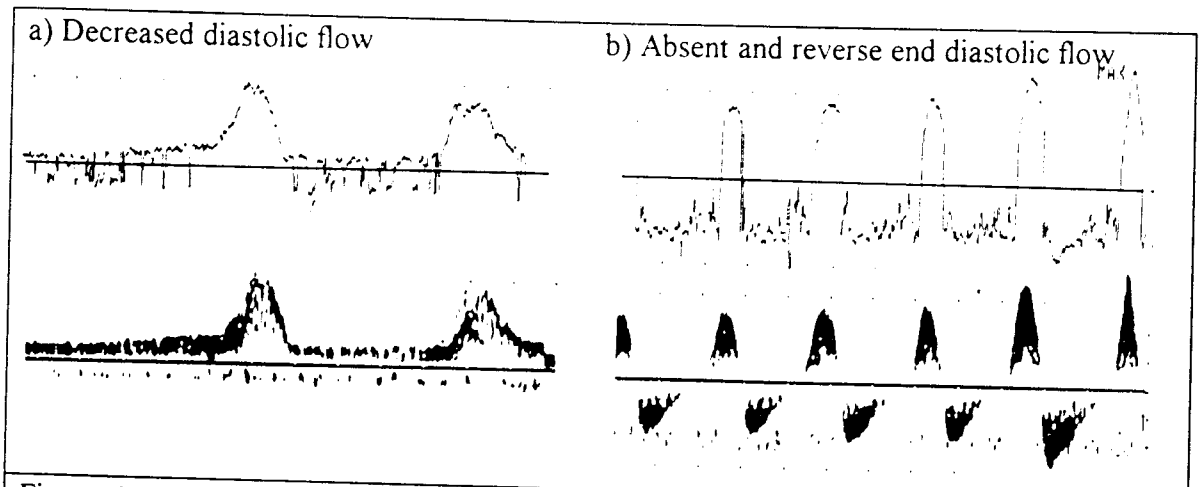

Figure 6-5 Vessels conducting pulsatile and laminar flow.

c) Absent end diastolic flow with variation in the venous blood flow

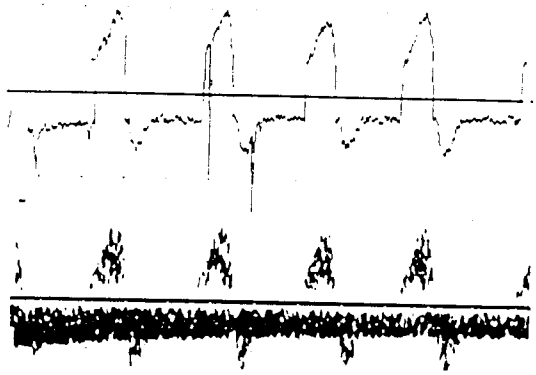

Figure 6-5 (cont) Vessels conducting pulsatile and laminar flow.

6.4.4 MATERNAL BREATHING

The MFW in Figure 6-6a section (i) follows the strong pulsatile signal until, due to sample volume movement, the MFW begins to follow the laminar flow as shown in section (ii). Figure 6-6a illustrates how the movement of the sample volume partially insonated the vessel conducting pulsatile flow, but did not affect the signal received from the vessel conducting laminar flow.

Partial insonation of the vessels within the sample volume results in only a portion of the flow profile within the vessels being insonated. The high pulsatile flow velocities, central within the vessel lumen, are not obtained and the sonogram is generated from predominantly low frequency spectral components. The resulting MFW is noisy and not representative of flow within the vessel as shown in Figure 6-6.

The overall effect of relative vessel movement with respect to the Doppler sample volume, is a periodic attenuation of the high frequencies of the pulsatile flow waveform.

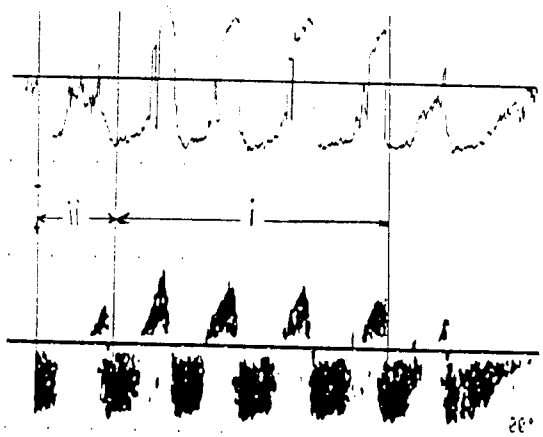

Figure 6-6 Pulsatile flow with vessel movement

6.5 DISCUSSION

In the four experiments above, each parameter investigated (Doppler gain, reverse flow, maternal breathing and flow in opposite directions) was shown to compromise the flow information presented by the MFW. The origin and implications of each parameter are discussed in this section.

6.5.1 DOPPLER GAIN

Doppler gain is a user-dependent variable set on the Doppler ultrasound machine by the operator. The gain setting can affect the MFW in one of two ways, either by introducing speckle or by causing input amplifier saturation.

Doppler sonograms from Fourier-transform based spectrum analysers exhibit a characteristic granular pattern called Doppler speckle. Speckle originates from large random fluctuations of the instantaneous spectral amplitude from the true amplitude (Hoskins et al., 1991). Doppler gain affects all amplitudes equally and therefore any increase in gain would increase the random fluctuations of the instantaneous spectral amplitude.

When the backscattered Doppler signal strength is low, due to attenuation from overlying tissue or small vessel size, the Doppler amplifier gain can be increased to improve the strength of the backscattered signal. If the gain is increased too much (greater than ±30dB's), input to the Doppler amplifier becomes saturated, which results in spurious high frequency components that present as background noise.

The effects of speckle and amplifier saturation are represented in Figure 6-2 which shows the increase in amplitude of the high frequency spikes as the Doppler gain is increased.

6.5.2 SIGNAL STRENGTH

The strength of the received Doppler signal depends predominantly on the extent of backscattering and the attenuation of the ultrasound wave. Both of these factors are inherent in Doppler ultrasound technology.

6.5.2.1 SCATTERING

Scattering of the input waveform provides the signal for imaging and Doppler analysis. It occurs when a wave travelling through tissue strikes a region of discontinuous density or compressibility. The scattering intensity increases with an increase in frequency. Lord Rayleigh (1871) cited in Evans et al.(1994) showed that a doubling in incident frequency causes the scattered intensity to increase 16 times.

The relationship between the scattered intensity and the insonation frequency affects the image resolution obtainable and the depth to which the ultrasound beam can penetrate. High insonation frequencies (>8MHz) offer a high scattering intensity but as a result, can only penetrate superficially (<2cm). Conversely, lower insonation frequencies (3MHz) have a lower scattering intensity but can obtain adequate imaging resolution and a greater depth of penetration (15cm)(Atkinson & Woodcock, 1982). In this investigation, a SIEMENS duplex Doppler 3.5MHz ultrasound probe was used with a focal length of 15cm.

6.5.2.2 *BLOOD*

Insonating Doppler ultrasound frequencies are scattered by blood particles moving within the foetal vessels. Blood is a non-Newtonian fluid consisting of various type of cells, namely erythrocytes, leukocytes and platelets suspended in a plasma. The erythrocytes are flexible bi-concave discs with an average diameter of seven micrometers and an average thickness of two micrometers. The shape of the cell has little effect on the scattering characteristics as the size of the erythrocyte is much smaller than the ultrasonic wavelength, effectively making it a point target. The degree of scattering depends only on the cell volume and the acoustic discontinuity between the erythrocyte and the suspending plasma, (Shung et al., 1976). Although they are not the largest of the blood cells, erythrocytes can be assumed to be the major source of ultrasound scattering since they constitute a significant percentage of the total blood volume (Table 6-1).

Table 6-1 The sizes and concentrations of blood constituents (Evans et al 1994).

	Concentration (Particles/mm^3)	Dimensions (μm)	% of total blood volume
Erythrocytes	5 x10^6	7	45
Leukocytes	8 x10^3	25	0.8
Platelets	2.5 x10^5	3	0.2

6.5.2.3 *SIGNAL ATTENUATION*

Signal attenuation is one of the major limitations of diagnostic ultrasound. The strong incident ultrasound signal is attenuated by overlying structures between the transducer and the vessel. The backscattered signal is attenuated by these structures as it travels from the vessel back to the transducer,(Evans, 1986).

Attenuation of acoustic energy within tissue occurs predominantly through relaxation losses. Relaxation losses occur when the stress imposed by the wave is relaxed by the flow of energy to various energy states of the tissue. For example, thermal relaxation is the conversion of wave energy to internal molecular energy, whereas the structural relaxation

is the conversion of wave energy into a structural change of the tissue. When the stress is released, the remaining energy is transferred back to the wave but usually with a phase delay. The phase delay causes interference of the propagating waves, thereby reducing the resultant amplitude. Many of these relaxation processes contribute concurrently to the wave attenuation, which makes it difficult to isolate the effect of a single relaxation event, (Wells, 1975). Table 6-2 shows the relationship between tissue types and the corresponding waveform attenuation in that tissue.

Table 6-2 Approximate attenuation coefficients of common tissues quoted in dB cm^{-1} for a specific frequency.

Tissue	Attenuation Coefficient(dB/cm) 1Mhz	Attenuation Coefficient(dB/cm) 3.5Mhz	Attenuation Coefficient(dB/cm) 6Mhz
Blood	0.2	0.6	1.0
Muscle	1.5	4.5	7.5
Liver	0.7	2.1	3.5
Brain	0.8	2.4	4.0
Bone	10	30	50
Fat	0.6	1.8	3.0
Water	0.002	0.006	0.01
Soft Tissue (Ave)	0.7	2.1	3.5

Derived from Narayana et al. (1984) - attenuation coefficient [dB/cm]

6.5.3 OPPOSITE FLOW IN ADJACENT VESSELS

The umbilicus consists of three thin vessels, one vein and two arteries. Simultaneous insonation of vessels during Doppler analysis is common, as both foetal arteries helix tightly around the foetal vein. In SGA foetuses these vessels are smaller and this phenomenon is even more pronounced. The results in Figure 6-4 and Figure 6-5 show the susceptibility of the MFW to simultaneous insonation of vessels since, as in each case, the resultant MFW is totally unrepresentative of the flow within either of the vessels.

The MFW, from which the PI is calculated, is determined from an algorithm that operates on the sonogram. The identification of the maximum frequency envelope of a Doppler waveform was considered an edge detection problem by Ballard & Brown (1982) cited in Hoskins et al. (1991). More recently digital maximum frequency followers applied to the Doppler spectrum have been described,(Mo et al, 1988 cited in Hoskins et al, 1991). These followers can be split into percentile and threshold-based techniques.

In the percentile method, the total value (Thres) of pixel values of a single spectral line is calculated, corresponding to the total power in the signal. The maximum frequency is the point where the sum of pixel values below that frequency exceeds a specified percentage of Thres, typically between 88 and 94%. The percentile method is sensitive to background noise such as interference from flow in nearby vessels, and vessel wall motion.

The SIEMENS Doppler machine used in this study, implements the threshold method. The maximum frequency follower algorithm starts from the high frequency end of the spectral line and works towards the lower frequencies. At each frequency the pixel value is compared to the threshold value. The highest frequency at which the pixel exceeds the threshold value is called the maximum frequency. This threshold is set dynamically and the performance of the system deteriorates if the level of noise exceeds this threshold.

The inherent limitation of either maximum frequency follower technique is the degree of noise present. These algorithms work successfully in large signal to noise ratio conditions but their accuracy is compromised under low conditions as is the case in SGA foetuses.

6.5.4 EFFECT OF THE DOPPLER WALL FILTER ON THE MFW

The Doppler effect may be expressed as follows - a moving target, insonated with a signal of a specific frequency, will cause a change in the frequency of the reflected signal at the point of observation. If the target is moving towards the observer, the reflected frequency will be greater than the incident frequency. Similarly, a target receding from an observer

will reflect a lower frequency than the incident beam frequency. In both cases the magnitude of change is dependent on the speed of the target.

$$f_D = \frac{2.f.v_r.\cos\theta}{c} \qquad \text{Equ 6-1}$$

f_D Doppler frequency shift,

f Insonating frequency,

v_r velocity of blood cells,

θ angle between the moving blood particles and the insonating beam,

c the average speed of sound in soft tissue 1560m/s.

The need for a wall or thump filter arises because the blood cells are not the only moving particles in the sample volume at any one time,(Taylor et al., 1988). The elastic walls of the thin umbilical vessels also move within the sample volume as a result of the pulsatile transluminal pressure. The amplitude of the Doppler signal received from the slow moving wall is much larger than the amplitude of the Doppler signal from the faster moving blood cells. The wall filter attenuates all the frequencies below the cut off frequency preventing high intensity signals, reflected from the vessel walls or surrounding visceral tissue from saturating the input Doppler amplifier,(Skidmore et al., 1980). The wall filter is usually adjustable in the frequency range 10-150Hz.

The wall filter does not affect the analysis of fast blood flow. However, when blood flow is reduced and the velocities of blood cells are comparable to the speed of the vessel wall, the wall filter does affect the flow profile extracted from the blood vessel. This is an intrinsic limitation of Doppler analysis and should be taken into account in the interpretation of the flow profiles extracted from SGA foetuses.

6.5.5 Maternal Breathing

The movement of the maternal diaphragm during respiration displaces the foetus. Under normal conditions the volume of liquor which surrounds the foetus acts as a buffer to this movement and prevents the foetus and accompanying umbilical cord from altering position significantly. When the liquor volume decreases however, as in SGA foetuses, the effect of maternal breathing on the foetus and the umbilical cord becomes more pronounced.

The effect of maternal breathing when monitoring SGA foetuses affects the relative displacement between the transducer and the vessel at any one time. Relative movement between the transducer and the vessel, is equivalent to the vessel moving within the ultrasound beam. This adds spurious artefact to the Doppler ultrasound signal thereby causing the Doppler waveform to be unrepresentative of the flow within the vessel, (Atkinson & Woodcock, 1982).

The frequency of maternal breathing was assumed consistent with that of a normal adult given in Berne & Levy (1990) as 14 times per minute. This phenomenon was encountered when capturing clinical data as discussed further in chapter seven.

6.6 Conclusion

The discussion above has focused on practical aspects pertaining to Doppler signals, in particular those extracted from growth-impaired foetuses exhibiting absent end diastolic flow. The observations made in this chapter are used in chapter seven to assess clinical Doppler waveforms. Clinical waveforms that exhibit artefact similar to those observed in this investigation will be rejected, thereby ensuring, that the waveforms are chosen for analysis represent the true foetal condition as accurately as possible.

The maximum flow waveform is a suitable non-invasive tool with which to assess the condition of small-for-gestational-age foetuses. It should not, however, be considered in

isolation but rather in conjunction with the sonogram. This will ensure that any artefact originating from the maximum frequency follower will not be interpreted as originating from the blood flow within the vessel.

Pulsed Doppler was used in this study because of its ability to isolate the source of the Doppler signal. This perceived benefit over continuous wave Doppler, was offset to some extent by the dependence of pulsed Doppler on vessel movement within the sample volume.

7. THE EFFECT OF MATERNAL HYPEROXYGENATION ON THE UMBILICAL BLOOD FLOW WAVEFORM.

7.1 INTRODUCTION

Foetal growth-impairment can be caused by placental insufficiency which results in foetal hypoxia, acidosis and absent end diastolic flow. During the early phase of foetal development, the ratio of foetal size to placental size is small. However, the relative growth of the foetus is larger than that of the placenta, and placental function becomes more critical after the 24th week. Prior to this stage, the demand of gases and nutrients by the foetus does not exceed the supply maintained by the placenta,(Nicolaides et al. 1988 , Bilardo et al., 1990).

Indicators such as femur length and bi-parietal diameter (BPD) provide a measure of the foetal size, which can be used to calculate the foetal growth over a period of time. A foetus is diagnosed as small for gestational age (SGA) if its size is below the 5th centile level as compared with an average foetus of the same gestational age (Figure 2-6). SGA foetuses are not always growth-impaired since some foetuses are, for genetic reasons, proportionately small for gestational age. They are otherwise healthy and have no placental abnormalities.(Hackett et al., 1987).

Severely growth-impaired small-for-gestational-age foetuses are usually hypoxic and acidotic, thus making it beneficial to deliver the foetus as soon as it becomes viable. At Groote Schuur Hospital (GSH) it is considered inadvisable to deliver a foetus before 28 weeks since its survival rate is only approximately 5%. Clinical intervention therefore, aims to optimise the foetal environment, in an attempt to reach the 28th week of gestation with minimal organ damage. Clinical treatment at GSH currently involves the administration of steroids to increase the rate of foetal lung maturation. A clinical trial was initiated by GSH, based on findings of Nicolaides et al.(1987), to determine whether in

addition to steroid treatment, maternal hyperoxygenation and bed rest could minimise in utero foetal compromise.

The study performed by Nicolaides et al.(1987) considered the benefit of oxygen treatment to SGA foetuses. This study found a decrease in the foetal mortality rate when oxygen therapy was implemented. However, the trial was not controlled and considered only six foetuses. The benefit of oxygen treatment or maternal hyperoxygenation has yet to be assessed using a large controlled sample.

The purpose of the pilot trial discussed in this chapter, was to determine clinical and statistical data that would be required to investigate oxygenation amongst a large controlled sample. The effect of maternal hyperoxygenation was to be assessed clinically using femur length measurements, BPD, liquor volume, foetal movements; and technically, using the umbilical blood flow waveform. Flow analysis involved characterising the blood flow waveform with suitable indices which were compared to those obtained from normal foetuses. This trial assessed the possibility of using the PI as an indicator of the benefit of maternal hyperoxygenation.

7.2 METHODS

7.2.1 CLINICAL TRIAL

The clinical trial was a prospective randomised comparison of continuous oxygen versus air therapy. It was limited to singleton pregnancies of 24-28 weeks gestation, where the foetuses presented with absent end diastolic flow persisting for a 12 hour period. Exclusion criteria included imminent eclampsia, maternal hypertension, chromosomal abnormalities, labour and an abnormal CTG.

Two measurements were made, twelve hours apart, in order to verify absent end diastolic flow. If this blood flow condition was confirmed, the mother was randomly assigned to

one of two groups. One group received normal room air and the other oxygen enriched air (40% oxygen). This was a blind trial where the type of gas received by each patient was undisclosed for the duration of the trial. Once participating in the trial, the mother was assigned bed rest and was required to wear a gas mask continually until delivery. Maternal treatment included aspirin (81mg) daily and steroids (Betamethasone 12 mg) from 29 weeks.

Subsequent measurements were then performed at 24hrs, 48hrs, 96hrs and weekly thereafter. Umbilical blood flow waveforms were gathered during each measurement and the foetus was clinically assessed according to a biophysical profile.

The foetus was delivered via Caesarean section as soon as it was viable. This was determined by a bubble test on the amniotic fluid obtained via amniocentesis.

7.2.2 DOPPLER WAVEFORM ACQUISITION

7.2.2.1 EQUIPMENT

The ultrasound image was obtained from a SIEMENS SL2 Duplex Doppler ultrasound machine with a 80Hz wall filter and 3.5MHz sector scanning transducer. The maximum flow waveform (MFW) was not offered via an output port of the ultrasound machine, but was available on an internal test point within the ultrasound machine.

This signal was processed by a unity gain buffering and anti-aliasing circuit. After extraction the maximum flow waveform was sampled using an Eagle Electric PC30D 12 bit analogue to digital conversion card. The data was written to a file and stored for later analysis. Analysis was performed using an IBM compatible 486DLC computer with customised analysis software written in Borland C++.

7.2.2.2 SAMPLING PROTOCOL

Spectral analysis performed on the maximum flow waveform determined the highest frequency component at any time in the foetal cardiac cycle, to be 30Hz. The maximum flow waveform was passed through a 2nd order low pass anti-aliasing filter with a cut off frequency of 35Hz. The filtered waveform was then sampled at 100Hz to satisfy the Nyquist criterion. Each record consisted of 1024 samples, representing a 10.24 second sample of blood flow in the umbilical artery as discussed in Appendix D.

The sampling protocol whereby maximum flow waveform data was captured is represented graphically in Figure 7-1.

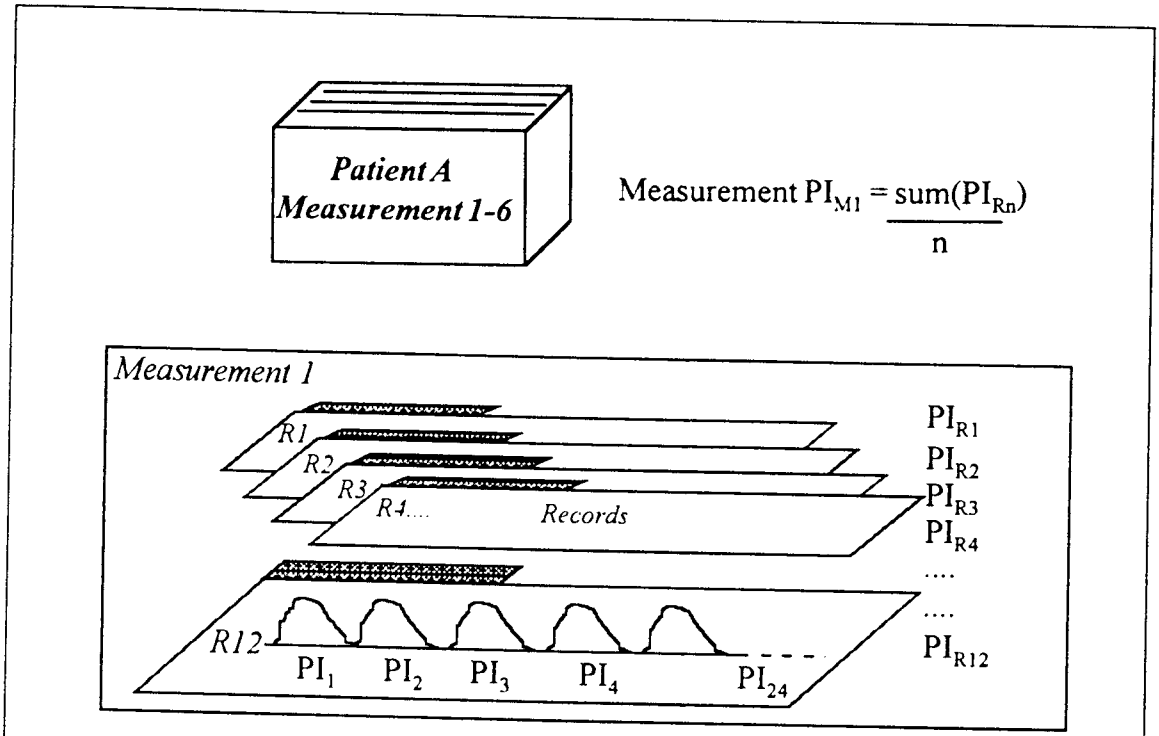

Figure 7-1 Sampling protocol

Each Doppler measurement performed consisted of between 10-14 records. Assuming an average foetal heart rate of 140-150 beats per minute, each record consisted of approximately 24 complete foetal cardiac cycles $PI_1, PI_2 .. PI_4 ... PI_{24}$. If the maximum flow waveform satisfied the validating criteria discussed in section 7.2.3, the pulsatility index

was then calculated for each of these cycles. The method used to determine the PI, representative of the entire measurement, is discussed in section 7.2.4.

7.2.2.3 PATIENT MEASUREMENT

All maximum flow waveform measurements were made relative to a zero flow baseline which was recorded at the start of each measurement.

The uterus was scanned using ultrasound imaging to locate the umbilical cord. The pulsed Doppler sample gate was placed over the umbilical artery and Doppler flow information was extracted from this site.

Any foetal, maternal or probe movement relative to the insonated vessels affects the Doppler signal obtained. This condition is particularly relevant for growth-impaired foetuses since the reduced liquor volume accentuated the maternal breathing movements and resulted in vessel movement within the sample volume.

7.2.3 DOPPLER WAVEFORM VALIDATION

The maximum blood flow waveform contains artefacts which degrade the signal quality. It was therefore necessary, before waveform analysis could be performed, to identify and exclude any known artefacts. In chapter six, sources of artefact such as excessive Doppler gain, low flow velocities, simultaneous insonation of adjacent vessels and vessel movement on the maximum flow waveform were identified.

These artefacts influenced the maximum flow waveform in predictable ways. It was therefore possible to define four conditions for waveform rejection. If any one or more of these conditions was found to be present in a waveform, the waveform was excluded from analysis.

1. Zero flow baseline drift or periodic flow modulation.
2. Unphysiological rate of change of blood flow.

3. Three or more high frequency spikes.
4. Noise spike or glitch period longer than the sampling period.

Artefact due to excessive Doppler gain, small signal strength and low flow velocities were indicated by conditions 3 and 4; simultaneous insonation of flow in opposite directions by condition 2; finally, the effect of maternal breathing by condition 1.

If a spike or glitch had a period equal to a sample period (0.01sec), it was assumed to originate from the processing hardware and was eliminated using the customised software.

7.2.4 WAVEFORM ANALYSIS

The pulsatility index was used to characterise the maximum umbilical blood flow waveform. The PI is a commonly used index which increases as waveform pulsatility increases. An increase in the waveform pulsatility is usually associated with a deterioration of foetal condition,(Rochelson et al. 1987).

Customised software was written to isolate each waveform. The PI's calculated from each individual waveform (as shown as PI_1, PI_2.. in Figure 7-1) were averaged to obtain a representative value for the record. This was done for each record resulting in an index matrix PI_{R1}, PI_{R2}....PI_{R10}.., PI_{R12} where subscript R denotes record.

Similarly, all the record indices - PI_{R1}, PI_{R2}....PI_{R10}.., PI_{R12} were averaged to determine a single pulsatility index, representative of the entire measurement. This PI, denoted as PI_M in Figure 7-1, was compared with previous measurements of the same foetus and was also used as a comparison between foetuses.

This form of analysis depends on the assumption that the intra-subject variability of the PI for each foetus is smaller than the corresponding inter-subject variability between foetuses. This assumption is validated in Appendix G.

7.3 RESULTS

7.3.1 PATIENT SUMMARY AND OUTCOMES

This trial lasted eight months, during which time data from seven patients was gathered.

Patient	Gest. (weeks @ entry)	Gas group	Maternal Complication	Foetal Outcome	APGAR Score	Foetal mass (age @ delivery)
A	24	AIR	Chronic H/T	I.U.D.	-	540g (28 wks)
B	27	AIR	Diabetic	Live Birth	3 and 6	650g (29 wks)
C	25	O_2	GPH	Live Birth	5 and 9	650g (28 wks)
D	25	O_2	GPH	Live Birth	5 and 7	1100g(28 wks)
E	24	AIR	GPH	I.U.D.	-	880g (27 wks)
F	25	AIR	GPH	Live Birth	3 and 3	760g (27 wks)
G	25	AIR	Chronic H/T	I.U.D.	-	570g (27 wks)

Table 7-1 Clinical trial summary

Abbreviations: GPH-gestational proteinuric hypertension, I.U.D-Intra uterine death, H/T-Hypertension, O_2-Oxygen, APGAR-scores out of ten to give an indication of the neonatal condition, 1 minute and 5 minutes after delivery.

Three of the seven foetuses in this study died before delivery. All foetuses were severely growth-impaired as their masses at delivery were all below the 10th centile for 27-29 week foetuses,(Theron & Thompson, 1995), Table 2-6.

7.3.2 PATIENT MEASUREMENT REGISTER

Each waveform was considered separately and accepted or rejected according to the validation criteria given in section 7.2.3. If more than 70% of the waveforms in any record were rejected according to the validation criteria, the record was also rejected. Table 7-2 shows the records for a single patient taken from the patient measurement register. In this

table the total number of records taken per measurement (TR) is compared with the number of acceptable records taken for each measurement (*AR*)

	Gest		M1	M2	M3	M4	M5	M6
Patient A	24	TR	10	7	5	9	10	13
		AR	*2*	*3*	*2*	*2*	*5*	*8*

Table 7-2 Patient measurement register
M denotes measurement number, Gest - gestational age at the first measurement.

The purpose of Table 7-2 is to demonstrate how few of the records captured for each measurement were accepted according to the validation criteria outlined in section 7.2.3. For example in measurement 1 of patient A only 2 out of 10 records were accepted for analysis.

7.3.3 LOW FREQUENCY FLOW MODULATION

Figure 7-2a shows a typical waveform that was captured during a patient measurement. This figure demonstrates the periodic modulation of the maximum flow waveform with time. Modulation of this type is considered as artefact and would result in the waveform being rejected due to criterion 1 of section 7.2.3. This characteristic was investigated further because many potential waveforms were rejected on the basis of this criterion.

Spectral analysis was performed on the record shown in Figure 7-2a to determine its constituent frequencies. The power spectral density function presented in Figure 7-2b shows that a large portion of the waveform energy is contained within the 0.2-0.5 Hz frequency range. This corresponds with the frequency of normal adult breathing,(Berne & Levy 1990). The origin of the maximum flow waveform modulation was thus ascribed to maternal breathing moving the vessel within the sample volume.

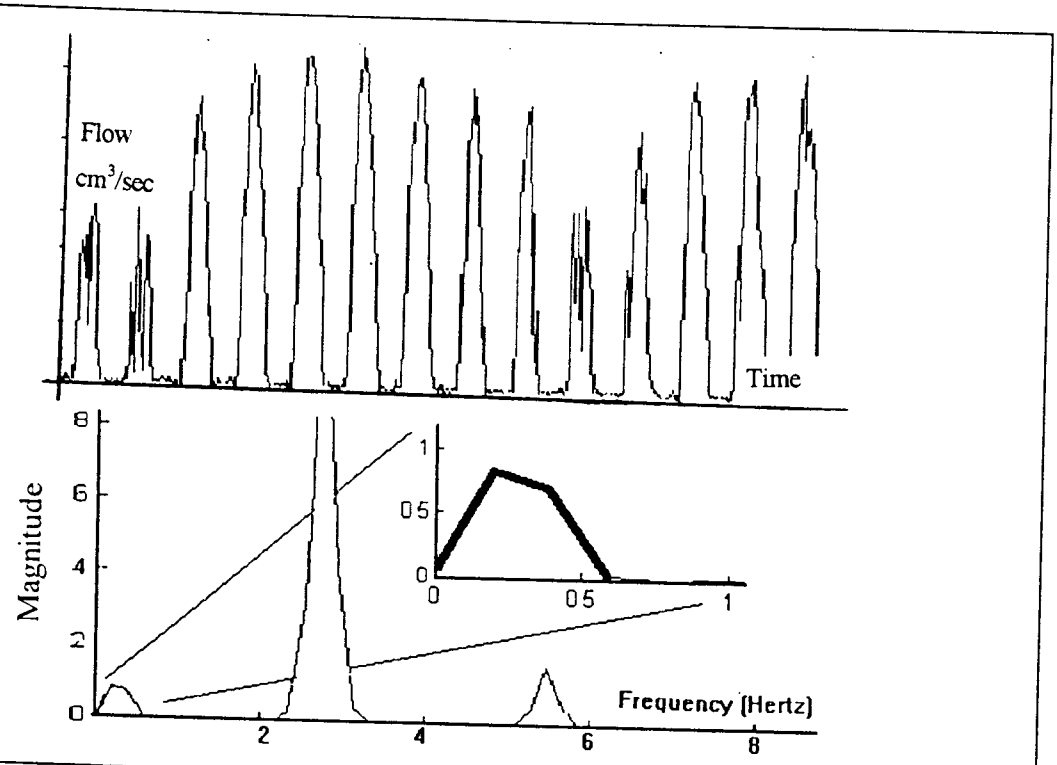

Figure 7-2a Maximum umbilical blood flow waveform with periodic vessel movement

Figure 7-2b Frequency spectrum of blood flow waveform.

7.3.4 PI INDEX VERSUS GESTATIONAL AGE

The data presented in Figure 7-3 represents the relationship between the pulsatility index and gestational age for all of the foetuses considered in this study.

Comparisons can not be made across a range of gestations for two reasons. Firstly, foetal compensatory mechanisms that are capable of alleviating, or at least offsetting, the effect of hypoxia and growth-impairment are dependent on gestational age. Secondly, the PI normally decreases with gestation age. Consequently, the PI which falls within the 95th centile for a 24 week old foetus, will fall outside this range for a 29 week old foetus. Figure 7-4, therefore, represents data taken from four patients who all started the trial at 25 weeks gestation.

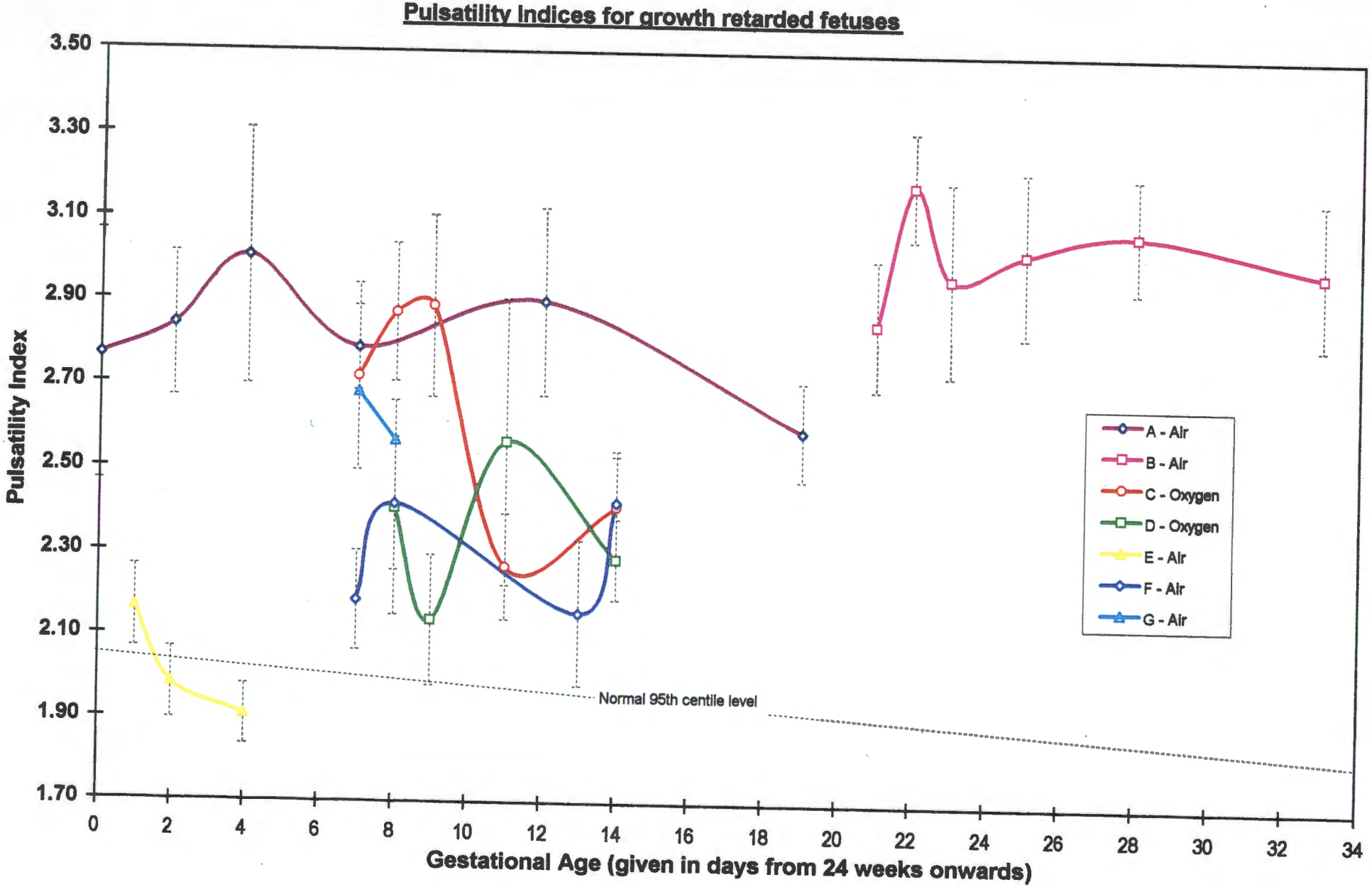
Pulsatility Indices for growth retarded fetuses
Pulsatility Index
3.50
3.30
3.10
2.90
2.70
2.50
2.30
2.10
1.90
1.70
0
2
4
6
8
10
12
14
16
18
20
22
24
26
28
30
32
34
Gestational Age (given in days from 24 weeks onwards)
A - Air
B - Air
C - Oxygen
D - Oxygen
E - Air
F - Air
G - Air
Normal 95th centile level

Figure 7.3

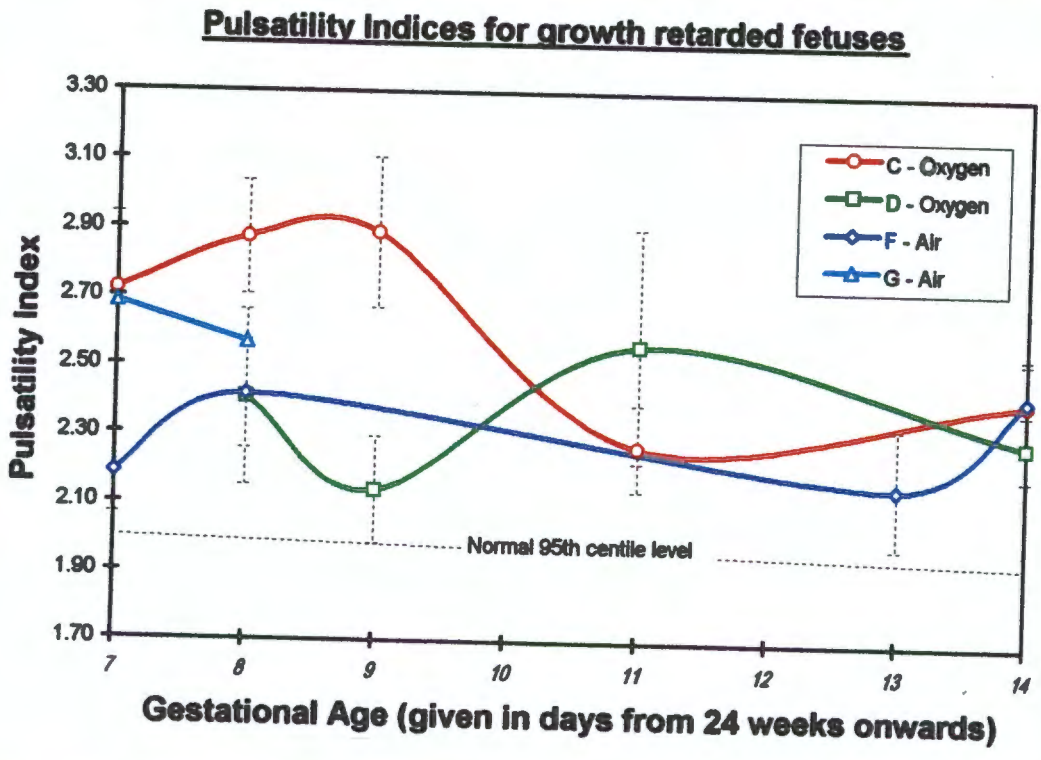

Figure 7-4 PI for SGA foetuses of 25 to 27 weeks gestation

7.4 DISCUSSION

The purpose of this discussion is twofold. Firstly, to give insight into the clinical and measurement protocols used, and secondly, to isolate basic relationships that may exist between PI, gestational age and maternal hyperoxygenation. No formal statistical trend analysis will be attempted as the sample size is too small.

7.4.1.1 GESTATIONAL AGE

Two clinical variables, namely gestational age and maternal pathology, compounded the accuracy with which measurements could be made. Some patients were unable to provide accurate menstrual dates, with the result that the gestational age had to be estimated using growth charts. This was inherently inaccurate since all foetuses included in this trial were

growth-impaired. This approximation limited the accuracy with which comparisons between foetuses could be made.

7.4.1.2 MATERNAL PATHOLOGY

Foetal growth-impairment and hypoxia can result from several maternal pathologies. For example, Table 7-1 shows three different maternal pathologies in the seven patients. Soothill et al.(1992) shows a broad range of foetal outcomes, depending on the maternal condition. Ideally, the maternal pathology should be common before any comparison can be made between two groups of patients, each receiving a different management protocol. Practically, however, isolating foetuses according to a specific maternal pathology would, according to the incidence noted thus far, result in a very long clinical trial.

7.4.1.3 SAMPLING PROTOCOL

The sampling protocol required approximately 10 records per measurement. Table 7-2 shows how few of the records captured met the validation criteria defined in section 7.2.3. Reduced liquor volumes, low volumetric blood flow conditions, small vessels, high ultrasound attenuation and vessel movement due to maternal breathing are all factors which degrade the Doppler signal. This effect is particularly pronounced in growth-impaired foetuses. Table 7-2 demonstrates the need for multiple records to be taken at each measurement since, for growth impaired foetuses, many of the captured waveforms are rejected as a result of measurement artefact. The number of records that can be captured, however, depends on the time over which the umbilical blood flow waveform shape can be assumed constant. This study found the waveform characteristics to remain constant over a 20-30 minute period.

7.4.1.4 DATA ANALYSIS

In Appendix G the co-efficient of variability (CV) was used to confirm that the variability between measurements (intra-variability), was less than the variability between patients

(inter-variability). The analysis technique as proposed in section 7.2.4 is thus a valid first order approximation for assessing a change in the umbilical blood flow waveform indices.

7.4.1.5 STATISTICAL EVALUATION

This pilot study captured data from seven patients, two of whom received oxygen and the other five normal room air. To determine the potential effect of maternal hyperoxygenation on the umbilical PI, measurements need to be taken from a statistically significant sample size. This sample size is calculated in Appendix G using information determined from this pilot study. A sample size of 64 patients (assuming 32 patients in both of the two groups) is required to determine a change in PI of 5%, similarly 16 patients are needed to determine a 10% change in PI, with a 95% confidence interval. In a seven month period this pilot trial monitored seven patients, where only two of these patients were administered oxygen.

7.4.1.6 VESSEL SAMPLING

Some studies on blood flow shunting in growth-impaired foetuses include blood flow signals from vessels other than the umbilical arteries.(Battaglia et al. 1992). In this study signal strength and resolution limitations prevented the Doppler signal from being isolated from the middle cerebral artery. In addition, noise interference from the foetal heart saturated the descending aortic flow measurement. Therefore, measurements and analyses were performed solely on the umbilical signal.

7.4.1.7 CLINICAL RESULTS

The final part of this discussion traverses the clinical results obtained from this study. Figure 7-3 plots the PI versus gestational age for all patients, and shows the PI of all but one patient, to be above the 95th centile. These raised values are indicative of foetal compromise with an associated risk to the foetus as illustrated by the intra-uterine death of foetuses A,E and G. For all three foetuses, the PI with respect to gestation shows a sharp decrease just prior to death. This trend is not consistent, since although the PI of foetus D

decreases sharply just before delivery, the foetus is born alive with an increasing APGAR score. The low APGAR score (5) of foetus D at birth might indicate that the foetal condition was deteriorating and without the oxygen treatment the foetal condition would have been further compromised.

Since the mechanisms which a foetus can employ to tolerate hypoxia depend on gestational age, comparison of the foetal response to maternal hyperoxygenation is only possible for foetuses of similar gestational age. This is particularly problematic where the accuracy of the gestational age is in question.

Figure 7-4 shows the PI versus gestational age for foetuses of approximately 25 weeks gestation. In this case study, of the four foetuses that could be compared, two (C,D) were randomly assigned to the group receiving oxygen enriched air and the other two F,G normal room air. Unfortunately foetus G died shortly after starting the trial. The remaining foetuses C,D and F were all of similar gestational age and had similar maternal pathology (GPH).

Of the three foetuses that survived, both foetuses receiving oxygen treatment were delivered alive with an improving APGAR score (5 to 9 and 5 to 7 for foetuses C and D respectively). Although foetus F was born alive, its APGAR score did not improve but remained constant at 3 (Table 7-1).

Comparison of this data shows graphs C and F exhibiting similar trends - initially rising, followed by an extended decrease before rising again. Graph D, however, showed tendencies completely opposite to those in graphs C,F. Consequently, it can be inferred that the effect of maternal hyperoxygenation has no obvious effect on the PI if the data obtained from this clinical trial is considered accurate.
The effect of maternal hyperoxygenation can only be speculated, as this pilot trial involved too few foetuses to reach a conclusive opinion.

7.4.1.8 ALTERNATIVE INDEX ANALYSIS

The clinical data analysed using the PI index was also analysed using the high resistance state index (HRSI), discussed in section 2-8. The HRSI is sensitive to the assessment of foetal compromise under absent end diastolic flow conditions,(Szentkuti et al. 1993). The two indices are compared in Figure 7-5. This graph plots the HRSI versus the PI for each measurement and shows an approximately linear relationship of the indices for a PI range of 2.3 - 3.0.

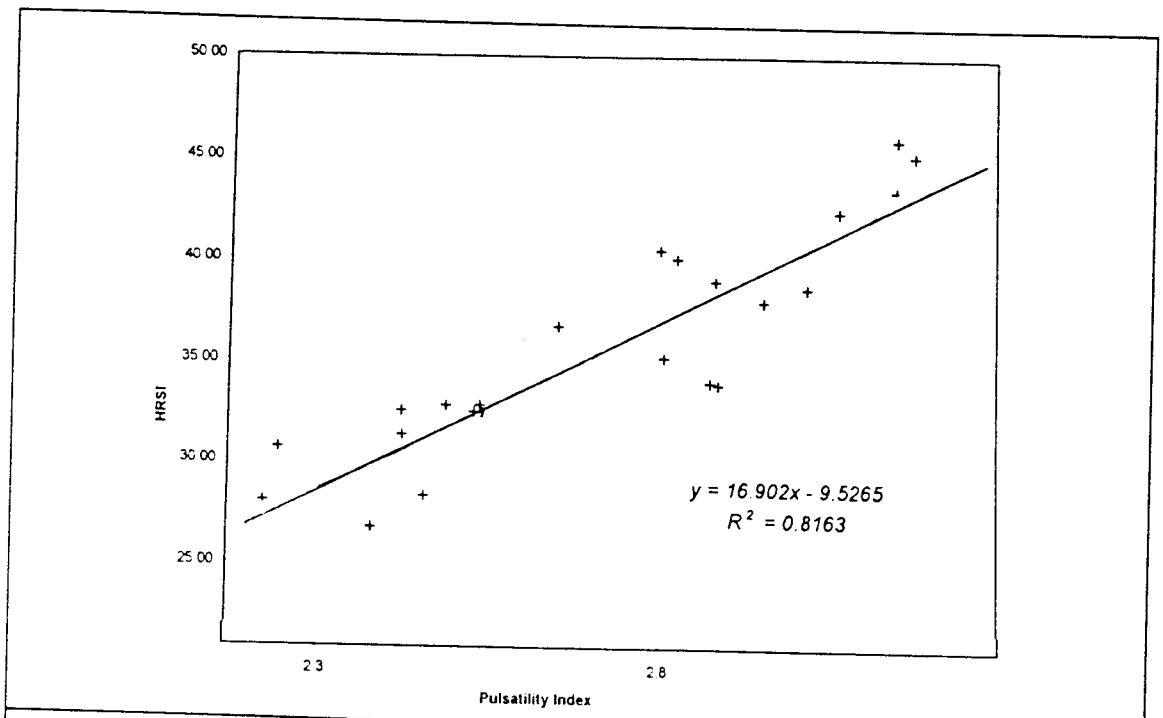

Figure 7-5 HRSI versus PI

7.5 CONCLUSION

This pilot study isolated many of the statistical and clinical considerations which need to be accommodated when using Doppler ultrasound in a larger, statistically significant, clinical trial. It was calculated that there would have to be at least eight patients in each of the two groups to isolate a change of 10% (95% probability) in the umbilical PI. Measurement and sampling protocols have been suggested to ensure accurate data

measurements. These techniques have been implemented and have proved suitable for the analysis of changes in the flow waveform shape. Analysis of the limited data available did not, however, display any apparent trends attributable to maternal hyperoxygenation. This does not imply that maternal hyperoxygenation has no effect on other aspects of foetal physiology, but rather that it had little effect on the umbilical flow waveform as characterised by the pulsatility index.

8. DISCUSSION

This study has investigated the theoretical and practical aspects which need to be considered when using Doppler ultrasound to assess the condition of small-for-gestational-age foetuses. The four objectives proposed in Chapter 1 (Page 4) have been addressed as follows:

1. A comprehensive survey of the literature was undertaken to gather information on the circulation of a foetus in its 28th gestational week. Objective information regarding the blood flow distribution, special anatomical adaptations, arterial dimensions and wall properties were obtained, for both normal foetuses and those experiencing adverse conditions.
2. A model of the foetal circulation was implemented by dividing the foetal vasculature into discrete units. Each individual vascular unit was characterised by electrical analogous flow parameters which were calculated from data in the literature. When appropriate data from human foetuses was not available the information was taken from studies of ovine foetuses. Different blood flow distributions, ranging from normal to hypoxic, were simulated by suitably adjusting the characteristics of each unit.
3. Limitations of Doppler ultrasound as an appropriate technique to assess growth impaired foetuses were investigated through tests performed on a flow phantom. The Doppler sample volume insonated two thin silicon tubes containing a flowing solution of microspheres to approximate the umbilical vessels and foetal blood flow respectively.
4. Finally, a pilot study was performed to define protocols and investigate potential problems that would be encountered when using Doppler ultrasound flow velocity indices to characterise the condition of the foetus. The findings of this study could be used to plan a large trial, involving a statistically significant number of patients.

The findings from each of these objectives are discussed in this chapter.

8.1 LITERATURE SURVEY

8.1.1 NORMAL FOETAL CIRCULATION.

Normal anatomical data was gathered from the literature for a normal foetal population in it's 28th gestational week. Suitable simplifications were made to enable the foetal vasculature to be represented in a model. Anatomical data of this type was scarce and parameters that could not be obtained from the literature, were gathered from post mortem studies. This study therefore obtained anatomical data from various sources and although the results correspond to those in the literature, an attempt should be made to standardise the origin of the anatomical data for future studies.

Data concerning the foetal blood flow distribution under different foetal conditions was only available for animal studies. The blood flow distributions of ovine foetuses, as measured by isotope labelled microspheres, were used to approximate that of a human foetus. The normal foetal circulations of human and ovine foetuses have been shown to be well correlated and therefore the changes in ovine circulation due to hypoxia and placental embolisation were considered appropriate for a human foetus.

As a result of insights gained from this study, the simplifying assumptions made regarding the blood viscosity, vessel radius and wall elasticity should be reconsidered in subsequent modelling.

- Foetal blood viscosity was approximated by that of adult blood and was assumed constant for all modelling conditions. This is a severe simplification of viscosity which is a function of many variables including vessel radius. Changes in modelled viscosity were found to affect the pulsatility of the output flow waveform shape significantly, suggesting a more detailed approximation to foetal blood viscosity in subsequent studies.
- Vessel wall radius affects the resistance of parabolic blood flow as described in Equ 4-1. An error of 10% in the radius measurement translates to an error of 32% in the calculated flow resistance, due to the inverse fourth power relationship between resistance and radius. This study was forced to use radius measurements from both in vivo and in vitro studies, both with large standard deviations, due to limited data. Until

comprehensive anatomical data is obtained from a large sample, the accuracy with which these parameters can be estimated will be an inherent limitation of blood flow modelling.

- Another factor that influenced the flow waveform shape significantly was Young's modulus, which offers an indication of the vascular wall elasticity. The value used in this study was the average modulus of adult vasculature determined from the literature, (McDonald, 1974). The range of Young's modulus for different tissues is small, but the actual value used in this study must still be verified as appropriate for the different foetal vessels at 28 weeks gestation.

The model used in this study did not include feedback control of physiological processes since it was configured to track individually defined foetal blood flow conditions. The chemo- and baro-receptors were found to be functional by the 28th gestational week and their effect could be incorporated into the model through the suitable control of the stroke volume, heart rate and peripheral impedance. It is extremely difficult to model these mechanisms employed by the foetus since these complex controls are still under clinical investigation.

8.1.2 COMPROMISED FOETAL CIRCULATION

The literature is inconclusive regarding the aetiology and progressive development of different circulatory pathologies which result in SGA foetuses. Incomplete trophoblastic invasion, hormonal vasoconstriction and incomplete placental development are all currently being investigated. Regardless of the origin, however, a compromise in the maternal or placental circulations restricts the supply of gases across the placenta resulting in foetal hypoxia. The effect of foetal compromise on the maternal physiology is currently under investigation and the reader is referred to Davey & MacGillivray (1988) for a detailed discussion.

Acute hypoxia is defined as a brief absence of nutrient and gaseous supply to the foetus ($\leq \pm 4$mins), whereas chronic hypoxia corresponds to a gradual decrease in the supply of gases and nutrients to the foetus occurring over an extended period. By the third trimester,

foetal compensatory mechanisms are sufficiently developed to limit the effect of adverse hypoxic conditions on the foetus. The foetal response to these adverse conditions, however, depends on the type of insult (acute or chronic) as well as the current state of foetal health.

This study found the umbilical PI inversely related to the percentage of blood flowing to the placenta. This result agrees with findings made by Maulik et al.(1992) who noted that for peripheral organs (including the placenta), "both in vitro and in vivo studies show an increase in PI with an increase in peripheral resistance". Blood flow distribution data collected by Block et al.(1990) and shown in Table 5-5, illustrates how foetal hypoxia can cause an initial increase in the percentage umbilical blood flow due to foetal blood flow shunting effects. This initial increase results in a decrease in the umbilical PI. When the foetal compensatory mechanisms fail, as would be the case for severe acidosis, the PI begins to increase with continued hypoxia. An increase in PI with continued hypoxia is illustrated by Downing et al.(1990).

8.2 FOETAL CIRCULATORY MODEL

Modelling the foetal vasculature by its electrical analogous equivalent, enabled existing circuit analysis techniques to be used. This approach enabled the foetal vasculature to be considered in discrete modules which allowed the complexity of each model unit to be varied. Two port analysis of the foetal vasculature provides the pressure and flow transfer function of the arterial system at the input or output of any model unit.

This model was not configured to perform transient analysis and therefore information regarding the manner in which the arterial system changed with time could not be obtained. Instead, the model isolated a single input frequency and determined the corresponding output as a function of the foetal vasculature. This approach was considered suitable for investigating discrete foetal states set by the properties of the foetal vasculature and the heart input. The outcome using this approach depends upon the condition of the foetal vasculature and the input waveform from the foetal heart. An improvement of this model would be to implement a control loop adjusting the cardiac parameters of heart rate and stroke volume.

Since the input to the model (the flow from the heart) is not known, it has been approximated by a simple waveform for the purposes of this model. The effect of varying the harmonic content and the waveform profile was investigated for both normal and hypoxic foetuses. The effect of the input waveform on the modelled umbilical PI was found to be negligible and therefore the potential inaccuracies incurred by this input approximation were considered acceptable. However, techniques more sensitive than the PI to blood flow waveform shape changes could, for example, be used to extract clinical information from the umbilical flow waveform regarding the cardiac contractility.

The impedance to flow of each modelled region was calculated by dividing the average arterial pressure by the average flow to that region. This was done for a number of foetuses with varying degrees of hypoxia. The average flow was obtained in each case from ovine flow measurements using microspheres. This is a simplification of the actual situation where a phase difference exists between the pressure and flow. These considerations were beyond the scope of this thesis but are recommended for further study.

8.2.1 SIMULATIONS

Simulations performed with this model demonstrated the following.

- Poiseuille's resistance to flow defined by Equ 4-1 assumes a parabolic flow profile, whereas inertance of blood in Equ 4-2 assumes plug flow. The plug flow inertance is converted to parabolic flow inertance by a scaling factor of 1.35 defined by Wormersley. Parabolic flow effects were compared to non-parabolic flow by the inclusion of frequency dependent parameters ε and M_{10} to the definition of flow resistance and inertance (Equ E-1, E-2). The resultant effect of frequency dependent flow components on the PI were negligible (less than 0.03%) and could therefore be ignored during subsequent analysis.
- The results shown in Figure 5-2 illustrate the foetal ability to tolerate a large degree of terminal vessel obliteration at 28 weeks gestational age. Any placental obliteration places the foetus at risk during later gestations when the requirements of the foetus on the placenta become critical. The findings of this model correspond well with those recorded by Thompson & Trudinger (1990). Both modelled results correspond well

with clinical data obtained by Morrow et al.(1989) which showed the placental flow resistance to remain constant until a large degree of placental embolisation had occurred, after which the resistance increased rapidly.

- The effect of blood flow shunting, as represented by the umbilical PI, was found to depend on the state of the foetus. The change in PI as a result of hypoxic conditions was larger for an unembolised placenta than the PI change for an embolised placenta. This finding complements the work done by Field et al.(1990) who showed that cerebral compensatory mechanisms only act over a limited range. Field showed that when the amount of oxygen in the foetal blood decreased below a threshold limit the compensatory mechanisms fail.
- A similar response to that found in the literature was noted when using the PI to model severely compromised foetuses. Under these conditions, the PI was found to decrease with a corresponding deterioration of the foetal condition. This response is different to the normal increase in PI for a corresponding deterioration in the foetal condition. The ability of the PI index to represent the condition of the foetus was thus shown to have a limited range. Results from this model, as shown in Figure 5-6, illustrate how the difference between diastolic and systolic extremes decreased faster than the mean flow value for large degrees of placental impedance. The physiological cause for this uncharacteristic change in the umbilical blood flow waveform shape has not as yet been investigated.

8.3 DOPPLER LIMITATIONS

A major advantage of Doppler analysis is its ability to monitor blood flow within the foetal vasculature without compromising the normal flow distribution. It is, however, inherently dependent on the attenuation of the ultrasound signal by intervening tissue, and the reflection of the incident wave by moving particles within the sample volume. Doppler analysis therefore has certain limitations which restrict its suitability for determining flow profiles under all conditions.

The signal strength received from growth-impaired foetuses, with small vessels and reduced blood volumes, is weak since the strength of the received Doppler signal is directly

proportional to the blood volume flowing within the sample volume. Increasing the gain to allow for the weaker signal is limited by the potential of the input amplifier to saturate. Weak signals are thus prone to artefact which corrupts the flow information of the Doppler signal and results in inaccurate waveforms. In this study these waveforms have been identified and rejected.

This feasibility study found that only a small fraction of the data rejected was due to noise and filtering artefact originating from the Doppler machine. The major fraction of rejected waveforms was as a result of artefact inherent in Doppler analysis. This study noted three predominant factors which compounded the accuracy of Doppler measurements on growth-impaired foetuses :

- Firstly, umbilical arteries normally helix tightly around the umbilical vein. In growth-impaired foetuses these vessels are very thin and narrow making it impossible to isolate the umbilical artery from the umbilical vein. The MFW is thus dependent on the ability of the maximum flow algorithm to differentiate between the origins of the two signals. Under these conditions, the resultant flow profile is determined from the simultaneous insonation of two vessels.
- Secondly, due to the reduced liquor volume, the effect of maternal breathing on the foetus is pronounced. This movement causes relative displacement of the foetal vessels within the sample volume and results in a Doppler MFW which unrepresentative of the flow profile within the vessel.
- Finally in growth-impaired foetuses, blood flow during diastole can decrease to the extent that it is absent or reverses direction. The Doppler wall filter removes the effect of all slowly moving particles that would otherwise saturate the Doppler circuitry. Under low flow conditions the wall filter removes the low velocity components of the flow waveform, resulting in an incomplete representation of blood flow within the vessel.

The artefact resulting from small flow volumes, vessel movement and low flow conditions has important implications for Doppler machines that offer automatic flow waveform analyses. Under these conditions, the sonogram should be used to verify the results of the maximum flow waveform algorithm. It is important to note that signal processing

algorithms that function well for normal foetuses, may introduce waveform artefact when used to process the small signals that originate from SGA foetuses.

Analysis using a pulsed wave Doppler extracts flow information from any particle moving within the sample volume defined by the Doppler beam and the timing of the pulsed gate. In this way the location from where the Doppler information is being determined can be defined. Continuous wave Doppler does not have a pulsed gate and therefore offers no range information. The sample volume is defined solely by the Doppler beam. Continuous wave Doppler is thus less dependent on relative vessel motion than pulsed Doppler. This study cannot offer an opinion as to which is more suitable for assessment of growth impaired foetuses since continuous wave Doppler was not used. Brar et al.(1989), however, showed no advantage of pulsed over continuous wave Doppler analysis. The choice of equipment thus depends on the trade-off between information pertaining to the sample volume location and the dependence on relative vessel movement.

8.4 CLINICAL TRIAL

This feasibility study performed a pilot clinical trial to determine the requirements necessary to initiate a statistically significant trial, with sufficient patients, to ascertain the effect of maternal hyperoxygenation. This involved developing a suitable clinical sampling protocol and obtaining relevant statistical variables to determine the required sample size.

Sample size

The sample size required to differentiate between two groups, one receiving oxygen enriched air, and the other room air, was calculated using the standard deviation determined in this pilot trial. Appendix G shows that at least 8 patients would be required in each group, to determine a change of 10%. This study found the incidence of foetuses with absent end diastolic flow to be low, since only seven patients were monitored during this seven month trial. A trial requiring a sample size of 16 would therefore need to be obtained from a relatively large geographic area.

Sampling protocol

This trial found that when monitoring growth impaired foetuses, at least ten records were required per measurement, due to the large percentage of sampled data which was rejected. Rejection criteria were established from potential artefact identified by the simulations done in Chapter 5 and flow phantom tests done in Chapter 7. These investigations found the predominant causes of artefact in growth-impaired foetuses to result from low signal strength, vessel movement and concurrent vessel insonation.

Data analysis

It is difficult to chose an index that is able to characterise umbilical blood flow over a wide range of conditions. The choice of index depends on many variables such as foetal condition, comparative data and noise susceptibility. Although the PI is not the ideal index with which to monitor foetal condition, it offers a simple method to represent the waveform pulsatility, which in turn is dependent on the foetal condition. Several disadvantages need to be considered when using the pulsatility index, for example:

- The PI is sensitive to small changes in the blood flow waveform, but has a large normal range. Large ranges were found when comparing data captured for a European population, ($PI_{95centile}$-$PI_{5centile}$=0.98; $PI_{50\ centile}$ = 1.12,(Arduini & Rizzo, 1992)) and a local population, ($PI_{95centile}$-$PI_{5centile}$=0.85; $PI_{50\ centile}$ = 1.15 ,(Pattinson et al., 1989). These large normal ranges limit the PI's ability to use small changes in the waveform shape, to isolate a deteriorating trend for a particular patient.
- The PI determines the difference between the systolic maximum and diastolic minimum and is therefore susceptible to noise. The PI of a cardiac interval containing spikes and glitches would thus not be representative of the blood flow during that interval.

Conversely, the pulsatility index :

- is used extensively in the literature to characterise blood flow thus enabling a large resource for comparison of results.
- does not saturate during absent flow like the resistive index and A/B ratio, but rather provides information under all flow conditions.
- offers similar insight into the foetal condition as compared with the HRSI, which is designed to be sensitive to absent and reversed flow.

Comparative limitations

The comparison of data to determine the effect of maternal hyperoxygenation was found to depend on the maternal pathology and the accuracy of menstrual dates.

- The gestational age of growth-impaired foetuses cannot be determined from normal growth charts. Therefore, the accuracy with which comparisons can be made depend on the accuracy of the maternal menstrual dates.
- A decrease in the foetal arterial oxygen content can be achieved through many different methods, for example, maternal hypoxemia, reduction in umbilical or uterine blood flow and placental embolisation. Table 5-5 shows how the foetal response differs according to the manner in which hypoxia was induced. This indicates that any type of comparative result can only be determined if the cause of the hypoxic insult is common between the foetuses.

Consequently, comparison of data to determine the effect of maternal hyperoxygenation, can only be made between foetuses which are exposed to similar maternal pathologies, and which are of similar gestations.

Pilot trial results

In this pilot study, data from seven patients was captured and analysed. Four of these were of the same gestational age and had similar maternal pathologies, allowing them to be compared directly. Three of these four foetuses survived. Both foetuses receiving oxygen treatment were delivered alive with an improving APGAR score (5 to 9 and 5 to 7 for foetuses C and D respectively). Whereas, although foetus F was born alive, its APGAR score (3) did not improve but remained constant (Table 7-1).

The PI calculations performed on the umbilical artery for each of these foetuses found no repeatable pattern in the umbilical blood flow response as a result of maternal hyperoxygenation. The clinical outcome of this small controlled trial supports the work done by Nicolaides et al. (1987), and indicates the need for a larger statistical trial that will be able to demonstrate the significance of the effect of maternal hyperoxygenation.

9. CONCLUSIONS AND RECOMMENDATIONS

The aim of this thesis was to investigate the feasibility of using the shape of the umbilical flow waveform, obtained clinically with Doppler ultrasound, to monitor the condition of growth impaired foetuses.

Based on the findings of this study, the following theoretical conclusions can be drawn and clinical recommendations made.

9.1 CONCLUSIONS

A model of the foetal circulation was developed that is representative of normal and compromised foetal flow conditions under the stated assumptions.

The Doppler umbilical blood flow waveform shape is an appropriate indicator of foetal condition, since a change in peripheral flow impedance and blood flow distribution, which depend on the foetal condition, can be observed by a corresponding change in umbilical blood flow waveform shape.

The pulsatility index, as determined from the umbilical blood flow waveform, is not the ideal index with which to characterise a change in foetal condition, due to its insensitivity to preferential blood flow shunting and limited range over which it can represent the foetal condition. The index does, however, provide a useful indicator of the placental impedance which has been shown to correlate well with the foetal condition.

9.2 CLINICAL RECOMMENDATIONS

The maximum flow waveform should be verified against the flow sonogram, when monitoring growth-impaired foetuses, to ensure an accurate representation of the flow profile within the vessel.

At least 10 records need to be obtained for each measurement when assessing growth-impaired foetuses to accommodate the loss of waveforms which are rejected due to artefact.

Before any conclusion is drawn as to the possible benefit of oxygen therapy, the potential damage caused to maternal and foetal tissue by prolonged oxygen treatment, must also be investigated.

It is recommended that in future studies an ultrasound machine be used that is capable of accurately determining flow within the middle cerebral artery.

Finally, findings of the electrical analogous flow model should be verified experimentally on ovine foetuses.

Appendix A SEGMENT LENGTH

The model in chapter four divided the artery into equal segments. The phase velocity and the wavelength of the wave travelling in the artery determined the length of each segment and in turn the number of segments required. For the lumped-parameter distributed-element approximation, each segment must be less than one tenth of the minimum wavelength present in the travelling wave. The minimum wavelength is defined by

$$\lambda_{min} = \frac{Vp}{f_{max}} \qquad \text{Equ A-1}$$

λ_{min} -Minimum wavelength.

Vp -Phase velocity of the travelling wave.

f_{max} -Maximum frequency present in the travelling wave.

The phase velocity of a wave travelling along a transmission line depends on the propagation factor gamma (γ). Gamma (γ) is a function of frequency (ω), resistance (R), inertance (L), equivalent conductance (Geq) and compliance (Ceq).

$$\gamma = \sqrt{(R + j.\omega.L) * (Geq + j.\omega.Ceq)} \qquad \text{Equ A-2}$$

The propagation factor (γ) can be separated into its real and imaginary components giving

$$\gamma = \alpha + j.\beta \qquad \text{Equ A-3}$$

$$\text{attenuation factor } \alpha = \sqrt{\frac{\sqrt{\omega^2.L^2.(Geq^2 + \omega^2.Ceq^2)} - \omega^2.L.Ceq}{2}} \qquad \text{Equ A-4}$$

$$\text{and phase factor } \beta = \sqrt{\frac{\sqrt{\omega^2.L^2.(Geq^2 + \omega^2.Ceq^2)} + \omega^2.L.Ceq}{2}} \qquad \text{Equ A-5}$$

Once the phase factor and the maximum frequency component of the travelling wave have been estimated, it is possible to solve for the phase velocity and the minimum wavelength.

$$Vp = \frac{2.\pi.f_{max}}{\beta} \text{ and} \qquad \text{Equ A-6}$$

$$\lambda_{min} = \frac{Vp}{f_{max}} \qquad \text{Equ A-7}$$

Therefore, the length of an arterial segment should be less than or equal to one tenth of the wavelength.

$$\text{Length}_{\text{arterial segment}} \leq \lambda_{min}/10 \qquad \text{Equ A-8}$$

Table A-1shows the phase velocity (Vp) and the corresponding wavelength (λ) for a range of wave harmonics propagating along specific arterial vessels. The phase velocity and wavelength present when no attenuation of propagation occurs (lossless), are given for comparison.

AORTA				
	radius = 0.315cm		wall thickness = 0.028 cm	
Harmonics	Vp (cm/s)	λ (cm)	Vp (lossless) (cm/s)	λ (lossless) (cm)
fundamental	640	274	715	306
2nd	663	142	723	155
3rd	674	96	725	103
4th	**681**	**73**	726	78
COMMON ILIAC ARTERY				
	radius = 0.144cm		wall thickness = 0.0055cm	
Harmonics	Vp (cm/s)	λ (cm)	Vp (lossless) (cm/s)	λ (lossless) (cm)
fundamental	367	157	402	172
2nd	397	85	447	95
3rd	**409**	**58**	461	66
4th	416	44	467	50
UMBILICAL ARTERY				
	radius = 0.107cm		wall thickness = 0.0011cm	
Harmonics	Vp (cm/s)	λ (cm)	Vp (lossless) (cm/s)	λ (lossless) (cm)
fundamental	167	71	178	76
2nd	193	41	213	75
3rd	**203**	**29**	227	32
4th	208	22	234	25

Table A-1 Phase velocity and wavelength calculations for various harmonics.

A heart rate of 140 beats per minute or a fundamental frequency of 2.3Hz was assumed.

The length of each segment must be $\leq \lambda/10$ (the frequency harmonic chosen for each vessel is indicated by the bold text) . These wavelengths are used in Table A-2 to determine the segment length.

Table A-2 Derivation of segment length for various arterial vessels

Aorta -	λ = 73cm
	minimum segment length $\equiv \lambda/10$ = 7.3cm
	Segments required = $^{\text{vessel length}}/_{\text{min segment length}}$ = 7.5/7.3 = 1.03
	Number of segments used = 4
	Segment length = 1.2cm
Common Iliac	λ = 58 cm
	minimum segment length $\equiv \lambda/10$ = 5.8cm
	Segments required = $^{\text{vessel length}}/_{\text{min segment length}}$ = 1.2/5.8 = 0.21
	Number of segments used = 2
	Segment length = 0.6cm
Umbilical -	λ = 29 cm
	minimum segment length $\equiv \lambda/10$ = 2.9cm
	Segments required = $^{\text{vessel length}}/_{\text{min segment length}}$ = 19.1/2.9 = 6.58
	Number of segments used = 8
	Segment length = 2.4cm

Appendix B UNIT VALIDATION

All values used in this document are given in CGS (centimetres, grams , seconds) units as used by McDonald (1974). The following conversion factors are required to convert pressure and flow to their CGS equivalent units.

Pressure : 1cmHg ≡ 133.3 dynes.cm^{-2}

Flow : 1ml /min ≡ $^{1}/_{60}$ cm^{3}.sec^{-1}

Table B-1 CGS units

	Equivalent	Units
Pressure		dynes.cm^{-2}
Flow		cm^{3}.sec^{-1}
Resistance to flow	pressure/flow	dyne.cm^{-5}.sec^{1}
Equivalent compliance	volume/pressure	dynes^{-1}.cm^{5}

The unit of resistance as determined by the ratio of pressure and flow, is equivalent to the unit of resistance as derived from Poiseuille's equation. This shown in the two equations below.

$$\text{Resistance to Flow} = \frac{\text{Pressure}}{\text{Flow}} \equiv \frac{(dyne.cm^{-2})}{(cm^{3}.\sec^{-1})}$$

The units for ratio of pressure to flow are therefore - : $(dyne.cm^{-5}.sec)$

$$\text{Poiseuille's Equation} \quad R = \frac{8.\mu.\partial x}{\pi.r^{4}} \equiv \frac{(dyne.cm^{-2}.\sec.cm)}{(cm^{4})}$$

The units for resistance to flow according to Poiseuille are - : $(dyne.cm^{-5}.sec)$

Appendix C TWO PORT ANALYSIS

Two port circuit analysis is a circuit simplification technique that enables each segment to be represented by an equivalent two dimensional matrix. Each matrix, or two port block, has a voltage and current input, and a voltage and current output. The relationship between these depends upon the electrical analogous components contained within each block.

There are several ways in which the input voltage (Vin) and current (Iin) and output voltage (Vout) and current (Iout) can be compared. For the purpose of this discussion, only those parameters which enable the successive cascading of two port blocks will be considered. These are described by Equ C-1 and Figure C-1 below.

$$\begin{bmatrix} Vin \\ Iin \end{bmatrix} = \begin{bmatrix} A_{11} & A_{12} \\ A_{21} & A_{22} \end{bmatrix} \begin{bmatrix} Vout \\ -Iout \end{bmatrix} \qquad \text{Equ C-1}$$

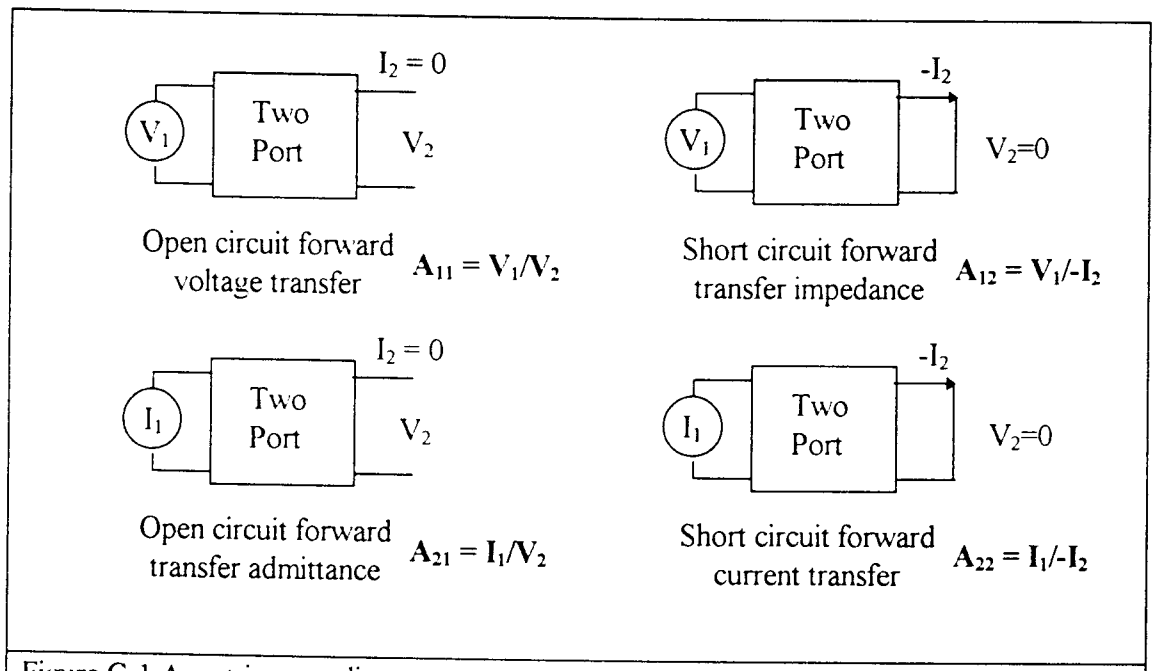

Figure C-1 A matrix cascading parameters

Equation C-1 can be expanded into the form shown in Equation C-2

$$Vin = A_{11}.Vout - A_{12}.Iout \qquad \text{Equ C-2}$$

$$I\,in = A_{21}.Vout - A_{22}.Iout \qquad \text{Equ C-3}$$

The placental impedance can be determined from Equation C-3

$$Vout = Zplacenta \times Iout \qquad \text{Equ C-4}$$

Inserting Equation C-4 into Equation C-3

$$Iin = A21.\,Zplacenta.\,Iout + A22.\,Iout \qquad \text{Equ C-5}$$

$$\text{or} \quad \frac{Iout}{Iin} = \frac{1}{(A_{21}.Zplacenta + A_{22})}$$

This ratio represents the current/flow transfer function of the foetal arterial network.

Only two types of circuits were required to model the foetal arterial system and these are shown with their equivalent two port cascade parameters in Figure C-2.

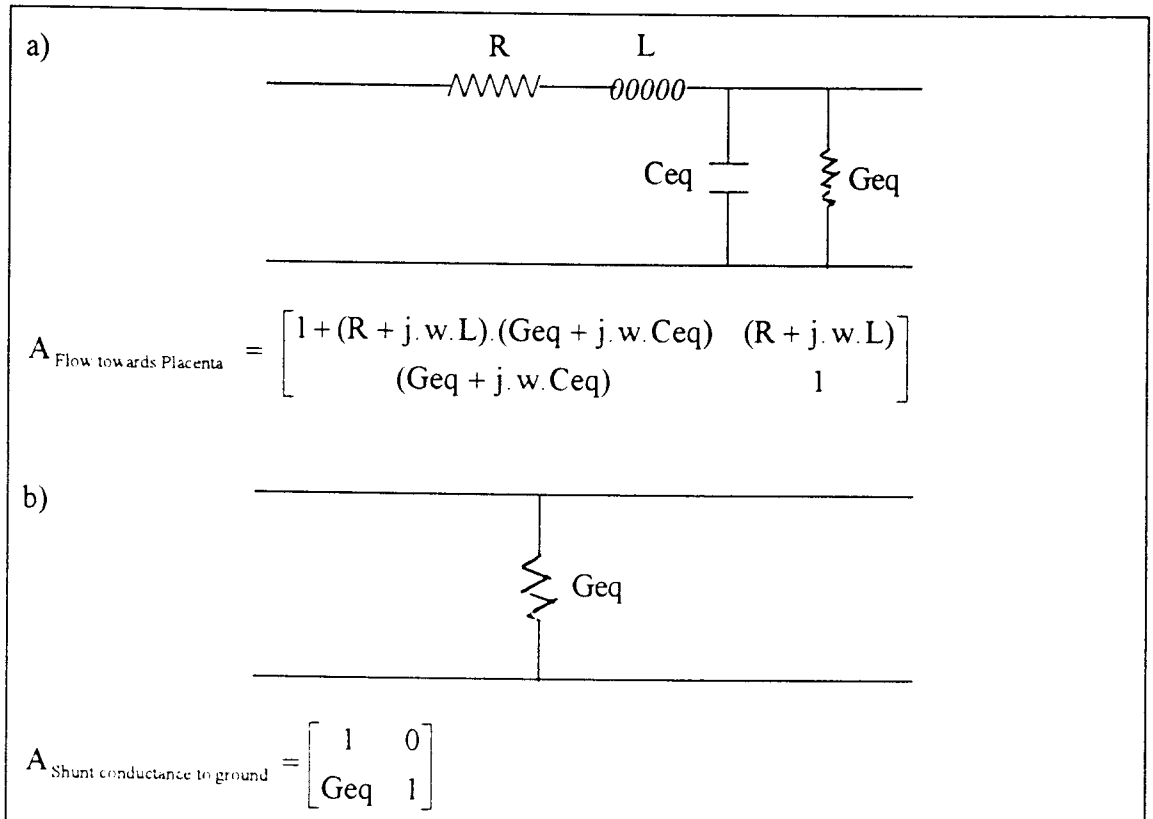

Figure C-2 Two port equivalents of vessels shunting blood towards a) and away b) from the placenta.

Both components namely those describing vessels conducting flow towards the placenta and those describing vessels conducting flow away from the placenta have been represented in terms of their A parameter matrix. Successive vascular components can be cascaded by matrix multiplication of their corresponding A parameters (Figure C-1). This analysis technique allows an equivalent A parameter matrix to be determined that is representative of the entire foetal circulation.

Appendix D SPECTRAL ANALYSIS

Figure D-1a below shows one cardiac cycle of a typical input waveform that has been sampled and zero padded to achieve the required frequency resolution for the frequency spectrum Figure D-1b.

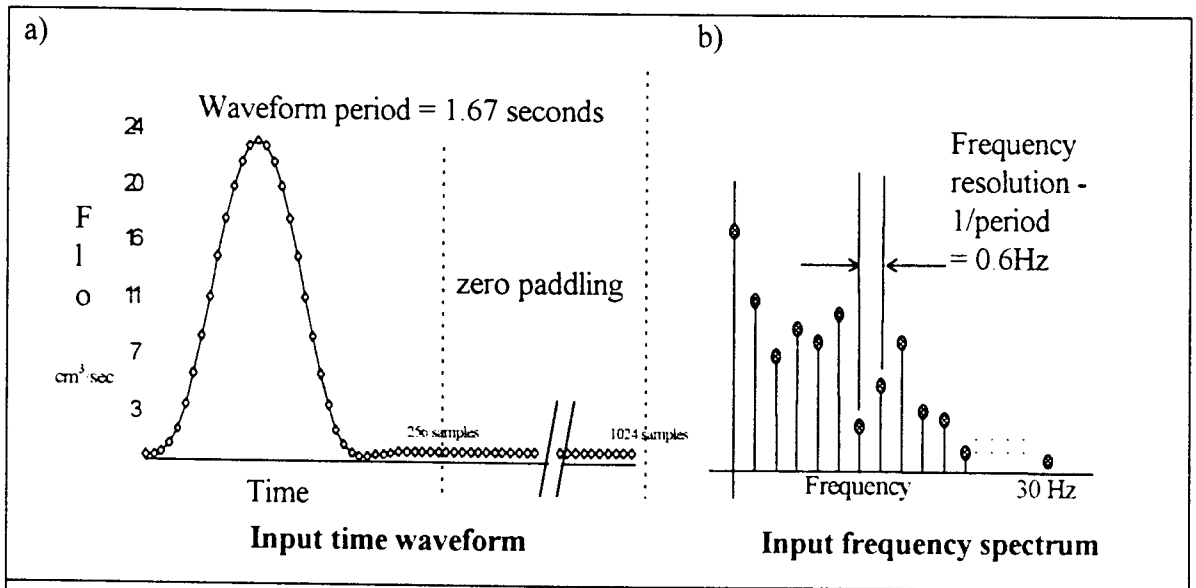

Figure D-1 Input flow waveform and corresponding frequency spectrum.

The normal foetal heart rate for a 28 week foetus is approximately 140 beats per minute, Polin & Fox (1992). This is equivalent to a heart beat frequency of 2.32 Hz and period of 0.43sec. The frequency resolution obtainable in spectral analysis is equal to the inverse of the sampling period (T) as shown in Equ D-1.

$$\text{frequency resolution} = \frac{1}{T} \qquad \text{Equ D-1}$$

A frequency resolution of 0.6Hz was determined to be adequate for the input flow waveform which according to Equ D-1 sets the sampling period at 1.67sec. The input flow waveform was therefore zero padded,(Stremler 1989), from 256 to 1024 samples to adjust the sampling period from 0.43sec to 1.67sec. (Figure D-1)

The individual spectra of the input waveform frequency response were thus determined with a resolution of 0.6Hz. This corresponds to the frequency resolution for which the arterial transfer function was determined in section 4.5.

Appendix E WORMERSLEY CONDITIONS

When a fluid flows through a tube the layer of fluid immediately in contact with the wall remains stationary. The laminae close to the wall begin to slide on one another subject to the force of viscosity and thus form a boundary layer. Initially the bulk of the fluid will move as a mass, affected very little by the forces of viscosity and will have a flat velocity profile. As flow proceeds down the tube, the boundary layer will become thicker as the viscous drag involves more and more of the fluid. In time, the boundary layer occupies the whole of the tube and steady viscous flow is established. Once steady flow has been reached, the velocity profile is parabolic. This progression is shown in Figure E-1.

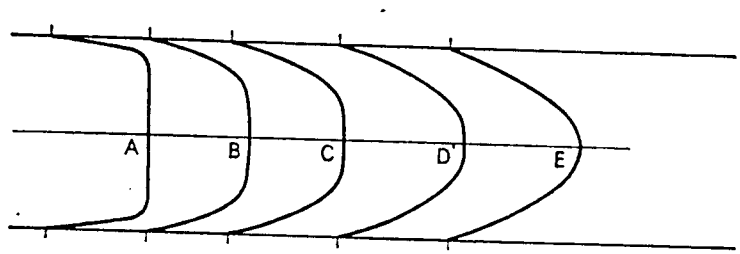

Figure E-1 Development of a steady parabolic velocity profile.

Under parabolic flow conditions, Poiseuille's equation Equ 5-1 is able to describe the relationship between pressure and flow for fluid in a tube. However, blood flow in the arterial system is not always parabolic due to the periodic heart beat and relatively short vessel lengths. Non-parabolic flow conditions violate Poiseuille's equation causing an inaccurate description of the relationship between pressure and flow. Womersley (1955) cited in McDonald (1974) derived an expression for impedance to blood flow from the relationship between flow and pressure gradient for laminar non parabolic flow in an elastic tube.

The impedance to blood flow is a complex quantity and can be described in terms of its resistive and inertive components per unit length δx.

$$R = \frac{\alpha^2 . \mu . \sin(\varepsilon_{10})}{\pi . r^4 . M_{10}'} \qquad \text{Equ E-1}$$

$$L = \frac{\rho . \cos(\varepsilon_{10})}{\pi . r^2 . M_{10}'} \qquad \text{Equ E-2}$$

A table of scaling factors M_{10}' and ε_{10} are defined in McDonald (1974). These terms incorporate the pulsatile effects of flow and reduce to Pouseille's equations under steady state flow conditions. The scaling factors are defined empirically in Equ E-3 and E-4.

$$M_{10}' = \text{modulus}\left\{1 - \frac{2.J_1}{\alpha . j^{3/2} . J_0}\right\} \qquad \text{Equ E-3}$$

$$\varepsilon_{10}' = \text{phase}\left\{1 - \frac{2.J_1}{\alpha . j^{3/2} . J_0}\right\} \qquad \text{Equ E-4}$$

Alpha is a dimensionless parameter that describes the type of flow. Figure E-2 shows the relationship between alpha and the type of flow. A smaller alpha value corresponds to parabolic type flow whereas a larger value indicates more plug-like or turbulent flow. For values of alpha less than approximately 2, the velocity profile remains close to parabolic at all times and the flow is called quasi-steady.

The equation for alpha is given by Equ 4-9.

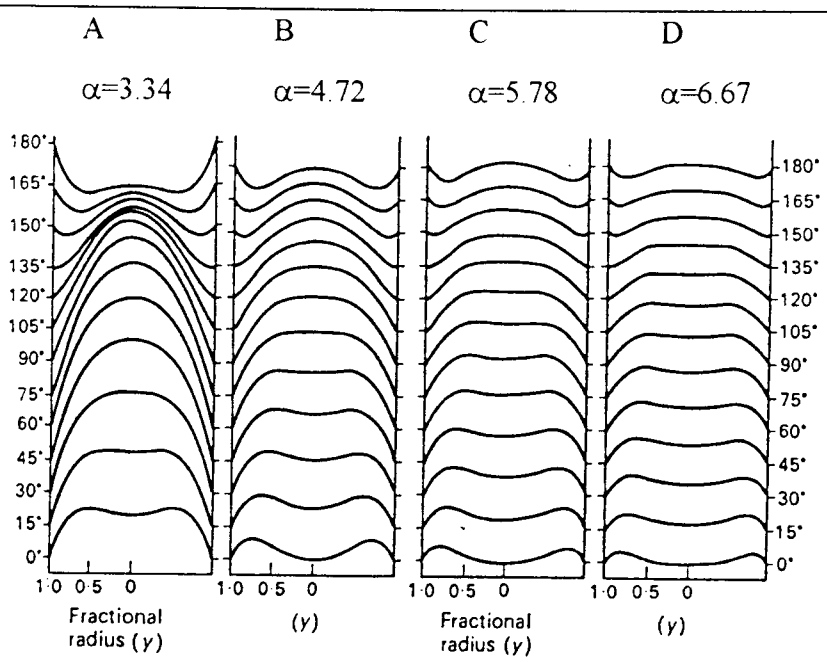

Figure E-2 Alpha and different types of flow

Appendix F SHUNT CONDUCTANCES

The normal percentage of the cardiac output being supplied to the brain and heart, is approximately 5%(Jensen et al. 1991),(Block et al. 1984). Thus the magnitude of the shunt conductance representing blood loss to the head and heart will be equal to 5% of the total shunt conductance. In this way, a value can be determined for each shunt region.

It is thus possible to alter the proportion of blood flow to the various regions, in order to determine the effect of preferential blood flow shunting on the umbilical flow waveform. The total conductance can be determined from Equ F-1

$$\text{Total conductance} = \frac{\text{average blood flow}}{\text{average arterial pressure}} = \frac{350ml/\min}{60\text{mmHg}} \qquad \text{Equ F-1}$$

$$= 7.3 \times 10^{-5}\ \text{dynes}^{-1}.\text{cm}^5.\text{sec}^{-1}$$

Region →	HAH		PLA		THR		ABD		ADR		BODY	
Pathology ↓	%	G	%	G	%	G	%	G	%	G	%	G
Control group	4.9	4	40	29	8.0	6	9	7	0.1	0.1	38	28
Hypoxic	9.8	7	45	32	6.0	4	6	6	0.2	0.1	32	26
Embolised	9.8	7	31	23	6.6	4	11	8	0.2	0.1	41	30
Hypoxic-embolised	17	12	32	23	4.5	3	10	7	0.4	0.3	35	26

Table F-1 Percentage conductance and absolute conductance per section shown for different pathological conditions as taken from Block et al.(1984). The absolute conductance values (G) are scaled by 10^{-6} $\text{dynes}^{-1}\ \text{cm}^5.\text{sec}^{-1}$.

Appendix G STATISTICAL ANALYSIS

INTER AND INTRA-VARIABILITY

The PI variability between measurements (intra-variability) was determined by the coefficient of variation (CV) for patients A and B. Similarly, the PI variability between patients (inter-variability) was determined for measurement 1 and 2.

Intra-Variability				**Inter - Variability**		
	Patient A	Patient B			M1	M2
M1	2.77	2.85		Patient A	2.77	2.84
M2	2.84	3.19		Patient B	2.85	3.19
M3	3.01	2.97		Patient C	2.17	1.98
M4	2.79	3.03		Patient D	2.41	2.14
M5	2.90	3.07		Patient E	2.19	2.42
M6	2.60	2.99		Patient F	2.72	2.87
				Patient G	2.68	2.60
Mean	2.82	3.02		Mean	2.54	2.57
Std Dev	0.14	0.11		Std Dev	0.28	0.43
CV	**0.05**	**0.04**		**CV**	**0.11**	**0.17**

Table G-1 Comparison of coefficient of variation for inter and intra variability

Std Dev - Standard deviation, CV - Coefficient of variation.

The CV (coefficient of variation) is a useful means of comparing the variation across populations especially when a difference in mean value, associated with those populations, is anticipated. The CV expresses the variation in a population in percentage terms relative to the mean of the population. CV is defined as the ratio of standard deviation to the mean.

Comparison of the coefficients of variability for inter- and intra-variability show intra-variability to be smaller by more than 50% in both cases.

SAMPLE SIZE

The sample size required to determine the effect oxygen on the PI is dependent on the difference that needs to be detected, and the level of confidence/significance that is to be attached to the finding and the variability of the result.

The sample size n is required to satisfy Equation G-1

$$n \geq 2.\left[\frac{Z.\sigma}{\text{Diff}}\right]^2 \qquad \text{Equ G-1}$$

Z - Standard normal deviate at the given significance level,

σ - Standard deviation

Diff - Detectable difference required

The standard deviation in PI was determined clinically as 0.1 and Z =1.9824 for the 95% confidence interval. The sample size was determined for a range of differences as shown in Table G-2.

Detectable Difference	1%	2%	3%	4%	5%	6%	7%	8%	10%
Sample Size (n)	786	196	87	49	32	22	16	12	8

Table G-2 Sample size versus required detectable difference of PI index

Appendix H DOPPLER FREQUENCY SPECTRUM

The spectrum of Doppler shift frequencies, under ideal conditions, represents a first order approximation of the range of velocities present in the vessel being insonated at any one time. The power in a specific frequency band of the Doppler spectrum is proportional to the number of erythrocytes moving at a specific velocity. Therefore, spectra corresponding to a flat velocity profile have much of their power concentrated in a relatively small range of frequencies. Conversely, the spectrum of a parabolic velocity profile has its power distributed over a wide range of frequencies. The distribution of power is illustrated in Figure H-1 where power is represented as the z or vertical axis, frequency on the y axis and time on the x axis.

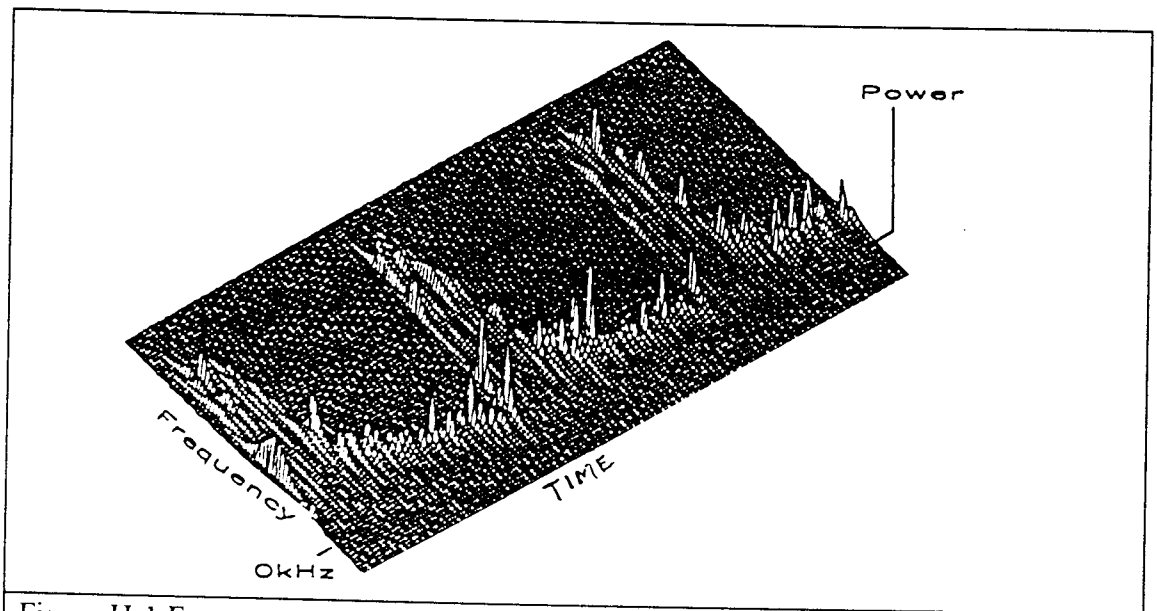

Figure H-1 Frequency power spectrum

SONOGRAM

The variation in shape of the Doppler power spectrum (Figure H-1) as a function of time is usually presented in the form of a sonogram. In this type of display, time is plotted along the horizontal axis, the range of Doppler shift frequencies along the vertical axis and the power of a particular frequency P(f,t) as the intensity of the corresponding pixel. Thus a single vertical line of a sonogram corresponds to a single power spectrum. A typical sonogram is shown in Figure H-2.

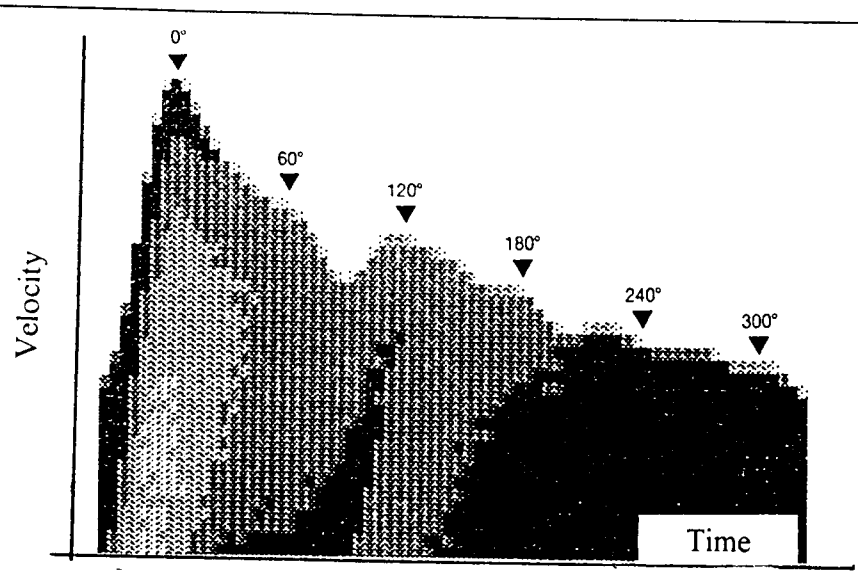

Figure H-2 Sonogram of the Doppler power spectral density.(Evans et al 1994)

Histograms of the velocity distribution are given, with their corresponding velocity profiles in Figure H-3. Peak flow has been marked, as in Figure H-2, by 0° . This notation allows each stage of the cardiac cycle to be represented in the form 0-360°.

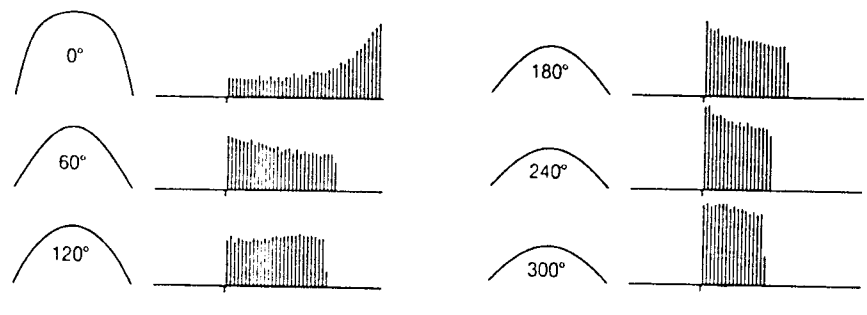

Figure H-3 Velocity flow profiles and corresponding velocity distribution histograms.

REFERENCES

Adamson SL. Morrow RJ. Bull SB. Langille BL
1989
Vasomotor responses of the umbilical circulation in fetal sheep.
American Journal of Physiology. 256: R1056-R1062

Alonso JG. Okai T. Longo LD. Gilbert RD
1989
Cardiac function during long-term hypoxemia in fetal sheep.
American Journal of Physiology. 257: H581-H589

Arbeille P. Maulik D. Fignon A. Stale H. Berson M. Bodard S. Locatelli A.
1995
Assessment of the foetal PO_2 changes by cerebral and umbilical doppler on lamb foetuses during acute hypoxia
Ultrasound in Medicine and Biology. 21(7): 861-870

Arduini D. Rizzo G. Romanini C. Mancuso S
1989
Foetal haemodynamic response to acute maternal hyperoxygenation as predictor of foetal distress in intrauterine growth retardation.
British Medical Journal. 298(6687):1561-1562

Arduini D. Rizzo G. Romanini C. Mancuso S
1990
Doppler assessment of fetal blood flow velocity waveforms during acute maternal oxygen administration as predictor of fetal outcome in post-term pregnancy.
American Journal of Perinatology. 7(3):258-262

Arduini D. Rizzo G
1990
Quantitative analysis of foetal rate: its application in antepartum clinical monitoring and behavorial pattern recognition
International Journal of Biomedicine and Computing. 25:247-252

Assali NS. Bekey GA. Morrison LW
1968
Foetal and neonatal circulation.
Academic Press. New York and London

Atkinson P. Woodcock JP
1982
Doppler ultrasound and its use in clinical measurement
Academic Press Inc. London

Battaglia C. Artini PG. D'Ambrogio G. Galli PA. Segre A. Genazzani AR
1992
Maternal hyperoxygenation in the treatment of intrauterine growth retardation
American Journal of Obstetrics and Gynaecology. 167(2):430-435

Behrman RE. Lees MH. Peterson EM. De Lannoy CW. Seeds AE
1970
Distribution of the circulation in normal and asphyxiated fetal primate.
American Journal of Obstetrics and Gynaecology. 108:956-969

Bekedam DJ. Mulder EJ. Snuijders RJ. Visser GH
1992
The effects of maternal hyperoxia on foetal breathing movements. body movements and heart rate variation in growth retarded foetuses.
Early Human Development. 27(3):223-232

Berne MB. Levy MN
1990
Principles of Physiology
Wolfe Publications. London

Bertolizio G. Arosio G. Frangipani GC. D'Aquino P
1966
The study of PO_2 and of acid-base equilibrium in the amniotic fluid during maternal hyperoxygenation
Annali di Ostetricia. Ginecologia. Medicina Perinatale. 88(4):301-306

Bilardo CM. Nicolaides KH. Campbell S
1990
Doppler measurements of fetal and uteroplacental circulations. Relationship with umbilical venous blood gases measured at cordocentesis.
American Journal of Obstetrics and Gynaecology. 162:115-120

Block BS. Schlafer DH. Wentworth RA. Kreitzer LA. Nathanielsz PW
1990
Regional blood flow distribution in foetal sheep with intrauterine growth retardation produced by decreased umbilical placental profusion.
Journal of Developmental Physiology. 13:81-85.

Block BS. Llanos AJ. Creasy RK.
1984
Responses of the growth-retarded foetus to acute hypoxemia.
American Journal of Obstetrics and Gynaecology; 148: 7-11

Bocking AD. White S. Gagnon R. Hansford H
1989
Effect of prolonged hypoxemia on foetal heart rate accelerations and decelerations in sheep
American Journal of Obstetrics and Gynaecology; 161:722-727

Brar HS. Medearis AL. DeVore GR. Platt LD.
1989
A comparative study of fetal umbilical velocimetry with CW and PW Doppler. in high risk pregnancies
American Journal of Obstetrics and Gynaecology; 160(2):375-378

Brosens I. Robertson WB. Dixon HG
1967
The physiological response of the veddels of the placental bed to normal pregnancy.
Journal of Pathology and Bacteriology. 93:569-579

Brosens I. Dixon HG. Robertson WB
1977
Foetal growth retardation and the arteries of the placenta bed.
British Journal of Obstetrics and Gynaecology. 84:656-663

Bunn A.E.
1980
Theory and physiological applications of pressure waves in compliant tubes.
Doctorate Thesis. Faculty Of Medicine. University Of Stellenbosch.

Carter AM
1989
Factors affecting gas transfer across the placenta and the oxygen supply to the foetus.
Journal of Developmental Physiology. 12:305-322

Chen HY. Chang FM. Huang HC. Hseih FJ. Lu CC
1988
Antenatal foetal blood flow in the descending aorta and in the umbilical vein and their ratio in normal pregnancy.
Ultrasound in Medicine and Biology. 14(14):263-268

Chudleigh P . Pearce MJ
1986
Obstetric ultrasound. how. why. when ?
Churchill Livingstone.. Edinburgh

Cohn HE. Piasecki GJ. Jackson BT
1980
The effect of foetal heart rate on cardiovascular function during hypoxemia.
American Journal of Obstetrics and Gynaecology. 138(8):1190-1199

Creasy RK. DeSwiet M. Kahanpaa KV. Young WP. Rudolph AM
1973
Pathophysiological changes in the foetal lamb with growth retardation
In:Comline RS. Cross KW. eds. Foetal and Neonatal Physiology
University Press. Cambridge

Creasy RK. Resnik R
1989
Maternal-Fetal Medicine. 2nd Edition.
Saunders. Philadelphia

Davey DA. McGillivray I
1988
The classification and definition of the hypertensive disorders of pregnancy
American Journal of Obstetrics and Gynaecology; 158:892-898

Dawes GS
1968
Foetal and Neonatal Physiology.
Year Book Medical Publishers. Inc. Chicago.

Dekker GA . van Geijn P
1994
Pathophysiology of preeclampsia and foetal outcome
In: van Geijn H. Copray F eds. A critical appraisal of foetal surveillance.
Elsevier Science

Demuylder X. Fouron JC. Bard H. Riopel L. Urfer H.
1984
The difference between the systolic time intervals of the left and right ventricles during fetal life.
American Journal of Obstetrics and Gynaecology. 149(7):737-740

Downing GJ. Yarlagadda P. Maulik D.
1991
Effects of acute hypoxemia on umbilical arterial Doppler indices in a foetal ovine model.
Early Human Development. 25:1-10

Edelstone DI. Heymann MA. Rudolph AM
1980
Effects of hypoxemia and decreasing umbilical flow on the liver and ductus venosus blood flows in fetal lambs.
American Journal of Physiology. 238:H656-H663

Evans DH. McDicken WN. Skidmore R. Woodcock JP
1994
The origin of the doppler spectrum
In : Doppler Ultrasound - Physics. Instrumentation and Clinical Applications.
John Wiley & Sons. Chichester

Evans JA
1986
Ultrasonic wave propagation in tissue
In: J.A Evans.. Ed. Physics in Medical Ultrasound.
Bocardo Press. Institute of Physical Sciences in Medicine. London

Field DR. Parer JT. Auslender RA. Cheek DB. Baker W. Johnson J
1990
Cerebral oxygen consumption during asphyxia in foetal sheep.
Journal of Developmental Physiology. 14:131-137

Fruchter O
1994
Does maternal hyperoxygenation result in fetal oxygenation?
American Journal of Obstetrics and Gynaecology; 169(6):1657-1658

Giles WB. Trudinger BJ. Baird PJ
1985
Foetal umbilical artery flow velocity waveforms and placental resistance:pathological correlation
British Journal of Obstetrics and Gynaecology. 92:31-38

Giles WB. Lingman G. Marsal K. Trudinger BJ.
1986
Foetal volumes blood flow and umbilical artery flow velocity waveform analysis: a comparison.
British Journal of Obstetrics and Gynaecology. 93:461-465

Gussani DA. Spencer JA. Moore PJ Bennet L. Hanson MA
1993
Afferent and efferent components of the cardiovascular reflex responses to acute hypoxia in term foetal sheep.
Journal of Physiology 461:431-449

Goodlin RC. Girard J. Hollmen A.
1972
Systolic time intervals in the foetus and neonate.
Obstetrics and Gynaecology. 39(2):295-303

Griffiths AC
1989
Differences in birth statistics from central Birmingham
British Medical Journal. 298(6666):94-95

Guiot C. Pianta PG. Todros T.
1992
Modelling the foeto-placental circulation: I. Adistributed network predicting umbilical haemodynamics throughout pregnancy.
Ultrasound in Medicine and Biology. 19(6-7):535-544

Guyton AC
1993
Medical physiology
Part VII. Sixth Edition. Saunders WB, Philadelphia.

Hackett GA. Campbell S. Gamsu H. Cohen-Overbeek T. Pearce JMF
1987
Doppler studies in the growth retarded foetus and prediction of neonatal necrotising enterocolitis. haemorrhage. and neonatal morbidity.
British Medical Journal. 294:13-16

Heymann MA. Rudolph AM
1975
Control of the ductus arteriosus. [Review]
Physiological Reviews. 55(1):62-78

Hibbard BM
1988
Principles Of Obstetrics.
Butterworths. London.

Hoskins PR. Loupas T. McDicken WN
1991
An investigation of simulated umbilical artery doppler waveforms.
Ultrasound in Medicine and Biology. Parts 1-3. 17(1):7-22,23-30,703-708

Howard RB. Hosokawa T. Maguire MH
1987
Hypoxia-induced fetoplacental vasoconstriction in perfused human placental cotyledons.
American Journal of Obstetrics and Gynaecology. 157(5):1261-1266

Huikeshoven FJ. Hope ID. Power GG. Gilbert RD. Longo LD
1985
Mathematical model of fetal circulation and oxygen delivery.
American Journal of Physiology. 249:R192-R202

Hytten F. Chamberlain G. eds
1991
Clinical physiology in obstetrics
Blackwell. Oxford

Itskovitz J. LaGamma EF. Rudolph AM
1987
Effects of cord compression on fetal blood flow and oxygen delivery.
American Journal of Physiology. 257:H100-H109

Jager GN. Westerhof N. Noordergraaf A
1965
Oscillatory flow impedance in electrical analog of arterial system.
Circulation Research. 16:121-133

Jensen A. Kunzel W. Kastendieck E
1985
Repetitive reduction of uterine blood flow and its influence on foetal transcutaneous PO2 and cardiovascular variables.
Journal of Developmental Physiology. 7:75-87

Jensen A. Hohmann M. Kunzel W
1987
Dynamic changes in organ blood flow and oxygen consumption during acute asphyxia in foetal sheep.
Journal of Developmental Physiology. 9:543-559

Jensen A. Berger R.
1991
Foetal circulatory responses to oxygen lack.
Journal of Developmental Physiology. 16:181-207

Jensen A. Roman C. Rudolph AM
1991a
Effects of reducing uterine blood flow on foetal blood flow distribution and oxygen delivery.
Journal of Developmental Physiology. 15:309-323

Kitanaka T. Alonso JG. Gilbert RD. Siu BL. Clemons GK. Longo LD
1989
Fetal responses to long-term hypoxemia in sheep.
American Journal of Physiology. 256:R1348-R1354

Koos BJ. Sameshima H. Power GG
1987
Foetal breathing. sleep state. and cardiovascular responses to graded hypoxia in sheep
Journal of Applied Physiology. 62(3):1033-1039

Liedtke AJ. Urschel CW. Kirk ES
1973
Total systemic autoregulation in the dog and its inhibition by baroreceptor reflex.
Circulation Research. 32:465-470

Low JA [Review]
1991
The current status of maternal and fetal blood flow velocimetry
American Journal of Obstetrics and Gynaecology, 164(4):1049-1063

Makowski EL, Meschia G, Droegemueller W, Battaglia FC
1968
Measurements of umbilical arterial blood flow to the sheep placenta and foetus in utero.
Circulation Research., 23:623-631

Maulik D, Yarlagadda P, Youngblood JP, Ciston P.
1991
Comparative efficacy of umbilical arterial Doppler indices for predicting adverse perinatal outcome
American Journal of Obstetrics and Gynaecology; 164(6 Pt 1):1434-1439

Maulik D, Arbeille P, Kadado T
1992
Hemodynamic foundation of umbilical arterial Doppler waveform analysis.
Biology of the Neonate, 62(4):280-289

McDonald DA
1974
Blood flow in arteries, 2nd Edition
The Camelot Press Ltd., Southampton.

Meyenburg M, Bartnicki J, Saling E
1992
The effect of maternal oxygen administration on foetal and maternal blood values using Doppler ultrsonography.
Journal of Perinatal Medicine, 19(3):185-90

Mires GJ, Patel NB, Dempster J
1990
The value of foetal umbilical artery flow velocity waveforms in the prediction of adverse foetal outcome in high risk pregnancies.
Journal of Obstetrics and Gynaecology, 10:261-270

Mo LY, Bascom PAJ, Ritchie K, McCowan LME
1988
A transmission line modelling approach to the interpretation of uterine doppler waveforms.
Ultrasound in Medicine and Biology, 14(5):365-376

Morrow RJ, Adamson SL, Bull SB, Knox Ritchie JW
1989
Effect of placental embolisation on the umbiclial arterial velocity waveform in foetal sheep
American Journal of Obstetrics and Gynaecology; 161:1055-1060

Muijsers GJ, van Huisseling H, Hasaart THM
1991
The effect of selective umbilical embolization on the common umbilical artery pulsatility index and umbilical vascular resistance in foetal sheep.
Journal of Developmental Physiology, 15:259-267

Narayana PA. Ophir J. Maklad NF
1984
The attenuation of ultrasound in biological fluids
Journal of the Acoustical Society of America, 76(1):1-4

Nicolaides KH. Bilardo CM. Soothill PW. Campbell S
1988
Absence of end diastolic frequencies in umbilical artery: a sign of foetal hypoxia and acidosis
British Medical Journal. 297:1026-1027

Nicolaides KH. Campbell S. Bradley RJ. Soothill PW. Gibb D
1987
Maternal oxygen therapy for intra-uterine growth retardation.
Lancet 1(8539):942-945

Owens JA. Falconer J. Robinson JS
1987
Effect of restriction of placental growth on foetal and utero-placental metabolism.
Journal of Developmental Physiology. 9:225-238

Pattinson RC. Theron GB. Thompson ML. Lai Tung M
1989
Doppler ultrasonography of the foetoplacental circulation - normal reference values.
South African Medical Journal. 76:623-625

Paulick RP. Meyers RL. Rudolph AM
1991
Vascular responses of umbilical-placental circulation to vasodilators in fetal lambs.
American Journal of Physiology. 261:H9-H14

Pearce JM.Campbell S. Cohen-Overbeek T. Hackett G. Hernandez J. Royston JP.
1988
References ranges and sources of variation for indices of pulsed Doppler flow velocity waveforms from the uteroplacental and foetal circulation.
British Journal of Obstetrics and Gynaecology. 95(3):248-256

Polin RA . Fox WW
1992
Foetal and Neonatal Physiology.
WB Saunders Company. London

Polvi HJ. Pirhonen JP. Erkkola RU
1995
The hemodynamic effects of maternal hypo- and hyperoxygenation in healthy term pregnancies.
Obstetrics and Gynecology. 86(5):795-799

Raymond SP. Whitfield CR
1987
Systolic time intervals of the foetal cardiac cycle.
Bailliere's Clinical Obstetrics and Gynaecology. 1(1):185-201

Reed KL. Anderson CF. Shenker L.
1987
Changes in intracardiac Doppler blood flow velocites in fetuses with absent umbilical artery diastolic flow.
American Journal of Obstetrics and Gynaecology. 157:774-779

Robinson JS. Jones CT. Kingston EJ
1983
Studies on experimental growth retardation in sheep. The effects of maternal hypoxemia.
Journal of Developmental Physiology. 5:89-100

Rochelson B. Schulman H. Farmakides G et al
1987
The significance of absent end-diastolic velocity in umbilical artery velocity waveforms.
American Journal of Obstetrics and Gynaecology. 156(5):1213-1218

Rochelson B
1989
The clinical significance of absent end-diastolic velocity in the umbilical artery waveforms.
Clinical Obstetrics and Gynaecology. 32(4):692-701

Rudolph AM. Heymann MA.
1967
The circulation of the foetus in utero: methods for studying distribution of blood flow . cardiac output and organ blood flow.
Circulation Research. 21(2):163-184

Rudolph AM. Heymann MA
1970
Circulatory changes during growth in the foetal lamb.
Circulation Research. 26:289-299

Rudolph AM
1974
Congenital diseases of the heart : Clinical-physiologic considerations in diagnosis and management.
Chicago: Year Book

Rudolph AM
1984
Oxygenation in the Foetus and Neonate - A Perspective
Seminars in Perinatology. 8(3):158-167

Sabbagha RE. Minogue J. Tamura RK. Hungerford SA
1989
Estimation of birth weight by use of ultrasonographic formulas targeted to large. appropriate. and small for gestational age fetuses.
American Journal of Obstetrics and Gynaecology. 162(5):1351

Sagawa K. Eisner A
1975
Static pressure-flow relation in the total systemic vascular bed of the dog and its modification by the baroreceptor reflex.
Circulation Research. 36:406-413

Schulman H. Winter D. Farmkaides G. Coury A. Schneider E. Penny B.
1989
Doppler examinations of the umbilical and uterine arteries during pregnancy.
Clinical Obstetrics and Gynaecology. 32(4):738-745

Shung KK. Sigelmann RA. Reid LM
1976
Scattering of ultrasound by blood
IEEE Transcripts of Biomedical Engineering. 23:460-467

Skidmore R. Woodcock JP. Wells PNT
1980
Physical interpretation of doppler shift waveforms
Ultrasound in Medicine and Biology. 6:219-231

Soothill PW. Ajayi RA. Nicolaides KN
1992
Foetal biochemistry in growth retardation.
Early Human Development. 29(1-3):91-97

Szentkuti A. Capper WL. Norman K. Wright AW. Odendaal H
1993
High resistance state index: a new method to assess foetal compromise in absent diastolic umbilical arterial flow.
Journal of Maternal-Foetal Investigation. 3(3):177

Taylor KJW. Burns PN. Wells PNT
1988
Interpretation and analysis of doppler signals
Clinical Applications of Doppler Ultrasound
Ravens Press. New York

Theron GB. Thompson ML
1995
A centile chart of birth weight for an urban population of the Western Cape.
South African Medical Journal. 85(12):1-5

Thompson RS
1987
Blood flow velocity waveforms.
Seminars in Perinatology. 11(4):300-310

Thompson RS. Stevens RJ
1989
Mathematical model for interpretation of Doppler velocity waveform indices.
Medical and Biological Engineering and Computing. 27:269-276

Thompson RS. Trudinger BJ
1990
Doppler waveform pulsatility index and resistance, pressure and flow in the umbilical placental circulation: An investigation using a mathematical model.
Ultrasound in Medicine and Biology. 16(5):449-458

Toubas PL. Silverman NH. Heymann MA. Rudolph AM
1981
Cardiovascular effects of acute haemorrhage in fetal lambs.
Amerian Journal of Physiology. 240:H45-H48

Trudinger BJ. Stevens D. Connelly A et al
1987
Umbilical artery flow velocity waveforms and placental resistance: The effects of embolization of the umbilical circulation.
American Journal of Obstetrics and Gynaecology. 157:1443-1448

Veth AFL
1976
Modelling the foetal circulation.
Institute of Medical Physics TNO. Netherlands.

Wells PNT
1975
Absorbtion and dispersion of ultrasound in biological tissue.
Ultrasound in Medicine and Biology 1:396-376

Wright AW
1994
Umbilical blood flow analysis to determine an index of placental impedance.
Cape Town. South Africa: UCT
MSc dissertation